Chapter 4

Fission Tracks in Zircons: Evidence for Abundant Nuclear Decay

Andrew A. Snelling, Ph.D.*

Abstract. Fission tracks are a physical record of *in situ* nuclear decay, their density being directly proportional to the amount of nuclear decay that has occurred. The aim of this study was to investigate whether the amounts of fission tracks in zircon grains in targeted rock units (that is, their fission track "ages") matched the radioisotope "ages" of those rocks. Stratigraphically well-constrained volcanic ash or tuff beds located in the Grand Canyon-Colorado Plateau "type section" of the Flood strata record were chosen—the Cambrian Muav and Tapeats tuffs from the western Grand Canyon (early Flood), Jurassic Morrison Formation tuff beds, southeastern Utah (middle Flood), and the Miocene Peach Springs Tuff, southeastern California and western Arizona (late Flood or post-Flood). The fission track "ages" of zircon grains separated from samples of these tuff units were determined by a specialized professional laboratory using the external detector method and a zeta (ζ) calibration factor. The observed fission track densities measured in all the zircons (and thus the fission track "ages") from the samples of the Jurassic and Miocene tuffs, and in some of the zircons from the Muav and Tapeats tuffs, were found to exactly equate to the quantities of nuclear decay measured by radioisotope determinations of the same rock units. Though thermal annealing of fission tracks had occurred in some zircon grains in the two Cambrian Grand Canyon tuffs, the U-Pb radioisotope system had also been thermally reset, the resulting reset ages in both instances coinciding

* *Geology Department, Institute for Creation Research, Santee, California*

with the onset of the Laramide uplift of the Colorado Plateau. The fact that the thermal annealing of the fission tracks and the thermal resetting of the U-Pb radioisotope system in those zircon grains were exactly parallel is unequivocal confirmation that the radioisotope ratios are a product of radioactive decay, in just the same way as the fission tracks are physical evidence of nuclear decay. Furthermore, because the resetting of the U-Pb radioisotope system in zircons will only occur at elevated temperatures, the fact that it has been reset in these zircons could therefore be due to them having been heated by accelerated nuclear decay. Even so, in spite of this thermal annealing and resetting, there remains sufficient strong evidence to conclude that both the fission tracks and radioisotope ratios in the zircons in the Cambrian Grand Canyon tuff beds record more than 500 million years worth (at today's rates) of nuclear and radioisotope decay during deposition of the Phanerozoic strata sequence of the Grand Canyon-Colorado Plateau region. Given the independent evidence that most of this strata sequence was deposited catastrophically during the year-long global Flood about 4500 years ago, then 500 million or more years worth (at today's rates) of nuclear and radioisotope decay had to have occurred during the Flood year about 4500 years ago. Thus, the fission tracks in the zircons in these tuffs are physical evidence of accelerated nuclear decay.

1. Introduction

The radioisotope dating of minerals and rocks is based on analyses of radioactive parent and radiogenic daughter isotope pairs, often ratioed against related stable isotopes because of the convenient measurement of isotope ratios using mass spectrometers. The interpretation that calculates ages from these radioisotope ratio analyses depends on crucial assumptions, in particular that the daughter isotopes have been derived by radioactive decay of the parent isotopes, and that radioisotope decay has occurred at a constant rate, as measured experimentally today. On the other hand, if either or both were shown to be false, then it could be argued that either the measured isotope ratios are merely an artifact of the mineral compositions and the geochemistry of the rocks and the

sources from which they were derived, or radioactive decay had been accelerated. If either or both of these possibilities were demonstrated to be true, then the interpreted radioisotope ages that are an integral part of the modern geological synthesis of the earth's history would be falsified. Indeed, the parent/daughter assumption is often not fulfilled, so those particular rocks cannot be radioisotope dated. And in many cases, the concentrations of the daughter isotope are independent of the parent isotope, which has led to alternative explanations for the daughter isotope concentrations apart from radioisotope decay, such as inheritance and mixing [*Snelling*, 2000a, 2005b].

One available method to test whether radioactive decay has really occurred *in situ* in rocks after they have formed is fission track dating. Fission tracks are a physical record in minerals of the nuclear decay of their trace U contents. The number and density of fission tracks that can be observed in certain minerals is directly proportional to the amount of nuclear decay that has occurred. If this method is valid, then it is possible to investigate whether the amount of radioactive decay implied by chemical analyses of the radioisotope ratios is matched by the required observable amounts of fission tracks. Such verification of the equivalent observable physical evidence of radioactive decay with the amount measured by radioisotope ratios would seem to rule out any claim that the interpreted radioisotope ages are merely artifacts of the chemical analyses and the assumptions implicit in these methods. Furthermore, demonstration that there is observable physical evidence that hundreds of millions of years of nuclear decay has occurred *in situ* in minerals within rocks since they formed implies that within the Biblical timescale of only 6000–7000 years for earth history those huge amounts of nuclear decay had to have occurred at accelerated rates. This then is the focus of the research being reported in this chapter.

Because fission track dating is a different nuclear decay dating method that is not as well known and understood as the radioisotope methods, some background information on how fission track dating is performed seems warranted. This is provided in an Appendix, drawn from *Faure* [1986], *Dickin* [1995], and *Faure and Mensing* [2005].

2. Previous Creationist Research on Fission Track Dating

There has been very little creationist research into fission track dating. In a review article concerning radioactive dating, *Chaffin* [1987] discussed the possibility that fission tracks might result from other isotopes with shorter half-lives than those of ^{238}U and ^{244}Pu. *Bielecki* [1994] reported his examination of fission track densities in obsidian from the Resting Spring Range near Shoshone, California. He found that the fission track densities were equivalent to the reported uniformitarian Miocene "age" of this obsidian. He had thought that if this rock was post-Flood then it might have fission track densities smaller than its claimed multi-million year age. However, the data did not support that hypothesis, the observed fission track densities being physical evidence of millions of years of nuclear decay. *Bielecki* [1998] reported on his literature investigation of the fission track densities in man-made and natural glasses of known historical age, as well as in natural glasses and volcanic debris of comparatively recent geologic age. He concluded that the spontaneous fission tracks in man-made and natural glasses are a reliable nuclear decay dosimeter for the recent past, and that the spontaneous fission track densities in glasses within volcanic strata throughout western North America of Pleistocene and Miocene geologic age indicate an over-abundance of nuclear decay has occurred since formation of those glasses. Because he was seeking to use spontaneous fission track densities as a means of distinguishing between Flood and post-Flood rocks he had to conclude his attempt to do that had failed.

Chaffin [2000] posed the question as to whether it is possible to determine what type of nuclide could produce the observed fission tracks within the time frame of a young earth, and assuming that fission decay constants had truly been the same throughout earth history. He found that when α-decay half-lives are compared with spontaneous fission half-lives there theoretically are some radionuclides that might have produced the observed spontaneous fission track densities within a young-earth time frame without recourse to postulating accelerated nuclear decay. The prime candidates would be three isotopes of the

trans-uranium element Cf which undergo both rapid α-decay and rapid spontaneous fission. However, it was admitted that it is impossible to distinguish the spontaneous fission of ^{252}Cf from that of ^{238}U by the lengths of the fission tracks, and it is impossible to confirm the presence of spontaneous fission of ^{252}Cf by analyzing for any infinitesimally small quantities of its decay product ^{250}Cm. On the other hand, because of the radiohalo evidence that millions of years of α-decay of ^{238}U has occurred [*Snelling*, 2000b; 2005a], the smaller quantities of spontaneous fission of ^{238}U that would have to have occurred contemporaneously would explain, and be commensurate with, the observed spontaneous fission track densities. Thus, because the physical evidence of millions of years of α-decay of ^{238}U would need to be explained by accelerated nuclear decay within a young-earth time frame, other nuclides with much shorter half-lives such as ^{252}Cf would also have experienced accelerated decay, rendering it unnecessary to attribute to ^{252}Cf the observed spontaneous fission track densities.

It can thus be concluded from these few studies that the physical evidence of millions of years of spontaneous fission of ^{238}U cannot be easily accounted for in a young-earth time frame without recourse to postulating accelerated nuclear decay. And even if there are fission tracks produced by isotopes with much shorter half-lives, they are virtually irrelevant in dealing with the observed spontaneous fission track densities that appear to match the physical evidence in radiohalos of millions of years worth of α-decay from ^{238}U [*Chaffin*, 2000]. Furthermore, the presence of spontaneous fission track densities in geologically recent natural glasses and volcanic strata commensurate with the presumed geologic ages of such strata and their ages measured by radioisotope decay cannot be ignored, particularly when such volcanic strata are deemed, in most creationist models of earth history, to have formed after the Flood during which the postulated accelerated nuclear decay would have occurred.

3. Rationale of the Present Study

The focus of the present research effort is not only to verify that

the fission tracks provide physical evidence of millions of years of nuclear decay, but to determine whether the observed fission track densities do or do not equate to millions of years of contemporaneous α-decay in the same rocks as determined from radioisotope dating analyses. For example, if the fossil content of a rock unit according to evolutionary criteria has been labeled as Cambrian and the radioisotope determinations have dated that rock unit as 540 million years old, then do the observed fission track densities yield fission track "dates" that are commensurate with both the biostratigraphic Cambrian designation and the radioisotope "age" determinations? If the answer is yes, then the physical evidence of nuclear decay in the form of the observed fission tracks confirms that the radioisotope determinations are indeed a record of radioisotope decay, rather than simply being just chemical analyses open to other interpretations. Furthermore, the fact that so many millions of years of nuclear decay has occurred implies that within the young-earth time frame such large quantities of nuclear decay have to be explained by an accelerated rate of nuclear decay. However, an additional outcome would potentially be the quantification of just how much accelerated nuclear decay had to have occurred, for example, during the Flood. Thus if the fission tracks observed in a Cambrian (early Flood) rock unit yield a fission track "age" of 540 million years equivalent to the rock unit's radioisotope "age," then it is possible to conclude that over 500 million years worth of accelerated nuclear decay must have occurred during the Flood year.

4. Sample Selection

To fulfill the objective of this study it was concluded that suitable samples needed to be obtained from stratigraphically well-constrained volcanic ash or tuff beds from which zircons would be extracted for fission track dating. Zircon would be the preferred mineral to be fission track dated because of its durability and high closing temperature, plus the fact that it can also be readily radioisotope dated using the U-Th-Pb system, or such data would already be available in the literature. Tuff beds would also be ideal because they represent time-

specific event horizons that are therefore specific time markers that can be geologically and radioisotope dated.

It was also decided that ideally the required volcanic ash or tuff beds should be located in the Grand Canyon-Colorado Plateau region because of that area already being well-studied by creationist geologists as a "type section" of the Flood [*Austin*, 1994]. Not only is there a very thick stratigraphic section, but most of the systems of the standard geological column are represented, spanning from the Precambrian crystalline basement (granites and metamorphic rocks that have been interpreted as Creation week rocks), up through Paleozoic and Mesozoic sedimentary strata deposited over an enormous geographical extent, to the uppermost Tertiary sedimentary strata (most or all of which would be interpreted as post-Flood) [*Austin*, 1994]. Sampling and fission track dating the zircons in the volcanic ash or tuff beds in this area would thus allow the results to be added to other studies in the region, and to be correlated with other data from the voluminous literature on this region.

Finally, it was decided that ideally it would be best to sample at least one Paleozoic tuff unit, one Mesozoic tuff unit and one Tertiary tuff unit, if such could be found in this Grand Canyon-Colorado Plateau "type section." Such tuff units would thus be representative of the early Flood, middle Flood and late Flood/early post-Flood periods that would potentially allow assessment of the behavior of nuclear decay through the Flood event and possibly into the post-Flood era, perhaps even constraining when the postulated accelerated nuclear decay occurred, and as also indicated previously, just how much accelerated nuclear decay might have occurred during the Flood. Fortunately, tuff units meeting these criteria were able to be found and sampled in the Grand Canyon-Colorado Plateau "type section."

4.1 Cambrian Tuff Units, Western Grand Canyon, Arizona

Naeser et al. [1989a] located, sampled and zircon fission track dated two thin bentonitic volcanic ash (tuff) units in the Tonto Group section in the western Grand Canyon. The outcrops sampled are to be found

at River Mile 179.8 (179.8 miles or 289.3 km downstream from Lees Ferry), a bench on the left below Lower Lava Rapid where a thin tuff bed sits on top of the Peach Springs Member of the Muav Limestone marking its contact with the overlying Kanab Canyon Member, and at River Mile 205.7 (205.7 miles or 331.0 km downstream of Lees Ferry), a prominent thin, green tuff bed near the base of a red-brown sandstone unit at the top of the Tapeats Sandstone where it transitions into the Bright Angel Shale above, as described by *Billingsley and Elston* [1989]. These two tuff units were not reported by *McKee and Resser* [1945] in their classic study of the Cambrian Tonto Group of the Grand Canyon, in which numerous stratigraphic sections were carefully measured and described in detail. Nor have they been referred to by *Middleton and Elliott* [1990, 2003] in their contribution to the present comprehensive textbook on Grand Canyon geology.

However, *Elston* [1989] provides a description of these two tuff units that accurately places their positions in the stratigraphy of the Tonto Group in the western Grand Canyon (Figure 1). The first of these tuff units is described as a 2–3 cm thick bentonite layer in a thin, thin-bedded interval of limestone that separates the single relatively uniform depositional unit of the Peach Springs Member from the overlying Kanab Canyon Member of the Middle Cambrian Muav Limestone. This thin ash-fall tuff bed evidently marks this contact in many places, and fifteen zircon grains from it have yielded a fission track age of 535±48 Ma [*Elston*, 1989; *Naeser et al*., 1989a]. The second and stratigraphically lower of these tuffs is described as an ash-fall tuff near the base of the red-brown sandstone at the top of an interval of shale and subordinate sandstone of Tapeats Sandstone lithology that overlies the early Cambrian *Olenellus* horizon, which in turn closely overlies the lower cliff-forming massive sandstone units of the Tapeats Sandstone, that can be traced to the Grand Wash Cliffs to the west. This 8–10 cm thick bentonitic tuff unit beneath the uppermost red-brown sandstone of the Tapeats Sandstone thus appears to approximately correlate with the *Zacanthoides* cf *walpai* horizon of the Toroweap stratigraphic section (Figure 1), considered by *McKee and Resser* [1945] to be of early Middle Cambrian age [*Elston*, 1989]. Twelve zircon grains from this

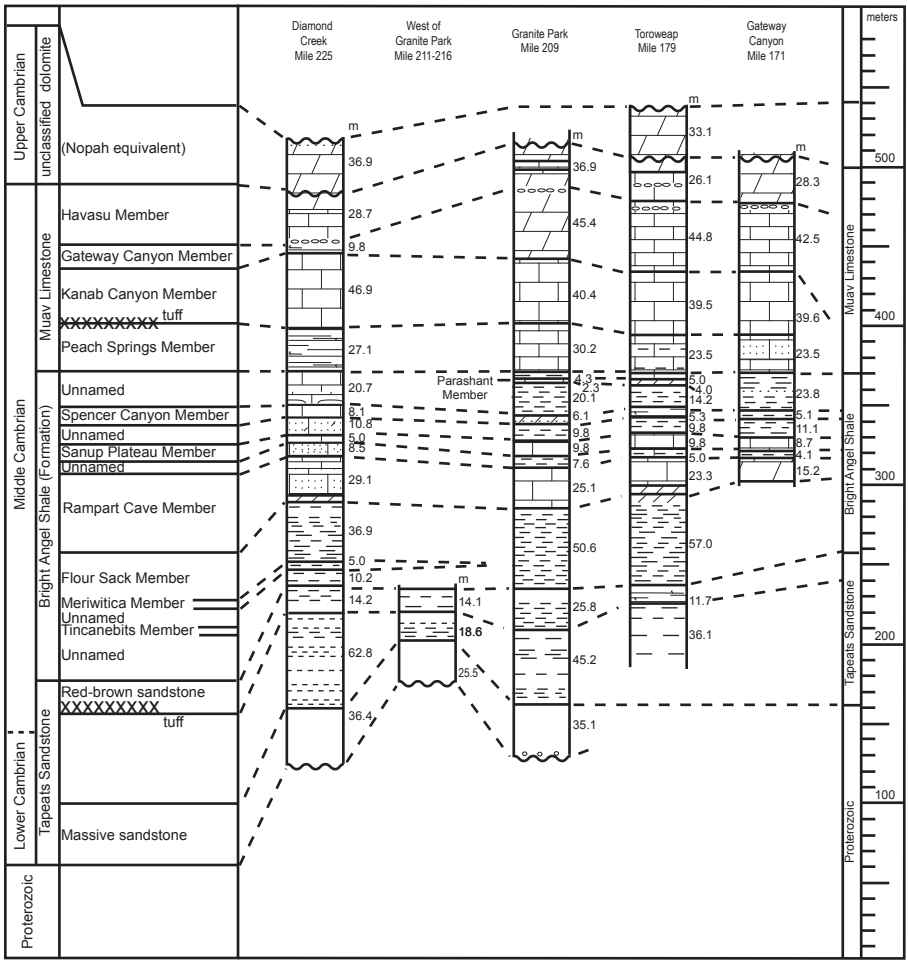

Figure 1. Correlation of the Cambrian Tonto Group showing facies changes in the western Grand Canyon (after *McKee and Resser* [1945]; *Elston* [1989]). The stratigraphic position of the thin Muav and Tapeats tuff units are indicated by xxxxxx.

tuff yielded a fission track age of 563±49 Ma [*Naeser et al*., 1989a].

Both of these tuff units were sampled for this study from these outcrops, two samples of the Muav tuff and a single sample of the Tapeats tuff. The details of these samples and the published ages of these two tuff units are shown in Table 1.

RATE Sample No.	Sample Source (Unit, Member, Formation)	Location	Latitude Longitude	Geological Age	Published Age (Ma) (±2σ)	Method	References
MT-3 MT-2	Tuff in middle of Muav Limestone	RM 179.8, Grand Canyon, Arizona	N 36°11.684' W 113°05.364'	Middle Cambrian	535±48	zircon FT (15 grains)	*Elston* [1989], *Naeser et al.* [1989a]
TT-1	Tuff in top of Tapeats Sandstone	RM 205.7, Grand Canyon, Arizona	N 36°00.201' W 113°20.487'	Middle Cambrian	563±49	zircon FT (12 grains)	*Elston* [1989], *Naeser et al.* [1989a]
NMF-64	Unit 64, top of Brushy Basin Member, Morrison Formation	Type Section A, Notom, Utah	N 38°15.279' W 111°05.733'	Late Jurassic	106±6 (Unit 64)	zircon FT (6 grains)	*Petersen and Roylance* [1982], *Kowallis and Heaton* [1987]
NMF-49	Unit 49, middle of Brushy Basin Member, Morrison Formation		N 38°15.117' W 111°06.168'		141± 6 (Unit 54) 145±13 (Unit 54)	zircon FT (8 grains) apatite FT (11 grains)	
					142±6 (Unit 49)	zircon FT (6 grains)	
BMF-28	Unit 28, top of Brushy Basin Member, Morrison Formation	Brushy Basin, near Blanding, Utah	N 37°38.338' W 109°34.188'	Late Jurassic	—	—	*Gregory* [1938]
BMF-14	Unit 14, bottom of Brushy Basin Member, Morrison Formation		N 37°38.297' W 109°34.906'		—	—	
MMF-1	Near top, Brushy Basin Member, Morrison Formation	Montezuma Creek, Utah	N 37°19.503' W 109°19.511'	Late Jurassic	147.6±0.8 (plag.) 149.2±0.4 (Kspar)	$^{40}Ar/^{39}Ar$ (single crystal laser-fusion)	*Turner and Fishman* [1991], *Kowallis et al.* [1991]
MMF-4	Near bottom, Brushy Basin Member, Morrison Formation		N 37°19.454' W 109°19.473'		149.4±0.7 (plag.) 149.8±0.3 (Kspar)		
PST-1	Peach Springs Tuff	Snaggletooth area, California	N 34°35.983' W 114°39.199'	Early Miocene	18.7±1.5*	sphene FT	*Young and Brennan* [1974], *Beusch and Valentine* [1986], *Gusa* [1986], *Glazner et al.* [1986], *Gusa et al.* [1987], *Nielson et al.* [1990]
PST-2	Peach Springs Tuff	I-40 road cut, Kingman, Arizona	N 35°10.729' W 114°04.435'		17.3±0.4 (?)	sanidine K-Ar	
PST-3	Peach Springs Tuff	Rte-66 road cut, Kingman, Arizona	N 35°11.316' W 114°02.233'		18.5±0.2	sanidine $^{40}Ar/^{39}Ar$ laser fusion	

*from Bristol Mountains, California, *Gusa* [1986] sample 15, collected by Miller, dated by Green [*Nielsen et al.*, 1990]

Table 1 (left). Details of the samples obtained for this study, including locations, geological age designations, and previously published age determinations. The latitude and longitude for each sample was determined by a hand-held Garmin G. P. S. II unit with an accuracy of between 3 and 10 m.

4.2 Jurassic Morrison Formation Tuffs, Southeastern Utah

The Morrison Formation (Middle? and Upper Jurassic) is one of the most colorful and widely recognized stratigraphic units in the western interior of the United States, primarily because in it are found some of the best preserved and most scientifically significant deposits of fossil dinosaur bones in the world [*Bilbey et al*., 1974; *Peterson and Turner-Peterson*, 1987; *Anderson and Lucas*, 1996; *Turner and Peterson*, 2004]. It has also received much attention because of the rich U deposits contained in its sandstones that in 1980 represented fully 50% of the U.S.'s U reserves. Characteristically 50–150 m thick but in places exceeding 250 m in thickness, the Morrison Formation has been recognized over an area of more than 600,000 square miles (more than 1.5 million km^2), stretching from southern Canada to central Arizona and New Mexico, and from southern Idaho and central Utah to Kansas. Although the internal stratigraphy of the Morrison Formation is locally complex, it is not so on a regional scale. The lower part is dominated by fine to coarse grained, cross-bedded, conglomeratic sandstone, intercalated with redbed mudstone and siltstone, known as the Salt Wash Member. It interfingers with the overlying claystone-dominated Brushy Basin Member. Many of the claystone units in this member are bentonitic and have been derived from volcanic ash, both primary ash-fall tuff and water reworked ash. Other distinctive units within the Morrison Formation have also been assigned member status where they have developed in local depositional basins [*Peterson and Turner-Peterson*, 1987; *Turner and Peterson*, 2004].

For the purposes of this study, the bentonitic mudstone units of the Brushy Basin Member of the Morrison Formation were targeted in southeastern Utah. Three stratigraphic sections that have been measured and well-documented in the literature were chosen for sampling, their locations being shown in Figure 2. At Notom, the

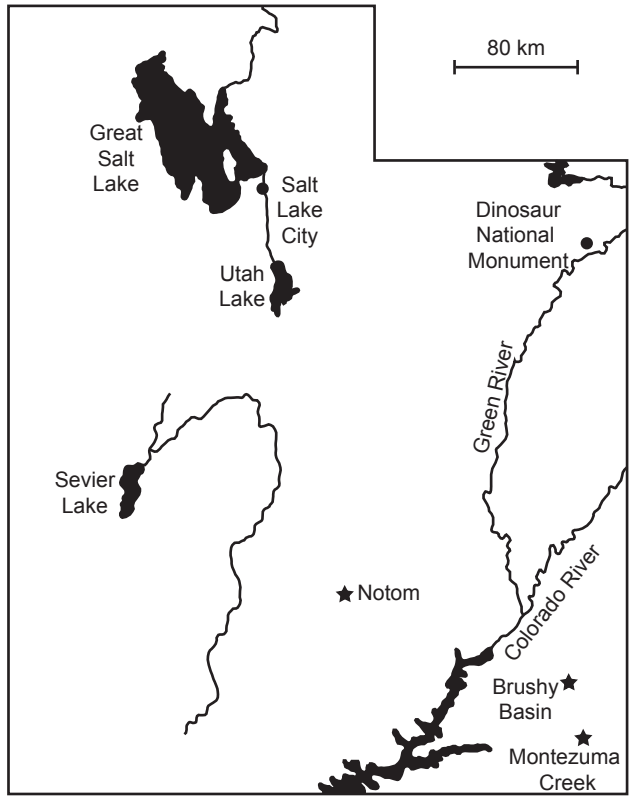

Figure 2. Map of Utah showing the location of the three Brushy Basin Member stratigraphic sections sampled in this study at Notom, Brushy Basin and Montezuma Creek.

Morrison Formation is unusually well exposed along the Waterpocket Fold beyond the eastern boundary of Capitol Reef National Park, which enabled *Petersen and Roylance* [1982] to measure and describe five stratigraphic sections. Their stratigraphic section A, shown in Figure 3, was sampled for this study, primarily because bentonites and bentonitic mudstones in this section have already been zircon fission track dated [*Kowallis and Heaton*, 1987]. Two samples were collected for this study from Peterson and Roylance's units 49 and 64, their stratigraphic position being shown in Figure 3. The second stratigraphic section of the Brushy Basin Member chosen for sampling was in the Brushy

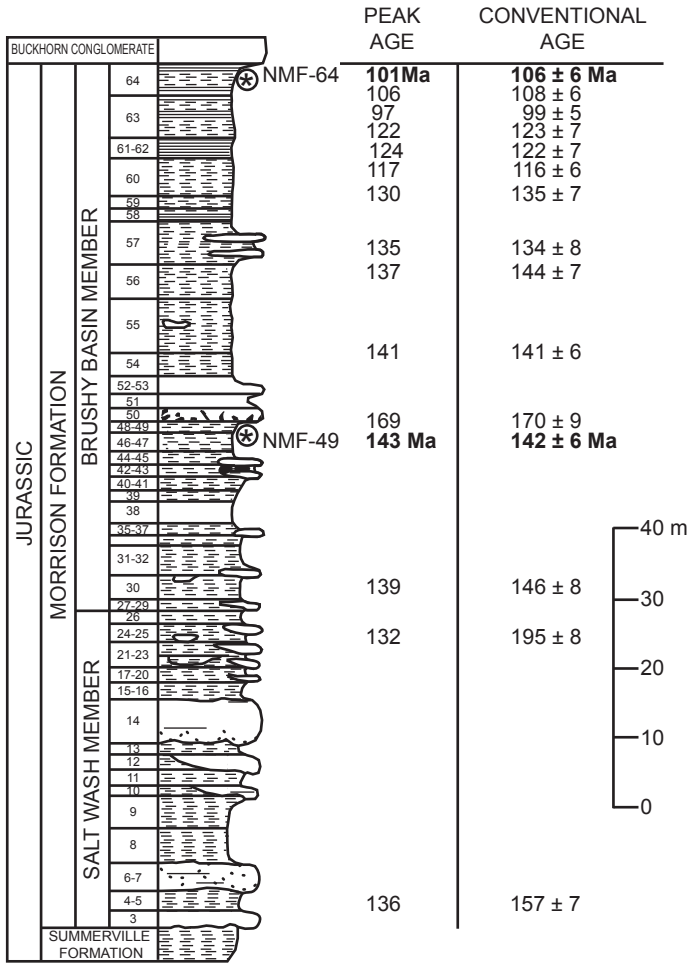

Figure 3. Schematic measured stratigraphic section showing the lithologies and unit numbers (3–64) in the Morrison Formation, and the location of some previously fission track dated samples from Notom, Utah (after *Petersen and Roylance* [1982]; *Kowallis and Heaton* [1987]). The stratigraphic positions of the samples obtained for this study (NMF-49 and NMF-64) are indicated. The peak age represents the age of the youngest peak in the age spectrum plotted for all grains in a sample, whereas the conventional age was obtained by combining all the count data from all grains in a sample [*Kowallis and Heaton*, 1987]. Fission track ages less than 142 Ma are Cretaceous, contrary to the accepted Jurassic stratigraphic age for the Morrison Formation.

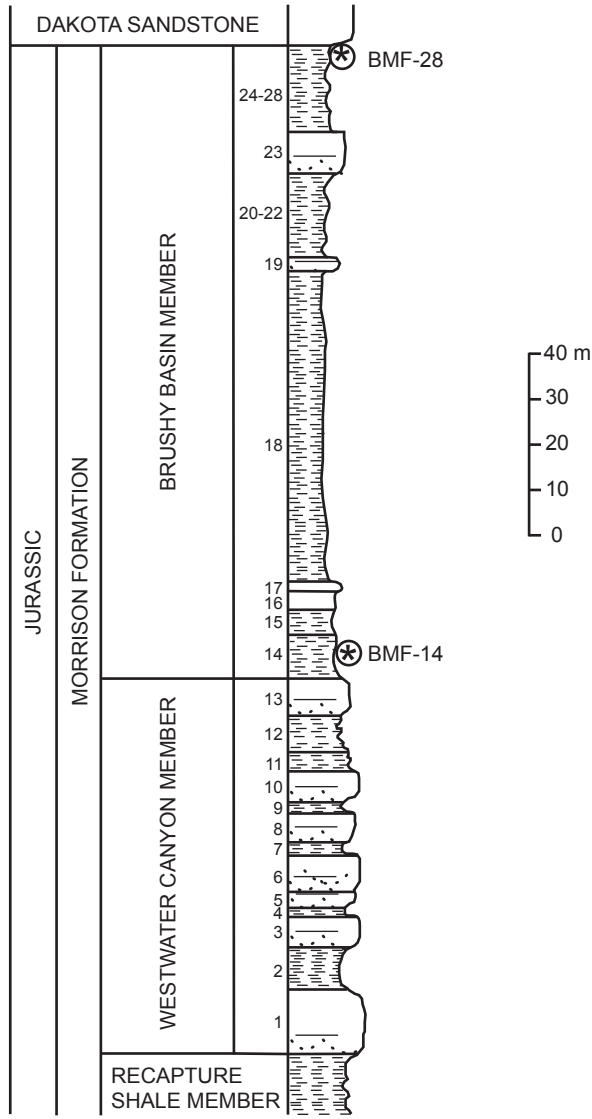

Figure 4. Schematic measured stratigraphic section showing the lithologies and unit numbers (1–28) in the Morrison Formation in the Brushy Basin, west of Blanding, Utah (after *Gregory* [1938]). The stratigraphic positions of the samples obtained for this study (BMF-14 and BMF-28) are indicated.

Basin just to the west of Blanding, section 25 of *Gregory* [1938], which is shown in Figure 4. Units 14 and 28 were sampled (as marked on Figure 4) because of the ease of identifying those bentonitic mudstone units which are adjacent to prominent sandstone units. Whereas the Brushy Basin Member in the Notom type section A is 79.5 m thick, here in the Brushy Basin section 25 due west of Blanding the Brushy Basin Member is 137 m thick, and comparison of these two sections in Figures 3 and 4 illustrate how difficult it is to correlate units within the member from section to section. Because *Kowallis et al.* [1991] have suggested that the unit at the top of the Notom section may not be the top unit of the Brushy Basin Member elsewhere, this could imply that it is not possible to correlate unit 64 at the top of the Notom section A with unit 28 at the top of the Brushy Basin section 25. It is also difficult to correlate the units in both these measured stratigraphic sections with the Montezuma Creek stratigraphic section measured by *Turner and Fishman* [1991] (Figure 5). The samples collected from this section were again chosen because of the ease of locating their positions within the stratigraphic section, being adjacent to prominent sandstone units, and because these same tuffaceous mudstone units had previously been ^{40}Ar-^{39}Ar dated by *Kowallis et al.* [1991]. All the location details and previous dating results for all the samples collected are summarized in Table 1.

4.3 Miocene Peach Springs Tuff, Southeastern California and Western Arizona

The Peach Springs Tuff is a Lower Miocene welded pyroclastic ash flow or ignimbrite that formerly blanketed a minimum area of 2000 square miles (more than 5000 km^2) on both sides of the western edge of the Colorado Plateau in northwestern Arizona, and filled northeast-trending, pre-Colorado River canyons cut through the Paleozoic rocks [*Young and Brennan*, 1974]. The tuff is characterized by abundant large (up to 5 mm) and clear sanidine phenocrysts, with subordinate subequal amounts of plagioclase, biotite, hornblende, sphene, apatite, and zircon in a groundmass that constitutes 80–90 volume percent

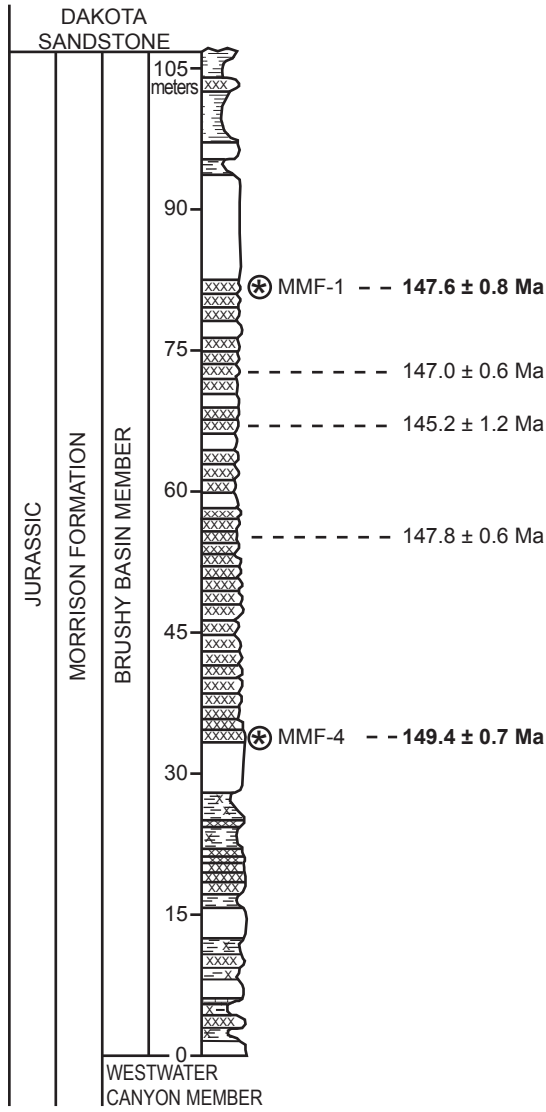

Figure 5. Schematic measured stratigraphic section showing the lithologies in the Brushy Basin Member of the Morrison Formation at Montezuma Creek, Utah (after *Turner and Fishman* [1991]). Tuff beds or tuffaceous intervals are marked with XXXX. The stratigraphic positions of the samples obtained for this study are indicated, as are the positions of previously obtained plagioclase ^{40}Ar-^{39}Ar dates (*Kowallis et al.* [1991]).

of the total rock [*Glazner et al*., 1986]. Rock fragments (often basalt) as large as 10 cm or more are sometimes present and are generally locally derived. This tuff was first recognized and described in the Peach Springs and Kingman areas of Arizona because of the extensive prominent outcrops, but it was subsequently proposed that the tuff may correlate with ash-flow tuff outcrops occurring to the west across the Mojave Desert in southeastern California as far as Barstow [*Glazner et al*., 1986] (Figure 6). However, because ash-flow tuffs are commonly difficult to correlate due to lateral and vertical variations in welding, mineralogy and chemistry, complex depositional mechanisms, and other complicating factors [*Hildreth and Mahood*, 1985], correlation of the Peach Springs Tuff over this expansive area has been based primarily

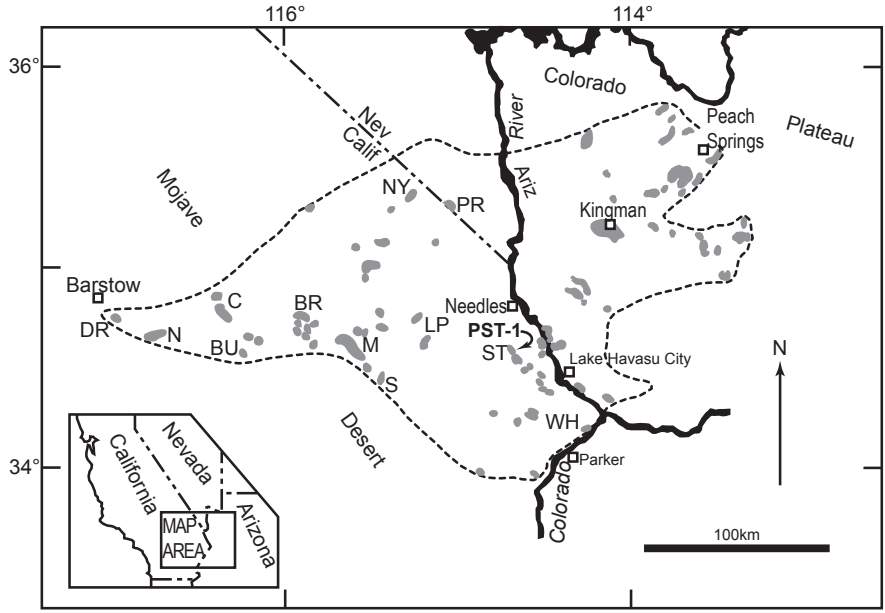

Figure 6. Map showing the distribution of the Peach Springs Tuff (after *Nielson et al.* [1990]). Abbreviations of ranges in California: BR, Bristol Mountains; BU, Bullion Mountains; C, Cady Mountains; DR, Daggett Ridge; LP, Little Piute Mountains; M, Marble Mountains; NY, New York Mountains; PR, Piute Range; S, Ship Mountains; ST, Snaggletooth area; WH, Whipple Mountains. The location of the outcrop from which sample PST-1 was obtained for this study is indicated.

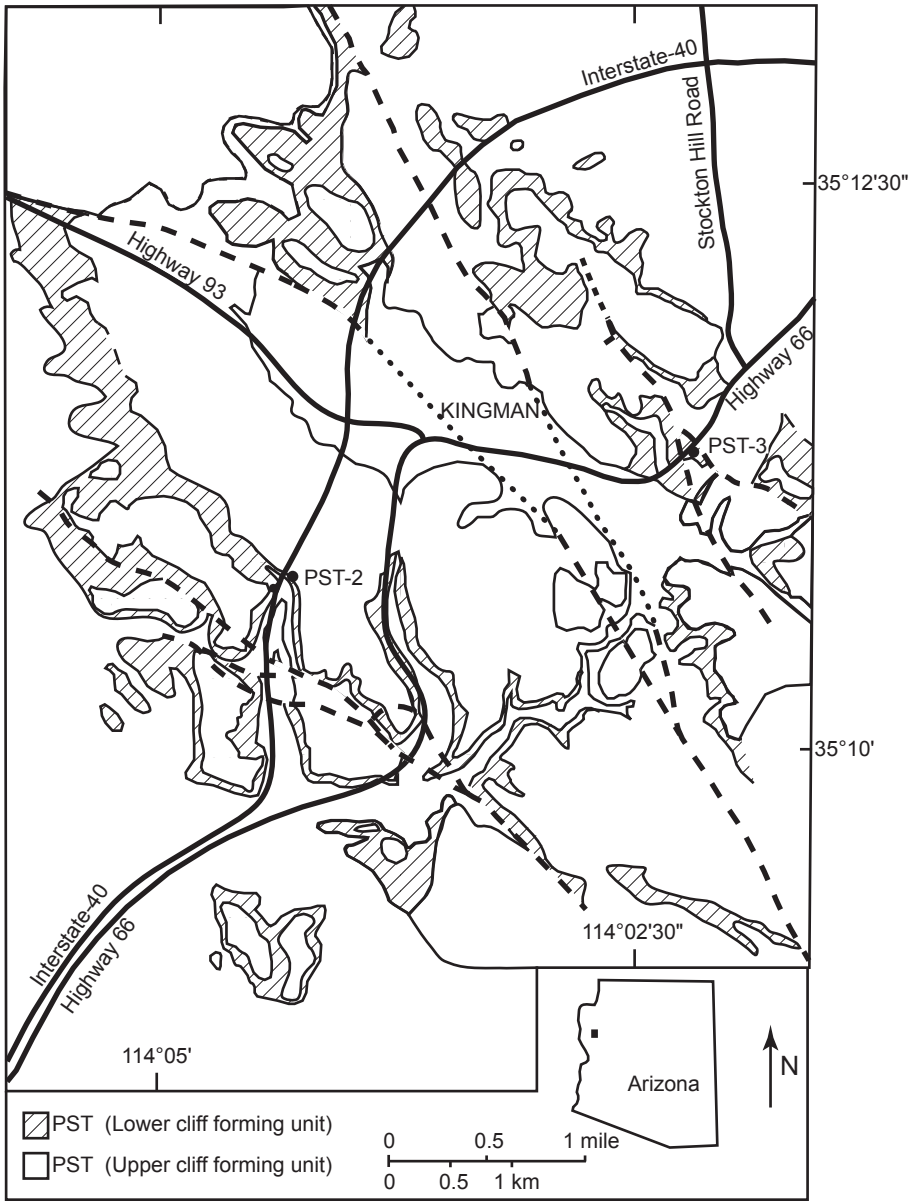

Figure 7. Map of the Kingman area, Arizona, showing the local extent of the Peach Springs Tuff (after *Buesch and Valentine* [1986]). The locations from which samples PST-2 and PST-3 were obtained for this study are indicated.

on field relations, such as its Lower Miocene stratigraphic position, and the phenocryst assemblage, particularly the presence of sphene, which has been confirmed by studies of the heavy mineral suites in the tuff by *Gusa* [1986] and *Gusa et al*. [1987]. Subsequent K-Ar and ^{40}Ar-^{39}Ar radioisotope dating of sanidine phenocrysts from seventeen locations [*Nielson et al*., 1990] has confirmed that the Peach Springs Tuff probably originally covered an area of approximately 35,000 km^2 over a lateral distance of 350 km (Figure 6), representing an erupted volume of volcanic ash of at least several hundred cubic kilometers [*Glazner et al*., 1986].

The Peach Springs Tuff (ignimbrite) exposed near Kingman, Arizona, probably forms a single, simple cooling unit, even though it is exposed as two cliffs [*Buesch and Valentine*, 1986; *Glazner et al*., 1986] (Figure 7). Two types of local facies have been described: (1) an "open valley facies" which occurs where the pyroclastic flow moved through relatively unobstructed valleys; and (2) an "edge facies" which occurs where the pyroclastic flow was affected by valley edges and paleo-topographic highs [*Buesch and Valentine*, 1986]. The open valley facies of the Peach Springs Tuff commonly has two cliff-forming zones, the lowest due to dense welding and the uppermost due to vapor phase crystallization and lithification. The areal extent of these two cliff-forming units in the Kingman area is shown in Figure 7, and the prominent stratigraphic section through the Peach Springs Tuff as exposed in road cuts along U.S. Interstate-40 near Kingman is reproduced in Figure 8. The internal stratigraphy of the Peach Springs Tuff is comparable to the "typical" ignimbrite sequence of *Sparks et al*. [1973], with a basal ground surge layer 1 m or less thick that is thinly laminated, overlain by the massive and very poorly sorted ignimbrite that in places is 70 m or more thick (Figure 8).

Three samples of the Peach Springs Tuff were collected for this study, based on prior knowledge of the presence of zircon in the tuff at those outcrops, on ease of access to, and identification of, well-documented outcrops, and on locations where the tuff has previously been sampled for dating. Details of these three samples are summarized in Table 1. The first sample was collected from the Snaggletooth area

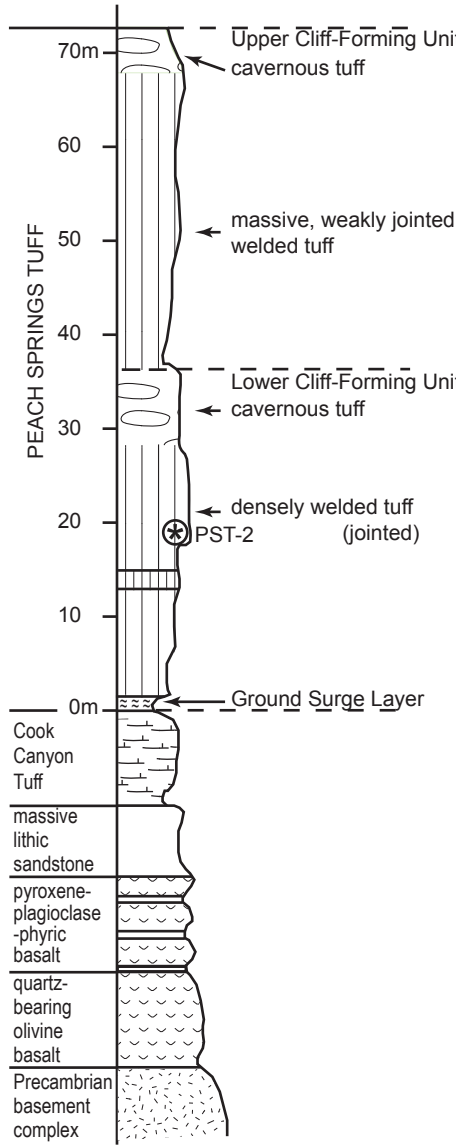

Figure 8. Schematic measured section through the Peach Springs Tuff (open valley facies) along Interstate-40 west of Kingman, Arizona (Figure 7), section 1 of *Beusch and Valentine* [1986], with underlying strata indicated. The stratigraphic position from which PST-2 was obtained for this study is shown.

in southeastern California (see Figure 6), the same outcrop as sample 10 of *Gusa* [1986] and *Gusa et al.* [1987]. The second sample was obtained in the U.S. Interstate-40 road cut near Kingman (Figure 7) that was the location of *Buesch and Valentine's* [1986] Peach Springs Tuff stratigraphic section 1 (Figure 8). The sample was obtained from a densely welded and jointed prominent layer in about the middle of the lower cliff-forming unit of the tuff (Figure 8). This also appears to be the approximate location of sample 1 of *Gusa* [1986] and *Gusa et al.* [1987], and possibly the sample from which sanidine phenocrysts were extracted and yielded a K-Ar date of 17.3±0.4 Ma, as reported by *Young and Brennan* [1974], *Glazner et al.* [1986], and *Nielson et al.* [1990]. Finally, the third sample was obtained from the same position in the same road cut on U.S. Highway 66 just east of downtown Kingman that was sampled for sanidine ^{40}Ar-^{39}Ar dating by *Nielson et al.* [1990], Stop 2 of *Buesch and Valentine* [1986] (Figure 7). Samples 2 and 3 are definitely from the lower cliff-forming unit of the Peach Springs Tuff (Figures 7 and 8), and sample 1 is probably also, given the relative stratigraphic position from which it was obtained from the outcrop of the tuff in the Snaggletooth area. In any case, given that the Peach Springs Tuff was erupted and deposited as a single cooling unit over an area of at least 35,000 km^2 in a period of days to weeks [*Glazner et al.*, 1986; *Nielson et al.*, 1990], sampling anywhere in the tuff at any stratigraphic level should yield the same age.

5. Analytical Procedures

The 3–5 kg tuff samples from each of these locations were sent to the Geotrack International laboratory in Melbourne, Australia. That laboratory was chosen because it specializes in fission track dating, its principal scientific staff having decades of experience in performing fission track analyses and in fission track research. At this laboratory the samples were reduced to chips of a few mm in size in a jaw crusher, and this material was then ground to sand grade in a rotary disc mill. The ground material was then washed to remove dust, dried, and processed by conventional heavy liquid and magnetic separation techniques to

recover the heavy minerals as separate fractions of zircon, sphene (titanite), and apatite.

The zircon grains from each sample were embedded in FEP teflon between heated microscope slides on a hot plate at ~350°C. The short time needed for this process, during which the zircon grains were subjected to this temperature, would not have allowed any annealing of fission tracks in the grains. The mounted grains were then ground and polished on diamond laps, and then etched in molten KOH:NaOH eutectic at 220°C [*Gleadow et al*., 1976]. Satisfactory etching of the spontaneous fission tracks in the zircons from each of the samples was achieved after etching for different lengths of time—15 hours for samples MT-2, TT-1, NMF-49 and NMF-64, 17.5 hours for sample MT-3, 43 hours for sample BMF-14, 47 hours for samples PST-1 and PST-3, 67 hours for samples BMF-28, MMF-1 and MMF-4, and 91 hours for sample PST-2. The longer time periods required on some samples potentially reflected their younger ages (and consequently lower degrees of radiation damage). Subsequent examination of the grain mounts showed that extremely high quality etched grains suitable for age determinations were present in all samples.

After etching, grain mounts were cut down to 1.5 × 1 cm, and cleaned in detergent, alcohol, and distilled water. The mounts were then sealed in intimate contact with low-U muscovite detectors within heat shrink plastic film, and then stacked between two pieces of U standard glass which had been prepared in similar fashion. The stack was then inserted into an aluminum can for irradiation.

Neutron irradiations were carried out in a well-thermalized flux (X-7 facility; Cd ratio for Au ~98) in the Australian Nuclear Science and Technology Organisation's HIFAR research reactor at Lucas Heights near Sydney. The total neutron fluence was monitored by counting the induced fission tracks in the mica external detectors attached to the two pieces of corning standard glass U3 included in the irradiation canisters at each end of the sample stack. A small flux gradient has often been present in the irradiation facility over the length of the sample package, this having developed only in late 1991 after extended refurbishment of the reactor. As a detectable gradient was found to be present, the

track count in the external detector adjacent to each standard glass was converted to a track density ρ_D and a value for each mount in the stack was calculated by linear interpolation. (If no detectable gradient had been present, the track counts in the two external detectors would have been pooled to give a single value ρ_D which would then have been used to calculate the fission track ages for each of the samples.)

After irradiation, the mica detectors were removed from the grain mounts and standard glasses and etched in hydrofluoric acid to reveal the fission tracks produced by the induced fission of ^{235}U within the zircon grains and the standard glass. In determining the induced track densities in the external mica detectors irradiated adjacent to the U standard glasses, twenty-five fields were normally counted in each detector, and the total track count N_D was divided by the total area counted to obtain the track density ρ_D. The positions of the counted fields are arranged in a 5×5 grid covering the whole area of the detector. For typical track densities of between $\sim 5 \times 10^5$ and 5×10^6 this is a convenient arrangement to sample across the detector while gathering sufficient counts to achieve a precision of approximately ±2% in a reasonable time.

The fission track ages were calculated using the standard fission track age equation and the ζ calibration method (equation 5 of *Hurford and Green* [1983]):

$$\textit{Fission track age} = \frac{1}{\lambda_D} \ln\left[1 + \left(\frac{\zeta \lambda_D \rho_S g \rho_D}{\rho_i}\right)\right] \qquad (1)$$

where: λ_D = total decay constant of ^{238}U (1.55125×10^{-10})
ζ = zeta calibration factor
ρ_s = spontaneous track density
ρ_i = induced track density
ρ_D = track density for U standard glass
g = a geometry factor (0.5)

Fission track ages were thus determined by the external detector method [*Gleadow*, 1981] (see the Appendix, Section A2). This method has the advantage of allowing fission track ages to be determined on single grains. For the analyses of the zircon grains in the samples in this

study, twenty zircon grains for each sample were normally analyzed. In those samples where the desired number of grains was not present, all available grains were counted, the actual number depending on the availability of suitably etched and oriented grains. Only zircon grains oriented with surfaces parallel to the crystallographic c-axis were analyzed. Such grains could be identified on the basis of their etching characteristics, as well as from morphological evidence in euhedral grains. The grain mounts were scanned sequentially, and the first twenty suitably oriented grains identified were analyzed.

All track counting was carried out by Dr. Paul Green using Zeiss® axioplan microscopes, with an overall linear magnification of 1068× using dry objectives. All tracks were counted with an eyepiece graticule divided into one hundred grid squares. In each grain, the number of spontaneous tracks, N_s, within a certain number of grid squares, N_a, was recorded. The number of induced tracks, N_i, in the corresponding location within the mica external detector was then counted. Spontaneous and induced track densities, ρ_s and ρ_i respectively, were calculated by dividing the track counts by the total area counted, given by the product of N_a and the area of each grid square (determined by calibration against a ruled stage graticule or diffraction grating). The fission track age of each zircon grain could then be calculated by substituting the track counts N_s and N_i for track densities ρ_s and ρ_i in equation (1), since the areas (N_a) cancel in the ratio.

Translation between zircon grains in each grain mount and the external detector locations corresponding to each grain was carried out using Autoscan™ microcomputer-controlled automatic stages [*Smith and Leigh-Jones*, 1985]. This system allowed repeated movement between each grain and detector, and all grain locations were stored for later reference if required.

The zeta calibration factor, ζ, had previously been determined empirically for zircon by analyzing a set of carefully chosen age standards with independently determined K-Ar radioisotope ages, following the methods outlined by *Hurford and Green* [1983] and *Green* [1985] (see the Appendix, Section A4). The zeta calibration factor used by Dr. Paul Green to calculate the fission track ages of the zircons in

the samples in this study was 87.7±0.8 for the U3 glass standard used. Further details and background information on the practical aspects of fission track age determinations can be found in *Fleischer et al*. [1975] and *Naeser* [1979].

6. Zircon Fission Track Dating Results

All samples yielded sufficient zircon grains for fission track age determinations to be obtained. Whereas around twenty grains from each sample were analyzed, sample NMF-49 only yielded nine suitable grains, but these were still deemed sufficient to provide a good fission track age estimate. Representative zircon grains from some of the samples are shown in Figure 9. *Green* [2001, 2002, 2003] reported that all analyzed grains were characterized by very high quality, well-etched surfaces suitable for analysis. In two other samples, BMF-28 and MMF-4, slightly fewer grains were analyzed due to the abundance in those samples of grains with highly zoned, non-uniform track densities and inclusions or other defects which rendered reliable track counting impossible. Otherwise, spontaneous track densities were typically in the range 2×10^6 to 3×10^7 tracks/cm^2, allowing reliable track counting. Typical fission tracks in the polished and etched surfaces of some of the zircon grains are shown in the photomicrographs of Figure 10.

Nevertheless, the etching process was highly selective, and so a large number of grains with higher and lower track densities were also present which couldn't be analyzed. At track densities higher than $\sim 3 \times 10^7$ tracks/cm^2, individual tracks cannot be resolved, while at track densities lower than $\sim 5 \times 10^5$ tracks/cm^2, etching becomes anisotropic and full track revelation is not possible. This would have the potential to severely bias the distribution of measured ages, so such grains were not used for the age determinations. However, the zircon grains in these samples are typical of zircon suites that show a sufficiently large range of U contents so that the zircons of whatever ages provide enough grains with spontaneous track densities suitable for track counting. Because of these factors, all the reported fission track age determinations on these samples were regarded as extremely reliable.

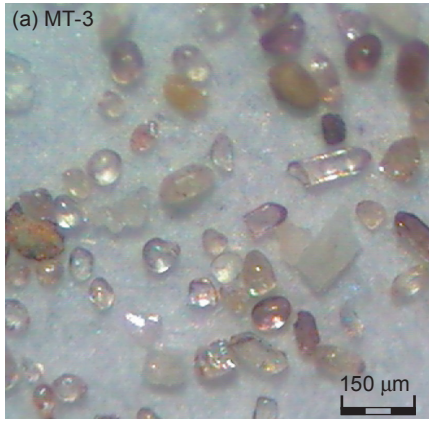
(a) MT-3
150 µm

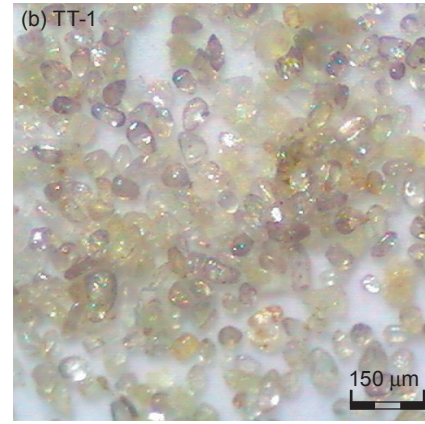
(b) TT-1
150 µm

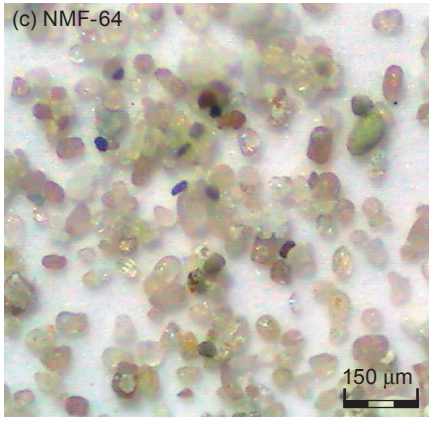
(c) NMF-64
150 µm

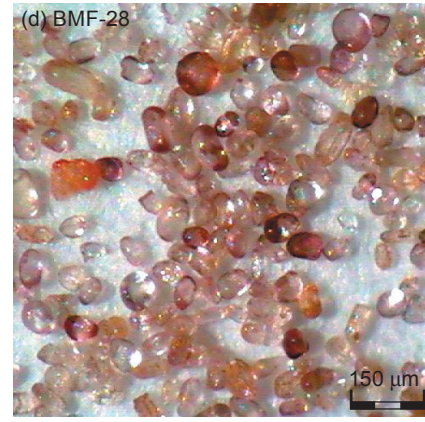
(d) BMF-28
150 µm

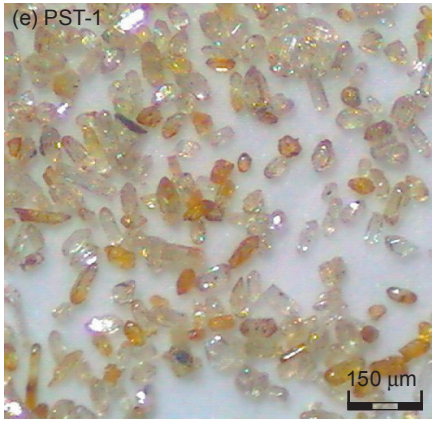
(e) PST-1
150 µm

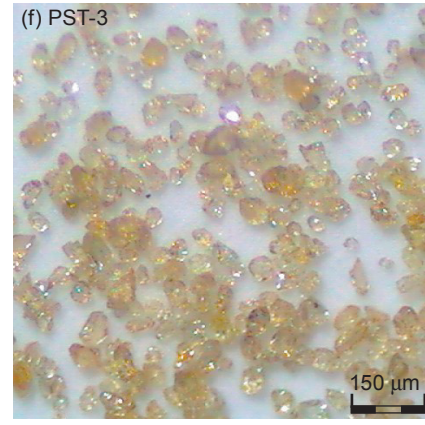
(f) PST-3
150 µm

Figure 9 (left). Some of the zircon grains from six of the tuff samples in this study: (a) MT-3, (b) TT-1, (c) NMF-64, (d) BMF-28, (e) PST-1, and (f) PST-3. For details of these samples see Table 1. The photographs were obtained under a binocular microscope, courtesy of Pat Kelly, Operations Manager, Geotrack International.

All twelve samples listed in Table 1, with details of outcrop locations and previous dating results, were processed at the Geotrack International laboratory and the zircon fission track ages determined were reported by *Green* [2001, 2002, 2003]. All results are summarized in Table 2, while the data and age determinations for all individual zircon grains analyzed in each sample are tabulated in *Green* [2001, 2002, 2003].

All the individual zircon grain fission track ages were calculated, as indicated previously, using the standard fission track age equation of *Hurford and Green* [1983], equation (1) above. The zeta (ζ) calibration factor used was 87.7±0.8 for the U3 standard glass as determined empirically by *Green* [1985] by direct comparison with K-Ar radioisotope ages for a set of carefully chosen age standards, following the methods outlined by *Hurford and Green* [1982, 1983]. Individual grain fission track ages were calculated from the ratio of the number of spontaneous fission tracks (N_s) to the number of induced fission tracks (N_s) counted for each grain, and the errors in the single grain ages were calculated using Poissonian statistics, as explained in more detail by *Galbraith* [1981] and *Green* [1981]. All errors are quoted as ±1σ. The pooled or maximum probability age for each sample was determined from the ratio of the total spontaneous and induced track counts (N_S/N_i) in all analyzed grains within each sample (Table 2). Errors for each pooled age were calculated using the "conventional" technique outlined by *Green* [1981], based on the total number of tracks counted for each track density measurement of all the analyzed grains for each sample.

The variability of fission track ages between individual zircon grains within each sample was assessed using a chi-square (χ^2) statistic [*Galbraith*, 1981], the results of which are summarized for each sample in Table 2. If all the grains counted in each sample belong to a single age population, then the probability of obtaining the observed χ^2 value,

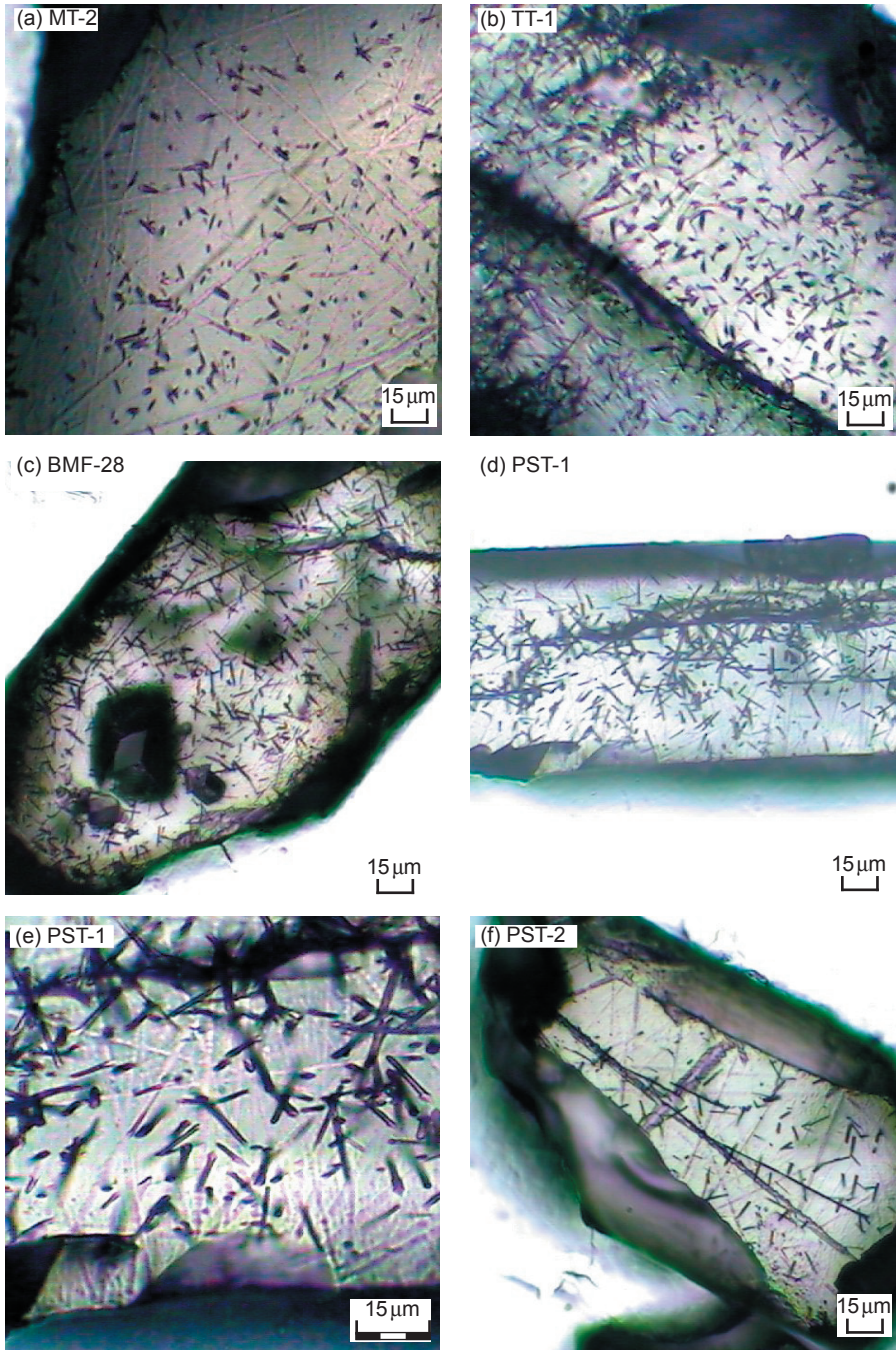
(a) MT-2
15 µm
(b) TT-1
15 µm
(c) BMF-28
15 µm
(d) PST-1
15 µm
(e) PST-1
15 µm
(f) PST-2
15 µm

Figure 10 (left). The spontaneous fission tracks in the polished and etched surfaces of some of the mounted zircon grains in five of the tuff samples in this study: (a) MT-2, (b) TT-1, (c) BMF-28, (d) PST-1, (e) PST-1 (high magnification), and (f) PST-2. Sample details are in Table 1. These photomicrographs were obtained courtesy of Pat Kelly, Operations Manager, Geotrack International.

for v degrees of freedom (where v = number of crystals – 1) is listed in Table 2, and in the data sheets for all the grains analyzed in each sample supplied by *Green* [2001, 2002, 2003], as $P(\chi^2)$.

A probability of greater than 5% can be taken as evidence that all grains are consistent with a single population of fission track ages for that sample. In that case, the best estimate of the fission track age of the sample is given by the "pooled age," calculated from the ratio of the total spontaneous and induced track counts (N_s/N_i) in all the grains analyzed in the sample. Errors for the pooled age are calculated using the "conventional" technique outlined by *Green* [1981], based on the total number of tracks counted for each track density measurement (see also *Galbraith* [1981]).

A $P(\chi^2)$ value of less than 5% denotes a significant spread of single grain ages in the sample, and suggests that real differences exist between the fission track ages of the individual zircon grains. A significant spread in grain ages can result either from inheritance of detrital grains from mixed source areas, or from differential annealing in zircon grains of different composition, within a certain range of temperature.

Calculation of the pooled age inherently assumes that only a single population of ages is present, and is thus not appropriate for samples containing a significant spread of individual grain fission track ages. In such cases, *Galbraith* [1981, 1984] has devised a means of estimating the modal age of a distribution of single grain fission track ages in a sample which is referred to as the "central age" of the sample. Calculation of the central age assumes that all single grain ages belong to a normal distribution of ages with a standard deviation, σ, known as the "age dispersion." An iterative algorithm, as yet unpublished [*Green*, 2001, 2002, 2003], is used to provide estimates of the central age with its

RATE Sample No.	Number of Grains	ρ_D (N_D) x 10^6 per cm^2	ρ_S (N_S) x 10^6 per cm^2	ρ_i (N_i) x 10^6 per cm^2	U content (ppm)	P (χ^2) (%)	Age Dispersion (%)	Fission Track Ages (Ma) (±1σ)			Age Spread (Ma) (±1σ)	
								Pooled Age	Central Age	Youngest Group (Pooled) Age	From	To
MT-3	23	1.208 (3684)	11.575 (4050)	4.053 (1418)	179	<1	57	149.6 ± 5.4	165.8 ± 20.7	**74.6 ± 3.9**	68.4 ± 8.3	473.5 ± 150.5
MT-2	20	0.585 (1866)	10.156 (3643)	1.650 (592)	150	<1	75	155.9 ± 7.9	139.0 ± 24.5	**62 ± 4**	34.9 ± 7.2	611.2 ± 254.9
TT-1	20	0.586 (1866)	10.307 (4547)	2.079 (917)	189	<1	105	126.3 ± 5.5	127.4 ± 30.5	**75 ± 7**	48.0 ± 14.9 (12.3 ± 1.2)	914.3 ± 414.8
NMF-64	20	0.590 (1866)	10.329 (3029)	1.419 (416)	128	<1	42	185.6 ± 10.7	178.6 ± 19.8	**132 ± 10**	93.1 ± 18.7	651.3 ± 210.4
NMF-49	9	0.588 (1866)	11.590 (671)	1.606 (93)	146	15	19	**183.4 ± 20.8**	178.7 ± 23.4	—	113.6 ± 42.0	343.1 ± 145.4
BMF-28	19	1.717 (2763)	6.301 (3101)	2.625 (1292)	81	<1	39	178.2 ± 7.0	173.7 ± 17.1	**136 ± 6**	104.2 ± 22.3	592.3 ± 137.4
BMF-14	20	1.706 (2763)	7.611 (2069)	2.954 (803)	92	<1	40	189.9 ± 8.9	188.3 ± 19.2	**144 ± 10***	98.2 ± 16.7	689.9 ± 187.6
MMF-1	20	1.728 (2763)	9.688 (2841)	3.318 (973)	102	<1	45	217.6 ± 9.3	205.1 ± 22.4	**137 ± 9**	87.6 ± 15.4	1036.2 ± 309.8
MMF-4	18	1.739 (2763)	7.697 (1671)	3.901 (847)	120	7	12	**148.8 ± 7.0**	148.2 ± 8.3	—	114.6 ± 18.6	233.5 ± 46.3
PST-1	20	0.591 (1866)	1.779 (1172)	1.871 (1233)	169	14	10	**24.6 ± 1.2**	24.5 ± 1.3	—	17.0 ± 4.6	34.5 ± 15.2
PST-2	20	0.580 (1803)	2.183 (1470)	2.658 (1790)	244	33	4	**20.9 ± 0.9**	20.9 ± 0.9	—	16.4 ± 3.7	27.3 ± 5.2
PST-3	20	0.593 (1866)	2.885 (1921)	3.591 (2391)	323	70	1	**20.9 ± 0.8**	20.9 ± 0.8	—	17.3 ± 2.2	29.3 ± 4.9

Notes: *12 euhedral grains yield a pooled age of 147.8±8.2 Ma.
ρ_S = spontaneous track density; ρ_i = induced track density; ρ_D = track density in external detector.
Brackets show number (N) of tracks counted – ρ_D and ρ_i measured in external detector; ρ_S measured in internal sample surfaces.
The "fission track" ages in **bold** were interpreted as the best estimates (statistically defendable) of the ages of the samples.
Ages were calculated using dosimeter glass U3, with a zeta (ζ) of 87.7±0.8 for all samples.
All samples were analyzed by Dr. Paul F. Green of Geotrack International, Melbourne.

Table 2 (left). Results of the zircon fission track dating of twelve tuff samples from the Grand Canyon-Colorado Plateau region. Counting data, statistics and calculated ages are shown. Full details discussed in the text.

associated error, and the age dispersion, which are all quoted for each sample in Table 2, and for all the single grain data in the laboratory reports. This treatment replaces use of the "mean age," which has often been used in the past for those samples in which $P(\chi^2) < 5\%$. For samples in which $P(\chi^2) > 5\%$, the central age and the pooled age should be equal, and the age dispersion should be less than ~10%, as is the case for the relevant samples listed in Table 2.

However, single grain fission track age data for each sample are best represented in the form of radial plot diagrams [*Galbraith*, 1988, 1990]. As illustrated in Figure 11, these plots display the variation of individual grain ages in a plot of y against x, where:

$$y = (z_j - z_o) / \sigma_j \tag{2}$$

$$x = 1 / \sigma_j \tag{3}$$

and z_j = the fission track age of grain j
z_o = a reference fission track age
σ_j = the standard error in age for grain j
y_j = the standardized estimates
x_j = the precision

In this plot, all points on a radial straight line emanating from the origin (since each such line has a slope $z_j - z_o$) define a single fixed value of fission track age (z_j), and at any point along the line the value of x is a measure of the precision of each individual grain fission track age. Therefore, precise individual grain fission track ages fall to the right on the plot (small error, high x or precision) (Figure 12a), which is useful, for example, in enabling precise, young grains to be identified. Error bars on all points plotted on the diagram are the same size. The age scale is shown radially around the perimeter of the plot (in Ma). If all

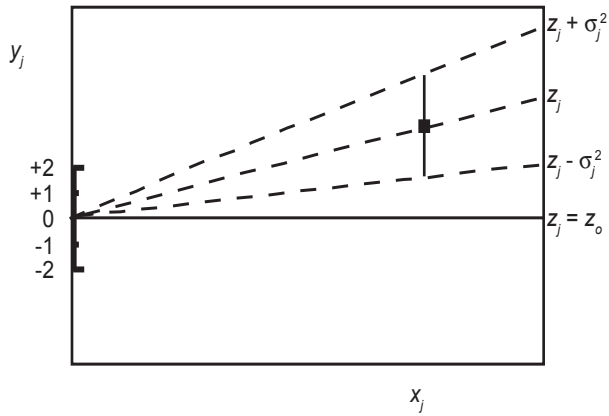

Figure 11. Basic construction of a normal radial plot (after *Galbraith* [1988, 1990]). Radial lines emanating from the origin with positive slopes correspond to fission track ages (z_j) greater than the reference age (z_o), while lines with negative slopes correspond to fission track ages less than the reference age. x_j is the precision and y_j the standardized estimate of the fission track age of grain *j*.

grains plotted on the diagram belong to a single age population, all data should scatter between $y = +2$ and $y = -2$, equivalent to a scatter within $\pm 2\sigma$. Scatter outside these boundaries would show a significant spread of individual grain ages, as also would be reflected in the values of $P(\chi^2)$ and age dispersion.

In detail, rather than using the fission track age for each grain as in equations (2) and (3), it is preferable to use the measured counts of the spontaneous and induced fission tracks in each grain so that:

$$z_j = \frac{N_{sj}}{N_{ij}} \tag{4}$$

and

$$\sigma_j = \left(\frac{1}{N_{sj}}\right) + \left(\frac{1}{N_{ij}}\right) \tag{5}$$

as the objective is to display the scatter **within** the individual grain fission track data from each sample in comparison with that allowed by the Poissonian uncertainty in the track counts, within the additional

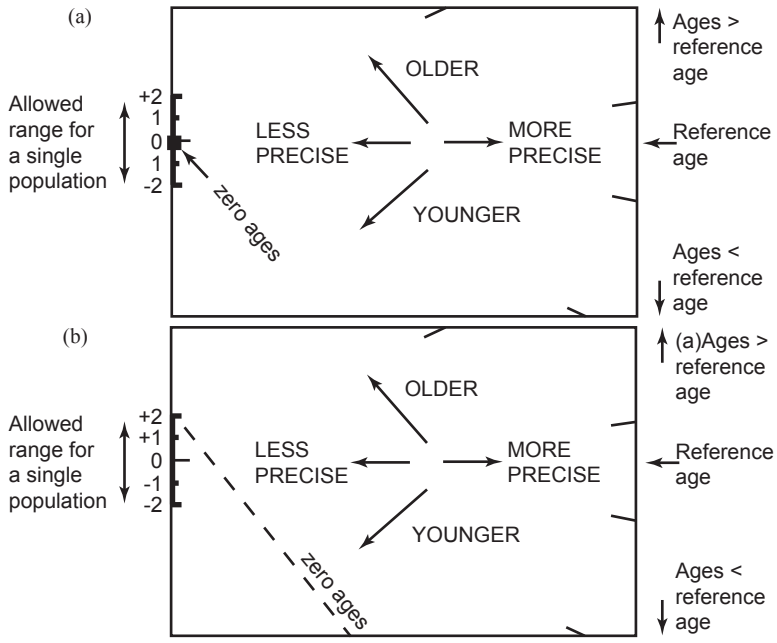

Figure 12. (a). Simplified structure of a normal radial plot (after *Galbraith* [1988]). Zero ages plot at the origin. The allowed range in y is in units of σ. (b). Simplified structure of an arc sin radial plot (after *Galbraith* [1990]). Zero ages plot along the dashed sloping line. The allowed range in y is in units of σ.

terms which are involved in determination of the fission track ages (ρ_D, ζ, etc.).

Zero ages cannot be displayed in such a plot (Figure 12a). This can be achieved using a modified plot [*Galbraith*, 1990], in which:

$$z_j = \text{arc sin} \sqrt{\left(\frac{N_{sj} + 3/8}{N_{sj} + N_{ij} + 3/4} \right)} \tag{6}$$

and

$$\sigma_j = \tfrac{1}{2} \sqrt{\left(\frac{1}{N_{sj} + N_{ij}} \right)} \tag{7}$$

Note that the numerical terms in equation (6) for z_j are standard terms,

introduced for statistical reasons. Using this arc-sin transformation, zero ages plot on a diagonal line which slopes from upper left to lower right (Figure 12b). Note that this zero ages line does not go through the origin. Figure 12 illustrates the difference between the conventional and arc-sin radial plots, and also provides a simple guide to the structure of these radial plots.

Use of arc-sin radial plots is particularly useful in assessing the relative importance of zero ages. For instance, grains with $N_s = 0$, $N_i = 1$ are compatible with ages up to ~900 Ma (at the 95% confidence level), whereas grains with $N_s = 0$, $N_i = 50$ are only compatible with ages up to ~14 Ma. These two data would readily be distinguishable on the radial plot, as the 0, 50 datum would plot well to the right (high x) compared to the 0, 1 datum.

Note that the x-axis of the radial plot is normally not labeled, as this would obscure the age scale around the plot. In general labeling is not considered necessary, as the focus is only on the relative variation within the data, rather than the absolute values of precision.

In this study the value of z corresponding to the pooled ($P(\chi^2)>5\%$) or central ($P(\chi^2)<5\%$) fission track age of each sample was adopted as the reference age, z_o. In Figures 13, 14 and 15 are the radial plots of the single grain fission track age data for the zircon grains analyzed in each sample, and alongside are conventional histogram plots of the number of grains which fall within a given fission track age range, another way of showing the spread and distribution of the individual zircon grain fission track ages within each sample. In Figure 13 are radial plots and histograms for the Cambrian Muav and Tapeats tuffs samples from the western Grand Canyon, in Figure 14 are the radial plots and histograms for the Jurassic Morrison Formation tuffs from Notom, the Brushy Basin and Montezuma Creek, Utah, and Figure 15 shows the radial plots and histograms for the three Miocene Peach Springs Tuff samples.

7. Discussion of Results

The results obtained in this study were discussed in detail by *Green*

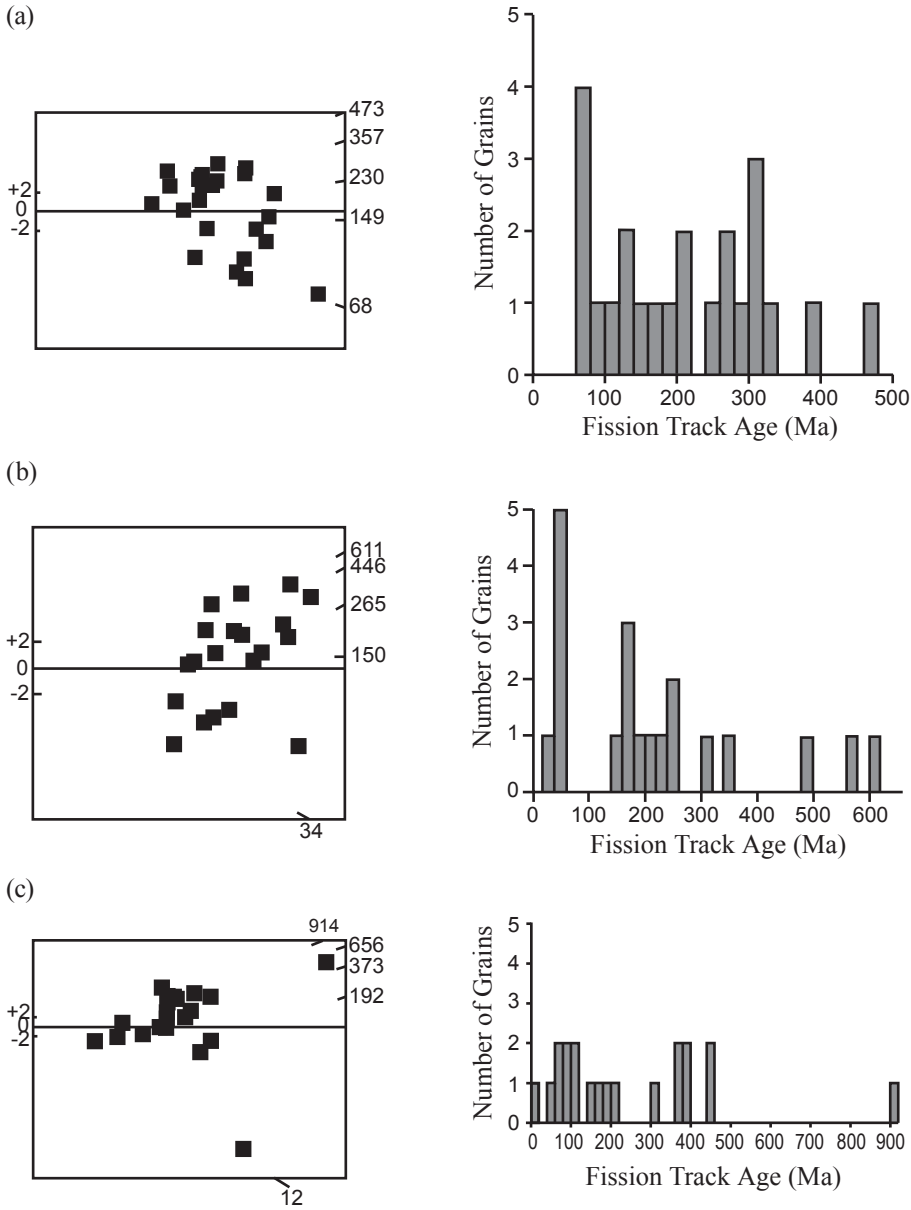

Figure 13. Radial plots (left) and histograms (right) of the individual zircon grain fission track ages in the early Middle Cambrian tuff samples from the western Grand Canyon: (a) Muav tuff MT-3, (b) Muav tuff MT-2, and (c) Tapeats tuff TT-1.

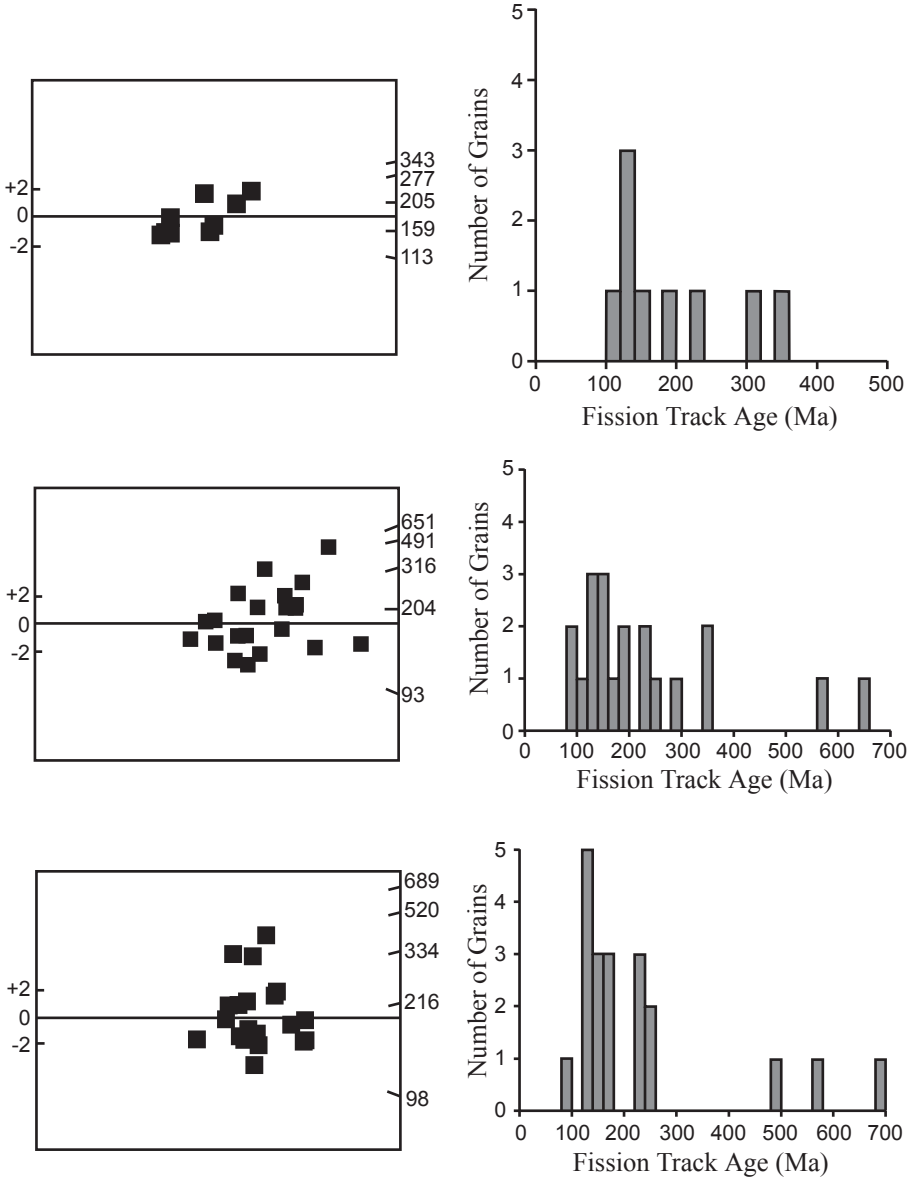

Figure 14. Radial plots (left) and histograms (right) of the individual zircon fission track ages in the Upper Jurassic Morrison Formation tuff samples from southeastern Utah: Notom tuffs (a) NMF-49, (b) NMF-64; Brushy Basin tuff (c) BMF-14.

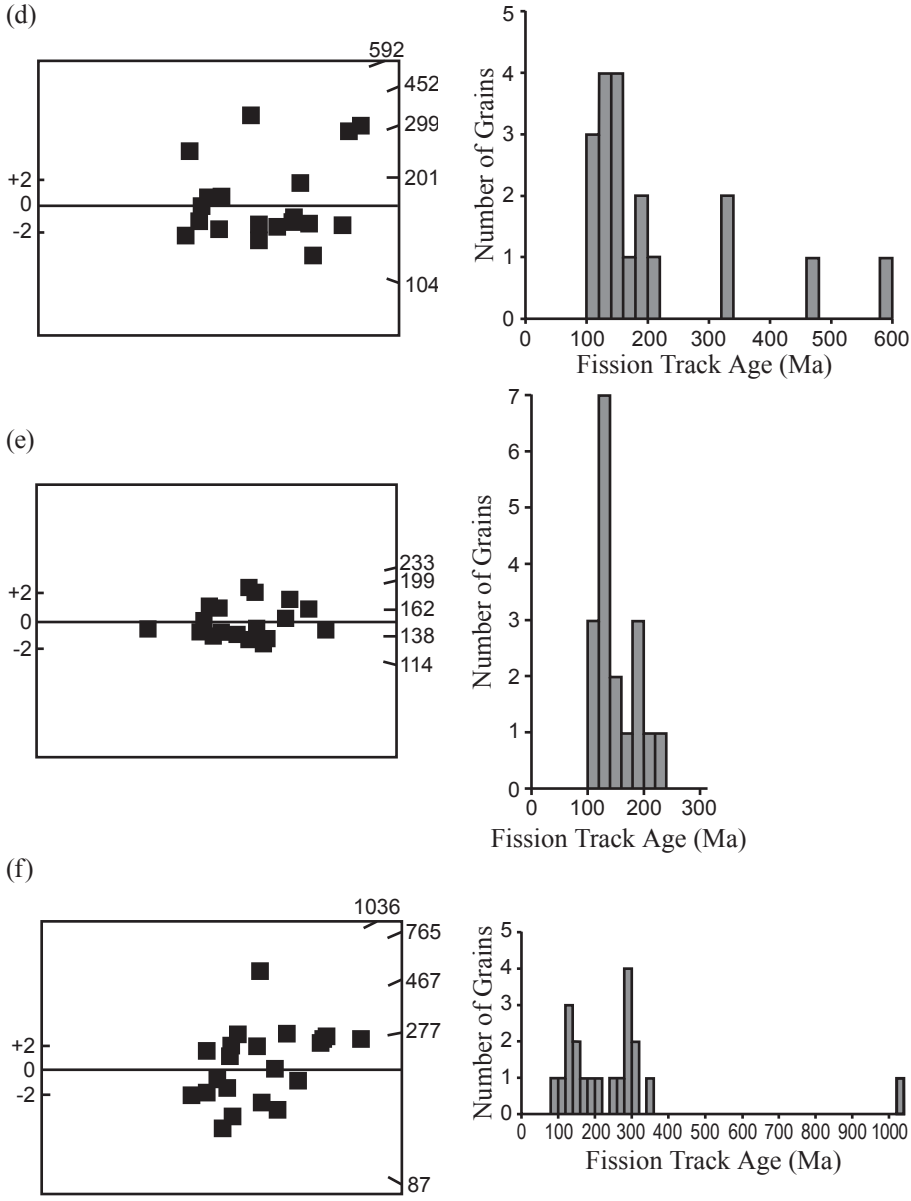

Figure 14 (continued). Radial plots (left) and histograms (right) of the individual zircon fission track ages in the Upper Jurassic Morrison Formation tuff samples from southeastern Utah: Brushy Basin tuff (d) BMF-28; and Montezuma Creek tuffs (e) MMF-4, (f) MMF-1.

(a)

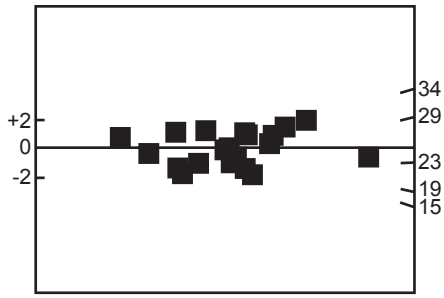
+2
0
-2
34
29
23
19
15

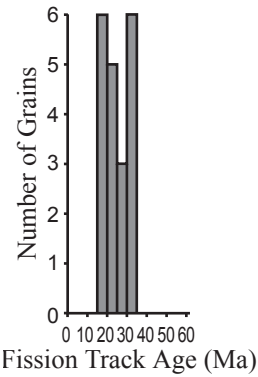
Number of Grains
0 1 2 3 4 5 6
0 10 20 30 40 50 60
Fission Track Age (Ma)

(b)

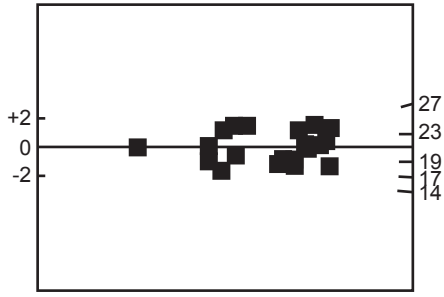
+2
0
-2
27
23
19
17
14

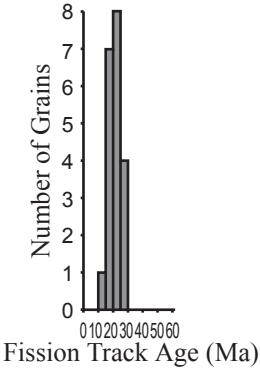
Number of Grains
0 1 2 3 4 5 6 7 8
0 10 20 30 40 50 60
Fission Track Age (Ma)

(c)

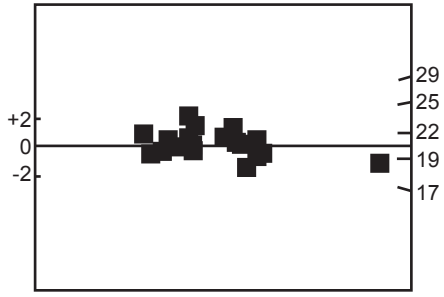
+2
0
-2
29
25
22
19
17

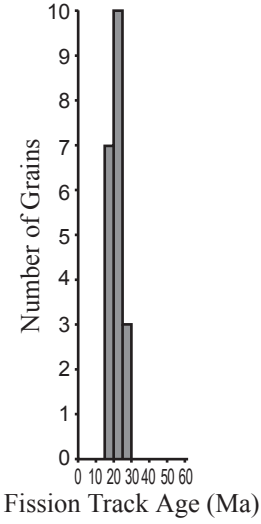
Number of Grains
0 1 2 3 4 5 6 7 8 9 10
0 10 20 30 40 50 60
Fission Track Age (Ma)

Figure 15 (left). Radial plots (left) and histograms (right) of the individual zircon grain fission track ages in the Miocene Peach Springs Tuff samples from southeastern California and western Arizona: (a) PST-1, (b) PST-2, and (c) PST-3.

[2001, 2002, 2003]. It should be noted that when the samples were submitted to the Geotrack International laboratory no specific location data for the samples were supplied, although some indication was given of the expected age of each sample. This procedure was adopted so that on the one hand the laboratory could optimize its analytical procedures, and yet on the other hand no bias would be introduced by the laboratory to obtain the ages required by prior knowledge of other age dating results on those sampled rock units. The discussion here is based on the information and results in Tables 1 and 2 respectively, and on the radial plots and histograms in Figures 13–15.

7.1 Cambrian Tuff Units, Western Grand Canyon, Arizona

It is immediately evident that the zircon fission track ages obtained in this study for the Muav and Tapeats tuffs from the western Grand Canyon did not match the early Middle Cambrian biostratigraphic ages [*McKee and Resser*, 1945] or reproduce the previously obtained zircon fission track ages of 535±48 Ma and 563±49 Ma respectively [*Naeser et al*., 1989a]. Only three of the sixty-three individual zircon grain fission track ages were close to the target early Middle Cambrian ages for these two tuff units, and even then the 1σ errors are exceedingly large (Table 2 and Figure 13).

The individual zircon grains in Muav tuff sample MT-3 show a statistically significant spread in fission track ages ($P(\chi^2)<5\%$), from a youngest limit of 68.4±8.3 Ma to an oldest limit of 473.5±150.5 Ma (all errors are quoted at the ±1σ level). A variety of grain morphologies were reported by *Green* [2001] to be present within the sample, from euhedral to rounded as well as intermediate forms. As the minerals in a cooling lava form they crystallize as euhedral grains. If the lava is then shattered by the volcanic eruption to produce ash, some of the grains will be abraded during their transport before deposition in the

resultant tuff bed. The degree of rounding of the grains will usually be an indication of how much abrasion and transport they have suffered. Another possibility is that rounded grains might represent grains that were eroded from other rocks (and thus inherited) as the volcanic ash was transported over them before deposition. The youngest group of ages within this sample were measured consistently only in euhedral grains (five in number), and these collectively define a pooled fission track age of 74.6±3.9 Ma (Table 2). The older ages were measured in grains having a variety of forms, including both euhedral and rounded grains as well as intermediate forms. No other distinct groupings are discernible within these older ages, as reflected by the radial plot of the single grain ages (Figure 13a), except that perhaps the histogram could indicate a grouping around 300 Ma.

The second sample of the Muav tuff (MT-2) is characterized by a central age of 139.0±24.5 Ma (Table 2). However, the individual zircon grains show a spread in fission track ages ($P(\chi^2)<5\%$) from 34.9±7.2 Ma to 611.2±254.9 Ma. Thus the numerical value of the central age has no significance other than characterizing the spread of ages within the sample. On the other hand, statistical analysis of the single grain ages [*Green*, 2002] suggests the presence of three dominant populations characterized by ages of 62±4 Ma, 200±15 Ma, and 432±66 Ma. However, the relevant histogram in Figure 13b, while justifying the existence of the two younger age groupings, does not support the oldest age grouping due to the large spread in the ages of the five grains represented. *Green* [2002] reported a variety of grain morphologies were present within this sample, from euhedral to rounded as well as intermediate forms, similar to sample MT-3 from the same outcrop (as would be expected). The youngest group of fission track ages were measured consistently only in euhedral grains (six in number), and these yielded the pooled age of 62±4 Ma. However, some grains belonging to the intermediate age group were also euhedral in form (three grains), while other grains in this group and all grains in the older age group showed rounded to sub-rounded forms.

The sample of the Tapeats tuff (TT-1) is characterized by a central age of 127.4±30.5 Ma. However, the individual zircon grains have fission track

ages from 12.3±1.2 Ma to 914.3±414.8 Ma, so the numerical value of the central age again has no significance. The youngest single grain fission track age measured in this sample (12.3±1.2 Ma) is distinctly younger than all other grains, and stands out prominently in the radial plot of single grain data in Figure 13c. Disregarding this grain, a statistical analysis of the remaining single grain fission track ages [*Green*, 2002] suggests the presence of three prominent populations characterized by ages of 75±7 Ma, 158±15 Ma, and 408±35 Ma. The existence of these three age groupings is justified from the relevant histogram in Figure 13c. *Green* [2002] reported a variety of grain morphologies were present within this sample, from euhedral to rounded as well as intermediate forms (which is similar to the samples from the Muav tuff). Four of the five grains comprising the youngest group of fission track ages were euhedral in form, while the fifth was sub-euhedral. Four grains belonging to the intermediate age group were also euhedral in form, and one of the older group was also euhedral. Other grains in the intermediate and oldest groups showed rounded to sub-rounded forms.

In summary, these three samples from the early Middle Cambrian Muav and Tapeats tuffs contain identical groups of euhedral grains within the youngest fission track pooled ages in the range 62–75 Ma, with all but two of the remaining forty-seven single grain fission track ages spread out up to the published 535–563 Ma zircon fission track ages for these tuffs [*Naeser et al*., 1989a]. This raises the obvious question as to why these samples from the same outcrops did not yield identical zircon fission track ages?

It is abundantly clear from the pattern of spread of the single grain fission track ages that an event at 62–75 Ma, recorded by the pooled single zircon grain fission track ages in the youngest age group in each of the samples, resulted in annealing of many of the zircon grains in these tuff units. Indeed, *Naeser et al*. [1989a] had found that apatite grains in Precambrian granitic rocks in the central and western Grand Canyon had been totally annealed by the onset of the Laramide uplift of the Colorado Plateau. The average fission track age for four apatite concentrates of the Proterozoic basement at Phantom Ranch was

62.4±5.2 Ma (±2σ). The identities of these samples in this study were thus revealed to Dr. Paul Green at Geotrack International, because his zircon fission track age determinations on the Grand Canyon tuff samples in this study were so different from the earlier results of fission track dating of samples from the same outcrops by *Naeser et al.* [1989a]. He responded with the comment:

> I can only understand these results in terms of the zircon fission track ages having been similarly reset as a result either of burial prior to the onset of Laramide uplift of the Colorado Plateau, or of igneous intrusions in the area, or a combination of both … this timing fits very well indeed with the youngest zircon ages in the three samples analyzed. I am surprised that those samples have been sufficiently hot to cause resetting of the zircon ages, which I would normally expect to require around 250 to 300°C. But we do have evidence to suggest that some zircons are more easily reset than others, so it's not totally unexpected [*Green*, personal communication, 27 March, 2003].

However, this interpretation of the zircon fission track ages obtained for the three tuff samples in this study appears to be at variance with the conclusion reached by *Naeser et al.* [1989a]. They concluded that fission track ages of ~1000 Ma obtained from zircons from Proterozoic rocks now exposed at river level indicate that those rocks have been at temperatures of 200°C or less for the last 1000 million years. A critical issue is the temperature at which fission tracks in zircons are annealed, which is not well known, the limited data available suggesting a temperature in the range 200±40°C [*Harrison et al.*, 1979; *Hurford*, 1985; *Zeitler*, 1985; *Naeser et al.*, 1989b]. Other estimates suggest a temperature of between 250°C and 300°C depending on the cooling rate [*Sharma et al.*, 1980; *Bal et al.*, 1983].

So why were the *Naeser et al.* [1989a] zircon fission track ages for these tuffs so much older? Those grains were analyzed by Dr. Charles Naeser at the U.S. Geological Survey, and perhaps he was only measuring the oldest population of zircons in those samples [*Green*, personal communication, 27 March, 2003] because he already knew the early Middle Cambrian biostratigraphic age for those samples. Certainly, in the samples in this study there is an older population of

individual zircon grain fission track ages which approaches the results of Naeser's analyses of his samples, but it is only represented by a few grains. However, all the grains that Naeser analyzed in his samples had very high spontaneous fission track densities and relatively low induced fission track densities, consistent with their older ages [*Naeser*, personal communication, 4 June, 2003]. Nevertheless, contrary to the *Naeser et al*. [1989a] paper, a total of twenty-three zircon grains were analyzed in their Muav tuff sample, and these included five younger grains with fission track ages of 249±50 Ma, 353±67 Ma, 297±128 Ma, 308±96 Ma and 183±34 Ma. In their Tapeats tuff sample there was also a younger grain with a fission track age of 387±74 Ma (all the errors in these ages being ±2σ). It should also be noted that in each sample there were two grains older than the published ages [*Naeser*, personal communication, 4 June, 2003]. Thus there was evidence of thermal resetting of some grains in the *Naeser et al.* [1989a] samples, but not complete resetting to coincide with the time of the Laramide uplift, as is so clearly evident in the pooled age for the youngest group of zircons in each of the samples in this study.

Another possible explanation of this discrepancy could be differences in the etching conditions used in the two laboratories. Naeser re-examined the mounts of zircon grains from his two samples and found a few under-etched grains in them [*Naeser*, personal communication, 5 June, 2003]. He thus suggested that it is quite probable that he and Green may have looked at different populations of grains in the respective samples. Because the time required to properly etch a zircon grain is a function of the total radiation damage the zircon has suffered, grains with high fission track densities will etch more rapidly than grains with low fission track densities. Thus Precambrian age zircons would be expected to etch in a few hours, while a Pleistocene zircon grain would probably take a week or more. As admitted by Naeser:

> When I etch a zircon mount I periodically check the progress of the etch. When I see a reasonable number of countable grains I will stop, even though there could be additional grains that could be counted if I doubled the etch time. It is a judgment call. Will I get more or fewer grains by continuing the etch? When I am dating Paleozoic or Precambrian samples I choose to

stop earlier rather than later [*Naeser*, personal communication, 4 June, 2003].

However, the Geotrack laboratory did not use a long etching time on the three Grand Canyon tuff samples in this study (refer back to Section 5 above). If anything, the short etching times used would have favored the exposing of older grains with higher spontaneous fission track densities than younger grains. Rather, because the Geotrack laboratory had no bias in knowing the supposed ages of the samples when working on them, they would have been more careful to look for a range of ages in the samples and count grains with a variety of fission track densities, morphologies, etc., compared to Naeser's approach, which would have been to count the grains with the highest fission track densities because of already knowing the "target age" [*Green*, personal communication, 4 June, 2003]. So by admission of both laboratories there is a possibility of bias being introduced in the etching times of the grains and in the grains chosen for analysis. Nevertheless, there is no "concrete" evidence to suggest that such would have had any more than a minimal effect on the resultant fission track age determinations on the respective samples in the *Naeser et al*. [1989a] study and in this study. Naeser may have missed zircon grains with younger fission track ages when he did his analyses, but it may have been more to do with the zircon grains that ended up in the sample mounts from the larger quantity of zircon grains separated from the samples (that is, bias unwittingly introduced in the sub-population of grains selected for mounting).

So are there any other clues, or means of finding out, about the thermal history of the Paleozoic strata in the Grand Canyon area that might confirm that conditions were in fact conducive to annealing of the fission tracks in the zircon grains in the Muav and Tapeats tuffs? The single zircon grain fission-track ages obtained from the samples in this study seem to clearly indicate that most of the zircons were reset during the Laramide uplift, so this means that if these tuff units were only subjected to temperatures <200°C since their formation, these zircon grains with young ages must have been anomalously sensitive to resetting. As indicated earlier, fission track ages of ~1000 Ma obtained from zircons from Proterozoic rocks now exposed at river level in the

Grand Canyon suggest that these rocks have only been exposed to temperatures of <200°C for the last 1000 million years. Furthermore, apatite fission track ages of Precambrian granitic rocks in the central Grand Canyon record the effects of the Laramide uplift at around 62.4 Ma, the original fission tracks in the apatite being totally annealed at temperatures between 105°C and 150°C [*Naeser*, 1981; *Naeser et al*., 1989a, b]. *Dumitru et al*. [1994] have shown from numerous apatite fission track data that between 2.7 and 4.5 km thickness of Mesozoic strata were eroded from the Grand Canyon area as a result of the erosion subsequent to the Laramide uplift. Thus the original late Cretaceous paleodepth of these Cambrian tuffs, combined with an assumed normal geothermal gradient, would have resulted in these tuffs being subjected to temperatures of 110–130°C. Furthermore, because the apatite fission track ages of the Grand Canyon Precambrian basement samples were totally reset at around 63 Ma, and the mean lengths of the fission tracks are slightly shorter than normal, *Dumitru et al*. [1994] concluded that the cooling as a result of the erosion of the overlying Mesozoic strata caused by the Laramide uplift was protracted (over millions of years in conventional terms). This conclusion was derived from comparison with the normal mean fission track lengths in rapidly cooled rocks and laboratory annealing studies [*Gleadow et al*., 1986; *Green et al*., 1989]. Such shortening of the fission tracks also reduces the fission track ages [*Green*, 1988], so it is necessary to correct for this to determine the time of this Laramide cooling. The corrected ages would be ~75 Ma. Significantly, that is the pooled age of the youngest group of zircon grains in two of the three tuff samples in this study, further confirming that the youngest groups of zircon grains in these samples do record the time of the Laramide uplift.

However, because all these claims concerning the thermal history since burial of these Cambrian tuff units in the western Grand Canyon are all based on fission track data, including the estimates of the temperatures at which fission tracks are totally annealed in apatite and zircon, it would be helpful to have confirmation of this claimed thermal history from other independent geological indicators. *Naeser* [personal communication, 21 June, 2003] referred to the work of *Wardlaw and*

Harris [1984] who used the color of alteration of conodont fossils in the Paleozoic rocks across Arizona, due to the heating resulting from burial and diagenesis of the sediments, as an indication of the thermal history of those Paleozoic strata. This method of using a Color Alteration Index (CAI) of conodonts (microfossils composed of apatite) to determine the temperatures of diagenesis and burial metamorphism of sediments was developed and calibrated by *Epstein et al.* [1977] and *Harris* [1979, 1981], and has been successfully applied and widely used since [*Harris*, 1979; *Rejebian et al.*, 1987]. Thus Wardlaw [*Naeser*, personal communication, 21 June, 2003] has concluded that the maximum temperature achieved in the Paleozoic strata of the Grand Canyon would have been <150°C, consistent with the conclusion reached by *Dumitru et al.* [1994] based on the apatite fission track data.

A further suggestion made by *Naeser* [personal communication, 4 June, 2003] was to have x-ray diffraction (XRD) analyses undertaken on the tuff samples to determine their illite/smectite ratios and their illite crystallinities, both of which could potentially indicate the maximum temperature to which the tuff units had been subjected. Experimental studies of the conversion of smectite to illite have demonstrated its potential use as a geothermometer [*Huang et al.*, 1993; *Essene and Peacor*, 1995], which has been confirmed by field studies [*Smart and Clayton*, 1985; *Pytte and Reynolds*, 1989; *Velde and Espitalié*, 1989; *Pollastro*, 1993; *Velde and Lanson*, 1993; *Hillier et al.*, 1995; *Renac and Meunier*, 1995]. Similarly, many studies have demonstrated the value of using illite crystallinity as an indicator to distinguish between diagenesis, very low-grade metamorphism and low-grade metamorphism [*Kubler*, 1964, 1967, 1968; *Kisch*, 1983, 1987; *Blenkinsop*, 1988; *Barrenechea et al.*, 1995; *Frey and Robinson*, 1999; *Kubler and Goy-Eggenberger*, 2001]. This advice was followed and portions of a sample from each of these tuffs were sent for XRD analyses to determine their illite/smectite ratios and illite crystallinities (see below for further details).

Another way of checking the supposed ages of the zircons in these tuff units is to apply the U-Th-Pb radioisotope dating technique to some of the individual zircon grains. Ideally the same grains on which the zircon fission track ages were obtained should be U-Th-Pb dated

so as to compare the two methods of age determination and thus see if they directly equate to one another. If they did, then this would settle the argument over whether the radioisotope ratios were derived by radioactive decay or are just geochemical properties of the rocks and minerals. It would be hard to deny that the radioisotope ratios were not derived from radioactive decay when the fission tracks as physical evidence of nuclear decay are present in the same zircon grains in the right quantities to match the radioactive decay measured by the radioisotope ratios. Another potential outcome is to thereby confirm just how much radioactive and nuclear decay has occurred in these Cambrian tuffs since they were deposited early in the Flood year, which thereby potentially indicates just how much acceleration of nuclear decay has to have occurred during the Flood year. And finally, if deep burial of these tuff units and the Laramide uplift have also effected the U-Th-Pb radioisotope system, then the U-Th-Pb dates of the zircon grains might match the pooled fission track ages for the youngest groups of zircon grains in these samples. If not, then even those grains (with the young fission track ages) should still yield Cambrian U-Th-Pb ages comparable with the *Naeser et al.* [1989a] zircon fission track ages. Unfortunately, because the zircon grains that had been fission track dated were still mounted and etched, it was not possible to U-Th-Pb radioisotope date those same grains, though attempts were made to organize this with a laboratory using an ion microprobe. Instead, some unmounted zircon grains from one of the Muav tuff samples and from the Tapeats tuff sample were submitted to a laboratory for TIMS (thermal ionization mass spectrometry) U-Th-Pb radioisotope analyses (see below for the results).

7.2 Jurassic Morrison Formation Tuffs, Southeastern Utah

It is immediately evident upon comparing the results on these six samples, two each from three different stratigraphic sections through the Morrison Formation in southeastern Utah, that the zircon fission track ages obtained in this study (Table 2) are directly comparable to previously published dating results (Table 1). Indeed, five of the six

samples yielded almost identical ages, the only somewhat different and older result being obtained on the Notom sample NMF-49 from which only nine zircon grains were recovered. Furthermore, in each of the three stratigraphic sections the two samples yielded zircon fission track ages commensurate with their stratigraphic order. The upper and therefore younger sample yielded a younger zircon fission track age for that tuff unit, and the lower or older tuff unit yielded an older zircon fission track age.

The nine individual zircon grains analyzed from sample NMF-49, the stratigraphically lower sample from the section at Notom (Figure 3), are consistent with a single population ($P(\chi^2)>5\%$), characterized by a pooled fission track age of 183.4±20.8 Ma (±1σ error) (Table 2). *Green* [2002] reported that a variety of grain morphologies were present within the sample, from euhedral to rounded as well as intermediate forms. The ages from euhedral grains (two in number) were consistent with the ages measured from obviously rounded grains (three in number). The ages from the other grains, with intermediate forms, were also consistent with the entire data set. Thus the individual zircon grain fission track data are consistent with a common origin for all these grains, the clustering of the data in both the radial plot and histogram of Figure 14a being consistent with a satisfactory pooled age using all nine grains. However, if the two oldest grains were eliminated from the analysis, because of potentially being outliers as evident in the histogram, the remaining seven grains would likely yield a pooled age almost identical with the published zircon fission track age on six grains for this same tuff unit [*Kowallis and Heaton*, 1987] (Table 1 here).

The sample NMF-64 from the uppermost tuff unit in the Brushy Basin Member of the Morrison Formation in the Notom section (Figure 3) is characterized by a central age of 178.6±19.8 Ma (Table 2). However, the individual zircon grains show a statistically significant spread in fission track ages ($P(\chi^2)<5\%$), from a youngest limit of 93.1±7 Ma to an oldest limit of 651.3±210.4 Ma (all errors ±1σ). Thus the numerical value of the central age has no significance other than characterizing the spread of ages within the sample. On the other hand, statistical analysis of the

individual grain fission track ages [*Green*, 2002] suggests the presence of two dominant populations characterized by ages of 132±10 Ma and 321±35 Ma. However, the relevant histogram in Figure 14b does not really support the existence of the suggested population of older grains, but the youngest group with a pooled age of 132±10 Ma is dominant and therefore can be justified as being the fission track age assigned to this sample and the tuff unit it represents. A variety of grain morphologies were reported by *Green* [2002] to be present within this sample, from euhedral to rounded as well as intermediate forms. All of the clearly euhedral grains analyzed (six grains) give ages which fall within the youngest group of ages. However, in addition, three grains falling within this youngest group are clearly rounded, while the older ages were measured only in rounded to sub-rounded grains. The presence of these rounded grains in addition to euhedral grains within the youngest age grain population, just as there are both rounded and euhedral grains within the single age population of sample NMF-49, perhaps suggests some degree of transport may have taken place prior to ultimate deposition of these tuff units. Note also that the older ages in this sample (see the histogram in Figure 14b) indicate that there may be a significant component of older non-volcanic material also present within this tuff unit.

Sample BMF-14 from the lowermost tuffaceous mudstone unit of the Brushy Basin Member in the Brushy Basin type section (Figure 4) is characterized by a central age of 188.3±19.2 Ma (Table 2). However, the individual zircon grains show a spread of fission track ages ($P(\chi^2)<5\%$) from 98.2±16.7 Ma to 689.9±187.6 Ma. So the numerical value of the central age again has no significance, other than as an estimate of the modal value of the distribution of ages within this sample. *Green* [2003] reported that the zircon grains obtained from this sample showed a variety of morphologies, from euhedral to well-rounded as well as intermediate forms. Data from only the euhedral grains (twelve in number) are all consistent with a single age population characterized by a pooled age of 147.8±8.2 Ma. Furthermore, a statistical analysis of the complete single grain fission track age data set [*Green*, 2003], using the approach outlined by *Galbraith and Green* [1990], suggests

the presence of three dominant populations characterized by ages of 144±10 Ma, 225±30 Ma, and 583±91 Ma. While the existence of the grain population with the highest age might seem justified in the radial plot of Figure 14c, the histogram shows a large spread for these three oldest grains. Nevertheless, the two clusterings on the histogram justifies the identification of the two younger populations, especially the strong clustering of so many samples that yields a pooled age for the youngest group of 144±10 Ma. This youngest group of single grain ages within this sample was measured consistently only in euhedral grains [*Green*, 2003], while grains giving older ages showed sub-rounded to well-rounded forms. This pooled age for the youngest group of zircon grains, comprising the majority of the grains analyzed within this sample, is consistent with the published fission track and radioisotope ages for the equivalent tuffaceous units in the other two Morrison Formation sections (Table 1). Furthermore, the dominance of euhedral grains in this age group suggests that this probably represents the timing of the volcanism contemporaneous with deposition of this tuffaceous mudstone unit.

Sample BMF-28 from the topmost unit of the Brushy Basin Member in the Brushy Basin section (Figure 4) is characterized by a central age of 173.7±7.1 Ma (Table 2). However, the individual zircon grains have fission track ages from 104.2±22.3 Ma to 592.3±137.4 Ma, so the numerical value of the central age again has no significance. However, a statistical analysis by *Green* [2003] of the complete single grain age data set, using the approach outlined by *Galbraith and Green* [1990], suggests the presence of three dominant populations characterized by ages of 136±6 Ma, 201±26 Ma, and 372±30 Ma. Examination of the radial plot in Figure 14d might suggest some evidence of structure in the older group, with populations of two grains each at 339±32 Ma and 564±119 Ma. However, with so few grains this further division is unwarranted by the available data. Furthermore, the histogram shows such a large spread of ages for these four grains that this oldest grouping doesn't appear to be justified. On the other hand, the histogram shows a strong clustering of younger ages with a distribution that would seem to justify a division into two populations of grains. Quite clearly the

youngest group with a pooled age of 136±6 Ma is dominant, because eleven of the nineteen grains analyzed fall into that youngest group. *Green* [2003] reported only a very small number of euhedral grains were present in this sample (four grains in number). These four grains show a similar spread of ages to the group as a whole (two fall into the youngest group and two into the oldest group), so therefore no significance can be attached to the grain morphologies. However, it is very significant that the pooled age of 136±6 Ma of the dominant youngest age group in this sample (from the topmost unit of the Brushy Basin Member in the Brushy Basin type section) is identical to the pooled age of 132±10 Ma of the youngest group of zircon grains in the sample from the topmost unit of the Brushy Basin Member in the Notom stratigraphic section (Table 2).

All individual zircon grains analyzed from sample MMF-4, from near the bottom of the Brushy Basin Member in the Montezuma Creek stratigraphic section (Figure 5), are consistent with a single population ($P(\chi^2)>5\%$) characterized by a pooled age of 148.8±7.0 Ma (±1σ error). The tight grouping of all eighteen analyzed grains consistent with a single fission track age population is clearly evident in both the radial plot and histogram of Figure 14e. *Green* [2003] reported that all eighteen zircon grains analyzed from this sample were euhedral in form, consistent with the rock unit being volcanic ash-rich. Thus these dated zircon grains most likely represent the primary volcanic component of this tuff unit. Note also that the central age for this sample is 148.2±8.3 Ma, identical to the pooled age (Table 2). What is even more noteworthy is that these fission track ages for this unit are also identical to the ^{40}Ar-^{39}Ar single plagioclase and K-feldspar crystal laser-fusion radioisotope ages obtained for this same unit (Table 1) by *Kowallis et al.* [1991]. This is unequivocal confirmation that the measured fission track physical evidence of nuclear decay is equivalent to the amount of radioisotope decay in the mineral grains that compose this tuff unit as determined by those radioisotope analyses. The zircon fission track age of this sample in this study is also almost identical to the zircon fission track age obtained for the sample (BMF-14) from the lowermost tuffaceous mudstone unit in the Brushy Basin Member in

the Brushy Basin type section (Table 2), consistent with a late Jurassic age for the deposition of the earliest units of the Brushy Basin Member of the Morrison Formation.

Sample MMF-1, from a tuff unit near the top of the Brushy Basin Member in the Montezuma Creek stratigraphic section (Figure 5), is characterized by a central age of 205.1±22.4 Ma (Table 2). However, the twenty individual zircon grains show a statistically significant spread in their fission track ages ($P(\chi^2)<5\%$), from 87.6±15.4 Ma to 1036.2±309.8 Ma (all errors ±1σ). Thus the numerical value of the central age has no significance other than characterizing the spread of ages within this sample. However, a statistical analysis by *Green* [2003] of the complete single grain age data set, using the approach outlined by *Galbraith and Green* [1990], suggests the presence of three dominant populations characterized by ages of 137±9 Ma, 277±17 Ma, and 1036±309 Ma. The oldest of these three groups can be seen on both the radial plot and histogram in Figure 14f to be represented by one grain that is an extreme outlier, which can therefore be discounted on the basis that it represents contamination of this tuff unit by older material. Otherwise, the two younger populations of zircon grains are clearly evident in both the radial plot and histogram of Figure 14f. *Green* [2003] reported that a variety of grain morphologies were present within this sample, from euhedral to rounded as well as intermediate forms. However, all the grains comprising the youngest group of ages (eight grains) are euhedral in form, while the only other euhedral grain gives an age that falls in the intermediate age group. All other grains belonging to the intermediate and oldest age groups are rounded in form, consistent with these representing older material that has contaminated the tuff. On the other hand, the complete dominance of euhedral grains in the youngest group of zircons with a pooled age of 137±9 Ma clearly suggests that this age represents the timing of the volcanism contemporaneous with the deposition of this tuff unit. Furthermore, even though this zircon fission track age is not quite identical to the ^{40}Ar-^{39}Ar single plagioclase and K-feldspar crystal laser-fusion radioisotope ages obtained on a sample from this same tuff unit by *Kowallis et al.* [1991] (Table 1 here), it is identical to the zircon fission

track ages obtained in this study on samples in a similar stratigraphic position from the Notom and Brushy Basin sections (Table 2). These results confirm the possibility, first suggested by *Kowallis and Heaton* [1987], that the uppermost units of the Brushy Basin Member of the Morrison Formation may in fact be of earliest Cretaceous age.

7.3 Miocene Peach Springs Tuff, Southeastern California and Western Arizona

The three samples of this tuff all yielded excellent results (Table 2), consistent with previously published dating results (Table 1). All twenty individual zircon grains analyzed from each of the samples PST-1, PST-2, and PST-3 are consistent with single populations ($P(\chi^2)>5\%$) characterized by pooled ages of 24.6±1.2 Ma, 20.9±0.9 Ma, and 20.9±0.8 Ma (±1σ errors) respectively, with identical central ages due to the narrow spreads in the data. This can be seen in the radial plots and histograms of Figure 15a, b and c respectively. *Green* [2002, 2003] reported that only euhedral grains were obtained from each of these samples, consistent with the nature of this welded crystal-rich tuff.

The two samples, PST-2 and PST-3, from the Kingman area (Figure 7) yielded identical ages which are only marginally older than the published sanidine K-Ar and ^{40}Ar-^{39}Ar laser-fusion radioisotope dates for these same outcrops (Table 2; *Nielson et al*., 1990). This outcome, given that the two samples in this study were analyzed in separate analytical runs, is reassuring that the laboratory's analytical procedures are identical from run to run. Furthermore, it demonstrates that the samples from different outcrops of the same rock unit are nonetheless representative of what is a homogeneous tuff unit. On the other hand, PST-1 from an outcrop about 100 km away to the southwest (Figure 6) has yielded a slightly older zircon fission track age. *Green* [2002] noted that the difference between the zircon fission track age of this sample compared with the identical zircon fission track ages for samples PST-2 and PST-3 is not statistically significant at 95% confidence limits. However, the high degree of internal consistency within the single

grain fission track age data from each sample suggests the difference between these ages could be real. Thus the outcrop from which sample PST-1 was taken could be slightly older than those outcrops from which samples PST-2 and PST-3 were taken. However, a sphene fission track age obtained for a sample from an outcrop even further to the west in the Bristol Mountains (Figure 6) is virtually identical to the zircon fission track ages obtained in this study for the two samples from the Kingman area (Table 2; *Nielsen et al.* [1990]). This supports the claim of *Gusa* [1986], *Glazner et al.* [1986], and *Gusa et al.* [1987], that all these outcrops belong to the Peach Springs Tuff. The only other possibility is that there is some contamination of the tuff with older material in the outcrop from which sample PST-1 was taken. There may be a hint of this possibility in the histogram in Figure 15a, where there appears to be a possible second, older population of grains close to the right of the main population of grains. That main population on its own would yield a pooled zircon fission track age identical to that for the outcrops in the Kingman area.

Nevertheless, for the stated purpose of this study it is clearly evident that these samples from this Miocene tuff unit have yielded a quantity of fission tracks in their zircon grains consistent with ages obtained by radioisotope dating of sanidine grains in samples from the same outcrops of this same tuff unit. This confirms that the radioisotope ratios have resulted from an amount of radioactive decay that has occurred equivalent to the physical evidence for nuclear decay provided by the fission tracks.

8. Additional Analytical Work on the Cambrian Tuffs, Western Grand Canyon, Arizona

8.1 X-Ray Diffraction (XRD) Determinations of their Mineralogy

Portions of Muav tuff sample MT-3 and the Tapeats tuff sample TT-1 were sent to Dr. Sam Iyengar, the technical director of the Technology of Materials laboratory in Wildomar, California, to be analyzed by x-ray powder diffraction (XRD) to determine their mineralogical constituents

in the fine (<2–4 μm) fraction. At the laboratory the samples were analyzed according to Laboratory Standard Operating Procedure-100 for clay mineral analyses. The samples were gently ground to break up the aggregates and then air-dried. They were then suspended and shaken in distilled water to promote dispersion. The time required to separate the <2–4 μm fractions was calculated from Stokes' law and the suspensions were allowed to stand for the appropriate time. The supernatant (with colloids) solutions were decanted into separate beakers. The process of adding water and allowing settling was continued until the supernatants became clear.

Portions of the clay suspensions in the beakers were used to make oriented clay mounts on Millipore filters. The suspensions were filtered through 45 μm filter papers on a Millipore filter set-up using a vacuum. They were then washed thoroughly with distilled water to remove excess salts. The clay cakes on the filter papers were transferred, while still wet, onto glass slides and kept in an ethylene glycol chamber for twenty-four hours. A drop of glycol was placed on the edge of each slide before the slides were placed in the chamber.

The oriented and glycolated clay mounts were then scanned from 3 to 30° 2θ using a Phillips' x-ray diffractometer running with Cu-K_{α} radiation at 35 kV and 20 ma.

8.2 U-Th-Pb Radioisotope Determinations on Zircons

The zircon grains separated from Muav tuff sample MT-3 and Tapeats tuff sample TT-1 by the Geotrack International laboratory that were not used for the zircon fission track analyses were sent to Dr. Yakov Kapusta in the geochronology and isotope geochemistry laboratory at Activation Laboratories in Ancaster, Ontario, Canada. There the grains were examined under a microscope and six grains from each sample were selected for U-Th-Pb radioisotope analyses. The six grains from the Muav tuff were abraded with air in order to clean their surfaces and to remove any secondary overgrowths and/or portions of any other mineral grains that might be still clinging to them. On the other hand, the six grains from the Tapeats tuff were chemically abraded in order to totally

eliminate any discordance caused by Pb loss. Thus the grains were first annealed at 900°C for sixty hours and then leached in concentrated HF at 170°C for twelve hours. They were then fluxed in warm 5N HNO_3 and rinsed with MQ water several times. These leached grains were then spiked with mixed Pb-U tracer and dissolved completely in concentrated HF at 210°C for forty-eight hours. All twelve abraded zircon crystals were then dissolved using the standard dissolution techniques (conversion to HCl and column chemistry) so that the relevant elements could be separated in solution for depositing on filaments for insertion in the mass spectrometer. Once prepared, the filament for each zircon grain was run in a thermal ionization mass spectrometer (TIMS) to determine the relevant radioisotope ratios and thus calculate the U-Pb ages for these zircon grains.

9. Results and Discussion of the Additional Analytical Work

9.1 The X-Ray Diffraction (XRD) Determinations

The XRD patterns for the oriented and glycolated clay fractions for both samples are shown in Figure 16. The appropriate peak positions for the various clay and other minerals present are marked on the oriented pattern. Both samples contain illite interstratified with smaller amounts of smectite. Discrete smectite, as estimated by expansion to ~17.8 Å upon glycolation, is also present, but in small amounts. The proportions of the various minerals in the clay (<2–4 μm) fractions of the two samples are listed in Table 3, along with the Kubler Index for illite crystallinity determined from the peak at 10.2 Å, in accordance with the internationally-recognized standard procedures [*Kisch*, 1991; *Warr and Rice*, 1994].

As already noted, the rationale for these XRD analyses of the clay minerals in these two tuff units is that the amount of smectite interstratified in illite has been used as a geothermometer. Its primary application has been to estimate the temperatures to which sediments containing organic matter have been subjected to by burial in sedimentary basins so as to determine whether maturation has

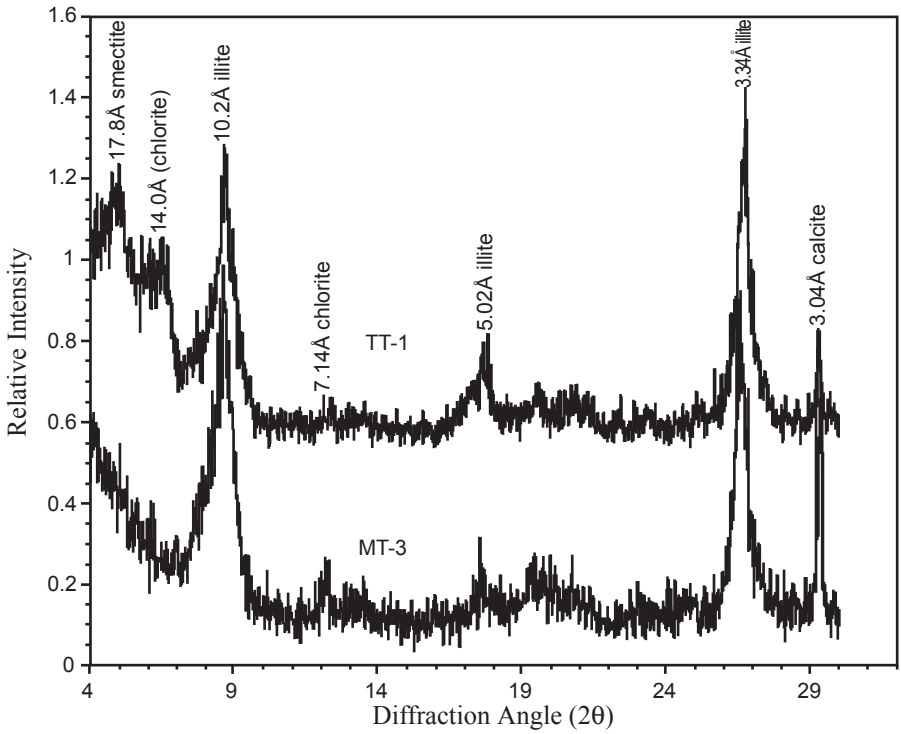

Figure 16. The XRD (x-ray diffraction) patterns for the oriented and glycolated <2–4 μm clay fractions of Muav tuff sample MT-3 and Tapeats tuff sample TT-1, showing the peak positions for the various clay and other minerals present (as marked).

Table 3. The mineral composition of the <2–4 μm fraction of Muav and Tapeats tuff samples MT-3 and TT-1 respectively determined by XRD analyses (Analyst: Dr. Sam Iyengar, Technology of Materials, Wildomar, California). The illite is interstratified with smectite. The smectite/illite ratio and the Kubler (illite crystallinity) Index for each sample has also been calculated.

Sample	Smectite (%)	Illite (%)	Smectite/Illite ratio	Illite/Smectite ratio	Kubler Index	Other Minerals (%)
MT-3	~20	~65	~0.3	~3.25	0.45	Chlorite (~10) Calcite (~5)
TT-1	~5	~80	~0.06	~16.0	0.65	Chlorite (<5) Calcite (~10)

occurred and hydrocarbons generated and released. The application of this geothermometer to these two tuff units seemed feasible, because a petrographic examination indicated they primarily consisted of a clay matrix in which the clay minerals appear to have accumulated at the time of deposition, rather than having formed *in situ* after deposition. In volcanic eruptions ash is produced by pulverization of the congealing lavas, so that the ultra-fine mineral fragments are then well mixed with super-hot steam as they are rapidly transported and deposited. It would have been the steam acting on the ultra-fine mineral fragments that would have reduced them to clay minerals by the time these tuff units were deposited.

However, the smectite/illite ratio relationship to temperature appears to be neither simple nor unequivocal, because of various factors such as the ion content and concentrations in interstitial waters and the geothermal gradient, not just at the present time but also during the history of the sediment pile. Nevertheless, *Hower* [1981] found clear relationships between depth, temperature and the percent illite in illite interstratified with smectite in the sediments intersected by oil wells in the Gulf of Mexico coast region (Figure 17) [*Pollastro*, 1993], one of which is directly comparable to the sedimentary strata sequence in the Grand Canyon-Colorado Plateau region. There *Dumitru et al*. [1994] estimated that the Cambrian strata of the Tonto Group would have been, prior to the erosion of the Mesozoic section from off the top of the Grand Canyon sequence, at a depth of burial of between 4.5 and 6 km, with the apatite fission track data suggesting temperatures of between 110° and 130°C. In Figure 17 the percent illite in the illite interstratified with smectite in the two samples from these Grand Canyon tuff units, as recorded in Table 3, have been plotted on the curve from oil well (B), and projected onto the depth and temperature axes. This suggests that with that geothermal gradient, these tuff beds would have been, prior to the erosion of the Mesozoic strata above, at depths of 4800–5600 m and subjected to temperatures of between 110° and 130°C, consistent with the estimates by *Dumitru et al*. [1994]. Confirmation that the interpretation of these results is entirely reasonable is the fact that these two tuff units plot on the depth axis in the correct stratigraphic order, the Muav tuff

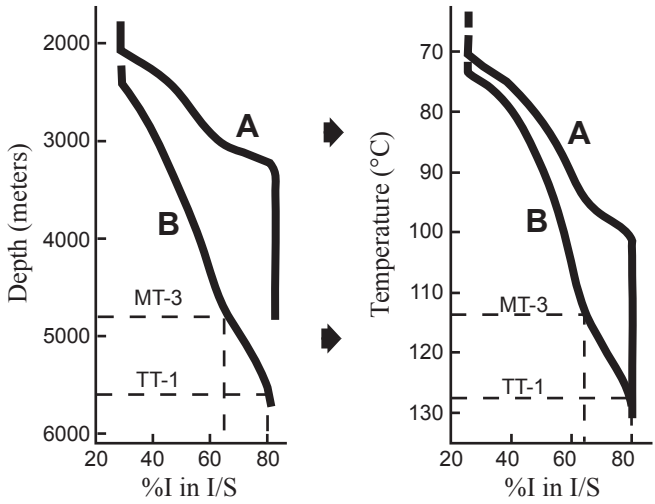

Figure 17. Proportion of illite (I) layers in mixed-layer illite/smectite (I/S) versus depth (left) and temperature (right) for samples from (A) an Oligocene well, and (B) a Miocene well, in the Gulf of Mexico coast region (modified from *Hower* [1981]). The %I in I/S data for the Muav tuff MT-3 and Tapeats tuff TT-1 samples are plotted on curve B and the interpreted depths and temperatures are projected from that curve.

being higher up the stratigraphic sequence above the Tapeats tuff by 200 m or more (Figure 1). *Dumitru et al.* [1994] based their estimation on a pre-Cretaceous geothermal gradient of 20–30°C/km, and the geothermal gradient in the Miocene oil well (B) (Figure 17) is of the order of 20°C/km. Such a geothermal gradient is not unreasonable in the time frame of the Flood event, given the catastrophic deposition of the thick Paleozoic and Mesozoic strata sequence [*Austin*, 1994] and the elevated temperatures of the waters depositing those sediments [*Austin et al.*, 1994]. Thus the estimates of depth and temperature based on the percent illite in the illite interstratified with smectite for these two tuff samples, though very approximate due to the likely large errors in the XRD determinations, are not unreasonable. Therefore, because of the consistency of these estimates with the apatite fission track data of *Naeser et al.* [1989a] and *Dumitru et al.* [1994], it seems reasonable to conclude that these two tuff units have since their burial only been

subjected to maximum temperatures of 110–130°C, well below the 200±40°C temperature for total annealing of fission tracks in zircon [*Harrison et al*., 1979; *Hurford*, 1985; *Zeitler*, 1985].

The significance of the Kubler Index values calculated from the XRD clay mineral analyses of the two samples from these two tuff units (Table 3) are harder to interpret from the available literature, which primarily focuses on low-grade metamorphism of sedimentary strata sequences. Estimating the temperatures to which these two tuff units were subjected based on these approximate Kubler Index values depends on the value of the Kubler Index used to define the boundary between diagenesis and the lowest grade metamorphism, which is otherwise defined by mineralogical changes in the clay minerals [*Kubler*, 1967; *Kisch*, 1987]. As indicated by *Blenkinsop* [1988], early studies using the Kubler Index for illite crystallinity all adopted different values of the index to define this crucial boundary, so standardization was warranted. Using the standardized definition of *Kisch* [1991] and *Brime* [1999] with a Kubler Index of 0.42 for the boundary between diagenesis and the lowest grade metamorphism, as successfully applied by *Brime et al*. [2003], the estimated Kubler Index values for the Muav and Tapeats tuffs (Table 3) indicate that they are on the lower temperature side of this boundary, as they only suffered diagenesis. Temperature estimates for that boundary place it at 150±50°C [*Frey and Kisch*, 1987; *Robinson and Merriman*, 1999; *Bucher and Frey*, 2002]. Thus the Kubler Index values for these two tuff units are consistent with the estimate of 110–130°C for the temperatures to which these tuff units have been subjected from both the apatite fission track data of *Naeser et al*. [1989a] and *Dumitru et al*. [1994], and their smectite/illite ratios.

9.2 Zircon U-Th-Pb Age Determinations

Some of the zircon grains in Muav tuff sample MT-3, and the six zircon grains selected from them when ready for analysis after being air abraded, are shown photographed in Figure 18. The six chemically abraded zircon grains from Tapeats tuff sample TT-1 are shown in Figure 19. There do not appear to have been any secondary overgrowths

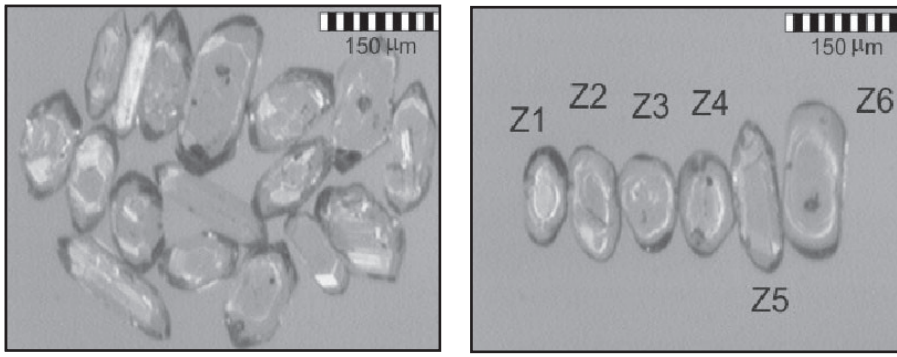

Figure 18. Zircon grains from Muav tuff sample MT-3. (a) Raw grains separated from the tuff. (b) The six selected grains after being air abraded to remove any overgrowths, metamict zones, or portions of other minerals still clinging to their outer surfaces. Photomicrographs courtesy of Dr. Yakov Kapusta at Activation Laboratories, Ancaster, Ontario, Canada.

on these selected and abraded grains, and the photographs don't show any obvious internal primary growth zones in them. The results of the U-Th-Pb radioisotope analyses of the twelve abraded zircon grains and the resultant calculated ages are shown in Table 4.

In the Muav tuff sample MT-3, only two of the zircons, z4 and z6, yielded concordant ages of 74.8±3.2 Ma and 169.0±0.5 Ma (2σ errors) respectively, and these results are plotted on the concordia diagrams in Figure 20. Otherwise, the individual ages derived for the zircon grains from the U-Pb radioisotope analyses range from a $^{206}Pb/^{238}U$ age of 68.2 Ma for grain z5 through to a $^{207}Pb/^{206}Pb$ age of 1621.2 Ma for grain z3 (Table 4). When the $^{206}Pb/^{204}Pb$ and $^{207}Pb/^{204}Pb$ ratios are plotted on a $^{206}Pb/^{207}Pb$ diagram the scatter in the data precludes the fitting of an isochron to them. However, when the data point for grain z6 is not included in the isochron plotting routine used, *Isoplot/Ex* [*Ludwig*, 2001], an isochron line fits the five remaining data points, with an MSWD (mean square of weighted deviates) value of 16 and corresponding to an age of 1609±204 Ma (Figure 21). This MSWD value is too high for this to be an acceptable isochron for an age determination (the ideal is a value of 1; *Dickin* [1995]), and the data point ignored is for grain z6 which yielded the best concordant U-Pb age (Table 4 and

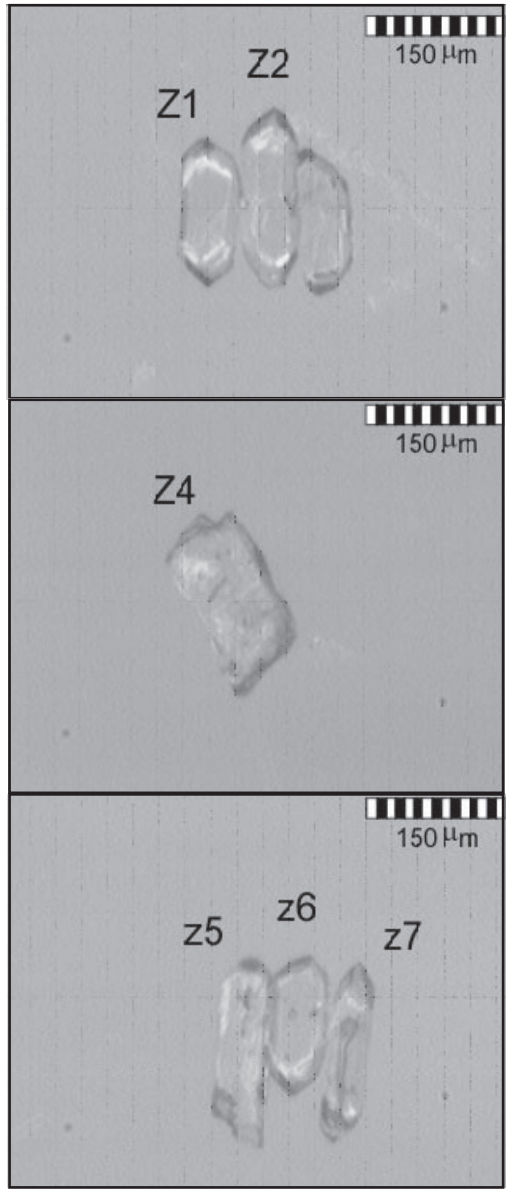

Figure 19. Zircon grains from Tapeats tuff sample TT-1. The six selected grains are labeled z1-z2, z4-z7 and are shown after being chemically abraded. Photomicrographs courtesy of Dr. Yakov Kapusta at Activation Laboratories, Ancaster, Ontario, Canada.

Table 4. The U-Th-Pb radioisotope analyses and ages of six abraded zircon grains (z1-z6) from Muav tuff sample MT-3, and of six abraded zircon grains (z1-z2, z4-z7) from Tapeats tuff sample TT-1, as analyzed by Dr. Yakov Kapusta, Activation Laboratories, Ancaster, Ontario, Canada.

Sample	Sample Fractions	Concentrations							Ratios						Ages (Ma)			
		Weight (µg) (a)	U (ppm)	Pb (ppm)	Pb(c) (pg) (b)	$^{206}Pb/^{204}Pb$ (c)	$^{208}Pb/^{206}Pb$ (d)	$^{207}Pb/^{204}Pb$	$^{206}Pb/^{238}U$ (e)	error (2σ%)	$^{207}Pb/^{235}U$ (e)	error (2σ%)	$^{207}Pb/^{206}Pb$ (e)	error (2σ%)	$^{206}Pb/^{238}U$	$^{207}Pb/^{235}U$	$^{207}Pb/^{206}Pb$	correlation coefficient
MT-3	z1	1.3	924	38.9	1.9	1568.5	0.096	146.39	0.040422	(.16)	0.52014	(.18)	0.09333	(.07)	255.4	425.2	1494.5	0.921
	z2	1.9	194	8.3	3.8	219.5	0.147	11.26	0.034146	(.58)	0.24153	(.85)	0.05130	(.57)	216.4	219.7	254.5	0.743
	z3	1.3	247	45.8	3.8	855.5	0.177	85.42	0.160868	(.16)	2.21465	(.20)	0.09985	(.12)	961.6	1185.7	1621.2	0.821
	z4	1.4	140	1.9	1.3	131.4	0.300	6.24	0.011645	(4.23)	0.07630	(4.96)	0.04752	(2.36)	74.6	74.7	75.3	0.880
	z5	2.2	76	0.9	1.8	82.9	0.206	4.25	0.010639	(3.03)	0.07514	(4.65)	0.05122	(3.31)	68.2	73.6	250.7	0.706
	z6	3.9	360	10.1	1.4	1686.5	0.161	83.38	0.026561	(.20)	0.18105	(.26)	0.04944	(.16)	169.0	169.0	168.6	0.799
TT-1	z1	2.6	353	5.1	0.4	2026.2	0.198	96.79	0.013431	(0.11)	0.08847	(0.29)	0.04777	(0.26)	86.0	86.1	88.1	0.460
	z2	2.7	214	10.5	0.2	7953.9	0.092	434.20	0.049947	(0.06)	0.37598	(0.10)	0.05459	(0.08)	314.2	324.1	395.7	0.595
	z4	5.8	267	85.7	3.2	9266.6	0.147	964.57	0.298127	(0.15)	4.23308	(0.16)	0.10298	(0.05)	1682.0	1680.5	1678.5	0.958
	z5	2.1	135	44.0	0.4	12950.6	0.187	1319.41	0.294489	(0.07)	4.13683	(0.09)	0.10188	(0.06)	1663.9	1661.6	1658.7	0.734
	z6	2.5	57	0.9	0.3	450.8	0.184	21.40	0.015362	(0.48)	0.10055	(1.64)	0.4747	(1.49)	98.3	97.3	73.2	0.448
	z7	1.7	301	4.7	0.3	1378.8	0.241	65.92	0.014073	(0.15)	0.09277	(0.28)	0.04781	(0.23)	90.1	90.1	89.9	0.583

Notes:

(a) Sample weights are estimated by using a video monitor and are known to within 40%.
(b) Total common-Pb in analyses.
(c) Measured ratio corrected for spike and fractionation only.
(d) Radiogenic Pb.
(e) Corrected for fractionation, spike, blank, and initial common Pb.

Mass fractionation correction of 0.15%/amu±0.04%/amu (atomic mass unit) was applied to single-collector Daly analyses and 0.12%/amu±0.04% for dynamic Faraday-Daly analyses. Total procedural blank less than 0.6 pg (MT-3) and 0.2 pg (TT-1) for Pb and less than 0.1 pg for U.
Blank isotopic composition: $^{206}Pb/^{204}Pb = 19.10\pm0.1$, $^{207}Pb/^{204}Pb = 15.71\pm0.1$, $^{208}Pb/^{204}Pb = 38.65\pm0.1$.
Age calculations are based on the decay constants of *Steiger and Jäger* [1977].
Common-Pb corrections were calculated by using the model of *Stacey and Kramers* [1975] and the interpreted age of the sample.

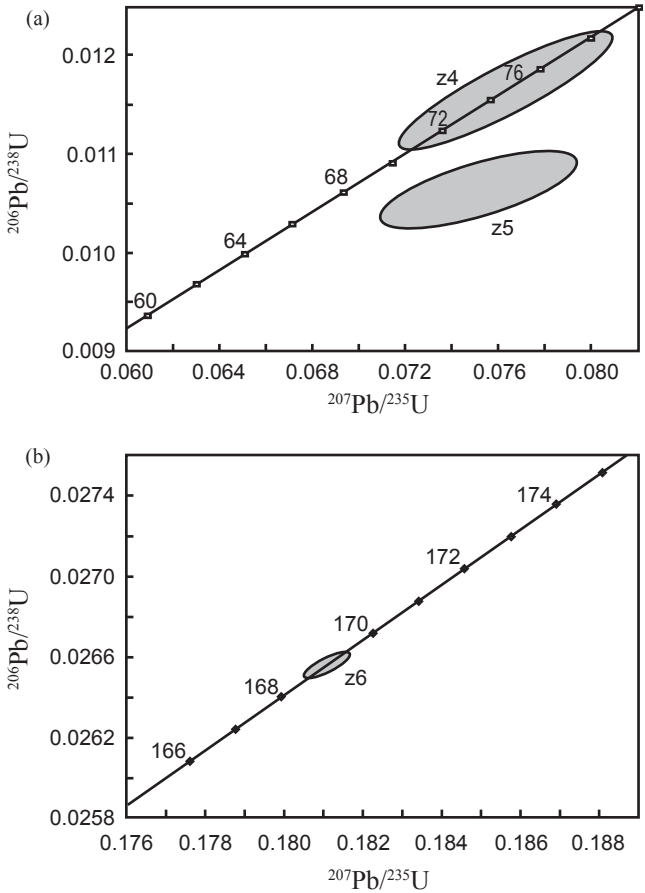

Figure 20. Concordia plots of the U-Pb radioisotope data obtained from zircon grains from Muav tuff sample MT-3. Only two grains yield concordant U-Pb ages: (a) z4 (74.6 Ma), and (b) z6 (169.0 Ma).

Figure 20). Therefore, if grain z6 is included in the isochron analysis, then the data points for grains z1 and z3 have to be rejected in order to fit an isochron to the remaining data. However, the resulting isochron justifies this procedure, because the four data points yield an isochron with an excellent fit measured by an MSWD value of 0.61 and a probability of 0.54 (Figure 21). The age for the isochron is 166±30 Ma (2σ errors), which not surprisingly is the same as the concordant U-Pb age of 169.0±0.5 Ma for grain z6 (Table 4 and Figure 20).

In the Tapeats tuff sample TT-1, all six zircon grains yielded essentially concordant ages. Grains z1, z6, and z7 yielded concordant ages of 86.2±0.3 Ma, 98.2±1.3 Ma, and 90.1±0.2 Ma (2σ errors) respectively, and these are plotted on the concordia diagram in Figure 22. Grains z2, z4, and z5 yielded older essentially concordant ages of approximately 319 Ma, 1681 Ma, and 1662 Ma respectively (Table 4). Otherwise, the individual grain ages derived from the U-Th-Pb radioisotope analyses range from a $^{207}Pb/^{206}Pb$ age of 73.2 Ma for grain z6 to a $^{206}Pb/^{238}U$ age of 1682.0 Ma for grain z4 (Table 4). When the $^{206}Pb/^{204}Pb$ and $^{207}Pb/^{204}Pb$ ratios are plotted on a $^{206}Pb/^{207}Pb$ diagram the scatter in the data precludes the fitting of an isochron to them. However, when the data points for grains z4 and z5 are not included in the isochron plotting routine used, *Isoplot/Ex* [*Ludwig*, 2001], an isochron line fits excellently

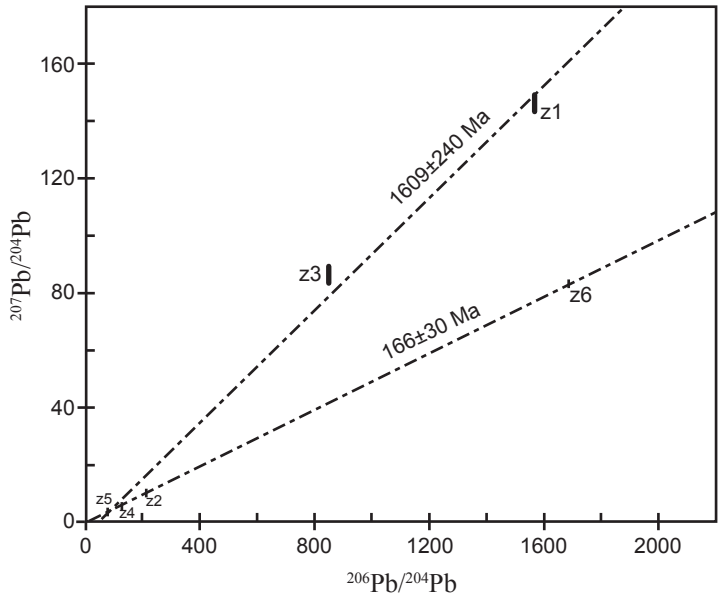

Figure 21. $^{206}Pb/^{204}Pb$ versus $^{207}Pb/^{204}Pb$ isochrons fitted to the Pb radioisotope data obtained from the six zircon grains from Muav tuff sample MT-3. Five grains (z1, z2, z3, z4, z5) yield an apparent isochron age of 1609±240 Ma, but with an MSWD of 16 the fit is poor. However, four grains (z2, z4, z5, z6) yield an isochron age of 166±30 Ma, with a good MSWD of 0.61 and a probability of 0.54.

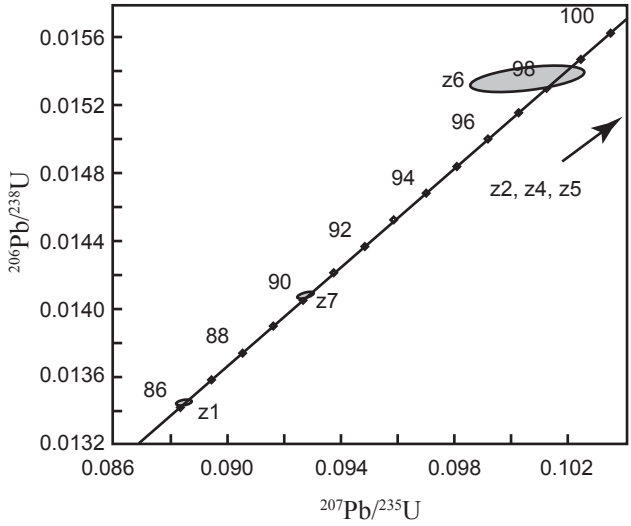

Figure 22. Concordia plot of the U-Pb radioisotope data obtained from three zircon grains (z1, z6, z7) from Tapeats tuff sample TT-1. The three concordant U-Pb ages are 86.2 Ma, 98.2 Ma, and 90.1 Ma respectively.

to the four remaining data points, with an MSWD value of 0.69 and a probability of 0.50 (Figure 23). This isochron corresponds to an age of 437±100 Ma (2σ errors). On the other hand, if the data point for grain z2 is excluded from the isochron plotting routine, the other five data points lie close to an isochron line with an MSWD value of 6.0, and corresponding to an age of 1774±200 Ma (Figure 23).

From all of these various U-Th-Pb radioisotope age determinations on the twelve zircon grains, the following observations can be made. First, none of the resultant ages matches either the biostratigraphic age of early Middle Cambrian for these Muav and Tapeats tuff units, or the zircon fission track ages of 535±48 Ma and 563±49 Ma respectively determined by *Naeser et al*. [1989a]. The only result that comes close is the Pb-Pb isochron age of 437±100 Ma for four grains from the Tapeats tuff sample. Second, the really old ages, for grains z1 and z3 from the Muav tuff and grains z2 and z4 from the Tapeats tuff (Table 4), suggest that the tuffs have a very small component of contamination by older sedimentary or igneous material. This is also hinted at in the histogram

for the Tapeats tuff sample TT-1 in Figure 13c and in the Pb-Pb isochron ages of 1609±204 Ma and 1774±200 Ma in Figures 21 and 23. Indeed, the zircon U-Pb ages of the granitic basement rocks in the western Grand Canyon [*Karlstrom et al*., 2003] fall within the ranges of these Pb-Pb isochron ages. If some older zircon grains have been inherited by these tuffs, most of the fission tracks in those grains have been inherited with them, having then survived the subsequent thermal annealing. Third, the concordant age of 74.8±3.1 Ma for grain z4 and the $^{206}Pb/^{238}U$ and $^{207}Pb/^{235}U$ ages for grain z5 from the Muav tuff (Table 4) coincide with the age of the Laramide uplift of the Colorado Plateau and the subsequent cooling due to the erosion of the Mesozoic strata sequence covering the Paleozoic strata in which these tuff units are found. These results are thus consistent with the pooled fission track age of 74.6±3.9 Ma for the youngest group of zircons in this same Muav tuff sample MT-3

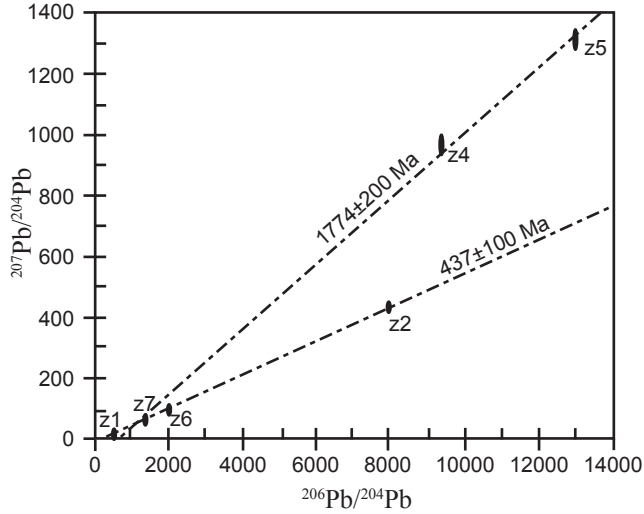

Figure 23. $^{206}Pb/^{204}Pb$ versus $^{207}Pb/^{204}Pb$ isochrons fitted to the Pb radioisotope data obtained from the six zircon grains from Tapeats tuff sample TT-1. Four grains (z1, z2, z6, z7) yield an isochron age of 437±100 Ma with a good MSWD of 0.69 and a probability of 0.50. Five of the grains (z1, z4, z5, z6, z7) yield an isochron age of 1774±200 Ma, and with an MSWD of 6 the fit is reasonable.

(Table 2), which is also matched in the youngest group of zircons from Tapeats tuff sample TT-1. And finally, fourth, the in-between spread of ages (even concordant U-Pb ages) is consistent with some thermal resetting of the U-Pb radioisotope system, due to the temperatures of 110–130°C of burial of these tuffs. This is also reflected in the spread of the zircon fission track ages obtained for the three samples of these tuffs in this study (Figure 13). Thus if the U-Pb radioisotope system has been thermally reset, it is not surprising that this is reflected in the thermal annealing of the fission tracks in the zircons in these tuffs, even though the estimated maximum temperatures of burial of 110–130°C are well below the temperature of 200±40°C for total thermal annealing of fission tracks in zircons. Thus, the suggestion by *Green* [personal communication, 25 August, 2003] that most of these zircons must have been particularly susceptible to thermal resetting seems to be consistent with all the evidence.

However, zircon is known to be stable up to 1690°C [*Finch and Hanchar*, 2003], and the closure temperature of the U-Th-Pb radioisotope system in unaltered zircon is very high at >900°C [*Ireland and Williams*, 2003]. Even though the crystallization of new zircon during metamorphism has been recorded for a wide range of temperatures and pressures, at pressure-temperature conditions lower than upper-amphibolite and granulite grades new zircon is rare [*Hoskin and Schaltegger*, 2003]. Thus, the U-Th-Pb radioisotope system in zircons has been routinely used to "date" what are claimed to be the earth's oldest rocks [*Parrish and Noble*, 2003], such as gneisses in Greenland [*Nutman et al*., 2000] and in Canada [*Bowring et al*., 1989] at 3800–4000 Ma. The U-Th-Pb radioisotope system in such zircons is reset at the temperatures of 600–750°C at which metamorphic gneisses and granites form, but is thermally stable below those temperatures, even though Pb loss due to diffusion can occur [*Baadsgaard*, 1973; *Cherniak and Watson*, 2003].

Therefore, thermal resetting of the U-Pb radioisotope system within most of the zircon grains in the Middle Cambrian Muav and Tapeats tuffs in Grand Canyon, as indicated by these U and Pb isotope measurements (Table 4), would seem to have been impossible at the 110–130°C burial temperatures experienced by the tuff. However, there is a possible

explanation. If this tuff bed and its contained zircons were buried at the outset of the Flood year, and during that year radioisotope decay was accelerated, then the heat generated locally within the zircon grains by this accelerated decay may possibly have raised the temperatures within the zircons sufficiently to reset the U-Pb radioisotope system in them by diffusion of Pb. The fission tracks in the zircons would also have thus been annealed. For such a scenario to work, the wet clay matrix surrounding the zircon grains within the tuff would need to have acted as an insulator that confined this heat to the zircon grains without the tuff matrix's temperature being raised beyond 110–130°C. However, there would then be the problem of dissipating this heat, so this scenario is somewhat speculative.

Nevertheless, assuming this scenario, what temperature might be required within a 50 μm long zircon grain for it to lose about 90% of its contained radiogenic Pb by 550 million years worth (at today's rate) of accelerated radioisotope decay within the Flood year? Using the same equation and data as *Magomedov* [1970] and *Gentry et al.* [1982] for Pb diffusion in zircon, it can be calculated that a temperature of about 725°C would be required. If the diffusion data of *Cherniak and Watson* [2001] were instead used in the calculation, then the required temperature would be much higher at about 1485°C. Both these temperatures are within the range in which zircon is stable and the U-Pb radioisotope system in it is thermally reset. However, in their determination of Pb diffusion in zircon, *Cherniak and Watson* [2001] did not take into account the effect of radiation damage on Pb diffusion, whereas the zircons on which *Magomedov* [1970] measured the Pb diffusion were metamict from radiation damage. If accelerated nuclear decay did occur in these zircon grains in the Muav tuff, then the intense blast of radiation would have undoubtedly caused much damage to their crystal structure, thus facilitating faster Pb diffusion from them and the resetting of the U-Pb radioisotope system. So it is unlikely these zircon grains had to reach a temperature of more than 725°C for the measured resetting of the U-Pb radioisotope system in them from 550 Ma to 70 Ma. The heat required for this resetting is potentially therefore evidence of accelerated nuclear decay.

10. Discussion of the Overall Study

As stated in the introduction to this chapter and in the section explaining the rationale of this present research study, this study was designed to test whether or not the radioisotope ratios measured in minerals and rocks are the product of the quantity of radioactive decay equivalent to the respective radioisotope ages inferred from them. Fission tracks were chosen for study because they provide physical evidence of nuclear decay. Samples were thus chosen from early Middle Cambrian, uppermost Jurassic, and Miocene tuff units in the strata sequence of the Grand Canyon-Colorado Plateau region for zircon fission track dating. The results have confirmed that the physical evidence of millions of years of nuclear decay provided by the observed fission track densities does equate to the millions of years of contemporaneous radioactive decay in the same rocks as determined by radioisotope dating methods. Thus the physical evidence of nuclear decay in the form of the observed fission tracks does confirm that the radioisotope determinations on these minerals and rocks are a record of radioisotope decay, rather than simply being just chemical analyses open to other interpretations. This confirmation that the fission track ages correspond directly to the radioisotope ages is clearly seen in the Jurassic Morrison Formation tuffs and the Miocene Peach Springs Tuff. Furthermore, even though there is clear evidence of thermal resetting of both fission tracks and the U-Pb radioisotope system in the zircons in the early Middle Cambrian Muav and Tapeats tuffs, there is still a direct correspondence between the observed quantities of fission tracks and the measured amounts of α-decay of U in the zircons in these tuffs, which corresponds to identical age determinations by both dating methods and identical evidence of thermal resetting. There is even identical evidence of minor contamination of these tuffs by older material. Thus, the claim that the radioisotope ratios measured in minerals and rocks have nothing to do with radioisotope decay, but are merely artifacts of the compositions of minerals and the geochemistry of rocks and the sources from which they were derived, cannot be sustained.

However, in response to this assertion it might be argued by some that

this direct correspondence between fission track and radioisotope ages is to be expected because the ζ calibration used in fission track dating is derived by using the fission track densities of standard minerals whose ages have been independently determined by radioisotope methods. In other words, the fission track dating method has been calibrated by radioisotope dating, and therefore one would automatically expect there to be a consistency between the two methods. However, in this present study all zircon fission track age determinations were performed in the same laboratory by the same investigator using the same value for the ζ calibration regardless of the resultant calculated fission track ages for the individual zircon grains from all twelve samples spanning from the Cambrian to the Miocene. In other words, the ζ calibration was a constant, and thus it was the fission track densities that varied according to the calculated fission track ages for the zircons in the samples. Thus the younger the age of the zircon the lower was the fission track density, and the older the age of the zircon, the greater the density of the fission tracks. Thus the quantities of fission tracks are directly proportional to the ages of the zircon grains, regardless of the value chosen for the ζ calibration, and thus regardless of that value being obtained using the fission track densities in samples whose ages had been determined by radioisotope determinations. Therefore, the accusation that the fission track ages may be an artifact of calibration against radioisotope ages simply cannot be sustained.

Furthermore, the presence of the fission tracks in the zircons shows that *in situ* U decay has indeed occurred, which implies that *in situ* generation of daughter products has also occurred. This is independent of any pre-existing daughter isotopes that may have been in the rocks. Thus it can be legitimately argued that the radioisotope ratios measured in the rocks are likely the result of *in situ* radioisotope decay, the amount corresponding to the fission track densities.

The remaining question is just how much nuclear decay has occurred during accumulation of the Phanerozoic strata sequence of the Grand Canyon-Colorado Plateau region? Because the zircon fission track ages are equivalent to the radioisotope ages of the Jurassic Morrison Formation tuffs and Miocene Peach Springs Tuff, then 145 or so million years

worth of radioisotope and nuclear decay has occurred during and since deposition of the Brushy Basin Member of the Morrison Formation. The initial zircon fission track age results from the Cambrian Muav and Tapeats tuffs were somewhat equivocal, because the only benchmark for them to be measured against were previous fission track age determinations that yielded nuclear decay ages more or less equivalent to the early Middle Cambrian biostratigraphic ages for these tuffs. The zircon fission track ages obtained in this study simply did not replicate the previously published zircon fission track dating results. However, the subsequent additional analytical work to determine the temperatures to which these tuff units were subjected by burial, and the U-Pb radioisotope age determinations of some of the zircons in two samples, have confirmed that this discrepancy between the two sets of zircon fission track age determinations has been caused by thermal resetting of both fission tracks and the U-Pb radioisotope system in many of the zircons in these tuffs. The fact that both the fission tracks and the U-Pb radioisotope system have been reset by equivalent amounts is reflected in both methods giving identical results for the onset of the Laramide uplift of the Colorado Plateau. This provides confidence to assert that **if** there had been **no thermal annealing** of the fission tracks **and no thermal resetting** of the U-Pb radioisotope system, then the previously published zircon fission track ages for these tuffs equivalent to their biostratigraphic ages would have been confirmed by both zircon fission track and U-Pb radioisotope age determinations in this study. This assertion is further confirmed by the fact that in both the previous and present zircon fission track dating analyses of samples from the same outcrops of these Cambrian tuffs, ages older than their biostratigraphic Cambrian age were found ([*Naeser*, personal communication, 4 June 2003]; and Table 2 and Figure 13). Such older ages were also found by the U-Pb radioisotope age determinations on zircon grains in this present study. In other words, one-to-one correspondence is routinely maintained between the spontaneous fission track densities in the zircons and their contained U-Pb radioisotope systems. Thus, it is concluded that **if** there had been **no thermal annealing** of the fission tracks in the zircons in these Cambrian tuffs, the fission track densities

would have recorded the physical evidence of more than 500 million years worth of nuclear and radioisotope decay (at today's decay rates).

Thus, if more than 500 million years worth of nuclear and radioisotope decay has occurred in the zircon grains within the Cambrian tuff units during and since their deposition, then this is consistent with more than 500 million years of elapsed time **only if** the nuclear and radioisotope decay rates have remained constant at today's measured rates throughout that elapsed time during which the Phanerozoic strata sequence of the Grand Canyon-Colorado Plateau region was accumulating. However, *Austin* [1994] maintains that most of that sedimentary strata sequence was deposited during the year of the catastrophic global Flood only about 4500 years ago, as recorded in the Scriptures (Genesis 7–9). *Austin* [1994] provides ample documentation of the evidence in the sedimentary strata sequence of the Grand Canyon-Colorado Plateau region that the sedimentary strata, whether sandstones, shales, or limestones, were deposited catastrophically over this vast area, consistent with a catastrophic global Flood of a year's duration. Similarly, these thin tuff units in the Muav Limestone and Tapeats Sandstone, sampled in this study, represent catastrophic event horizons, as do the tuffs in the Morrison Formation and the Peach Springs Tuff. Indeed, there is no present-day analog for the scale of the eruption responsible for the Peach Springs Tuff, when at least several hundred cubic kilometers of volcanic ash was deposited over a lateral distance of 350 km and an area of at least 35,000 km^2 [*Glazner et al.*, 1986]. So, if the geologic evidence for catastrophic deposition of the strata sequence in the Grand Canyon-Colorado Plateau region is consistent with the Biblical record of a year-long global catastrophic Flood only 4500 or so years ago, then by implication 500 or more million years worth (at today's rates) of nuclear and radioisotope decay, that has occurred during deposition of much of this strata sequence during that year-long global Flood, must therefore have been occurring at accelerated rates. Furthermore, the occurrence of ^{238}U and Po radiohalos together in the same biotite grains in granites is consistent with accelerated radioisotope decay and rapid granite formation during the Flood [*Snelling and Armitage*, 2003; *Snelling et al.*, 2003b; *Snelling*, 2005a]. Thus the fission tracks in

the zircons in these Cambrian tuff units in the western Grand Canyon provide physical evidence of at least 500 million years worth (at today's rates) of nuclear and radioisotope decay during the Flood.

Of course, such a conclusion presupposes the correctness of interpreting the evidence for catastrophic deposition of the strata sequence in the Grand Canyon-Colorado Plateau region in terms of a year-long global Flood only 4500 or so years ago. The question arises as to whether there is independent evidence that quantifies the timescale for the Flood and since, and for the age of the earth, for that matter? Yes, the diffusion of He, a by-product of U and Th decay, from where it has been generated in zircons within granites indicates a diffusion age of only thousands of years, even though the U-Th-Pb radioisotope dating of the same zircon grains records many millions of years of radioisotope decay [*Humphreys et al*., 2003a,b, 2004; *Humphreys*, 2005]. Also, the presence of primordial ^{14}C in organic matter such as coal and fossil wood, and in diamonds, that are supposedly hundreds of millions of years old and therefore ^{14}C "dead," is only consistent with a young earth and a recent, year-long, global catastrophic Flood [*Baumgardner et al*., 2003a,b; *Baumgardner*, 2005]. Furthermore, the occurrence of ^{238}U and Po radiohalos together in the same biotite grains in granites is consistent with accelerated radioisotope decay and rapid granite formation during the Flood [*Snelling and* Armitage, 2003; *Snelling et al*., 2003b; Snelling, 2005a]. Thus on this basis, the quantities of fission tracks found in the zircons from the tuff units examined in this study are evidence for hundreds of millions of years of accelerated nuclear decay during a global, catastrophic Flood in the recent past.

This conclusion of course raises many questions. How would the enormous amount of heat generated by accelerated decay be removed? And the radiation involved would surely have killed off living organisms? Would the decay of all radioisotopes have been similarly accelerated by the same factor? And by what mechanism was the decay accelerated? These issues are too complex to be dealt with here, but are discussed by *Chaffin* [2000, 2005], *Humphreys* [2000, 2005], *Austin* [2005], and *Snelling* [2005a, b].

There is one final consideration. *Bielecki* [1994, 1998] had hoped

that if accelerated nuclear decay had occurred during the Flood year and fission tracks are a physical measure of the amount of accelerated nuclear decay that has occurred in Flood rocks, then perhaps there should be a lack of spontaneous fission tracks in post-Flood rocks, because they would have been deposited after accelerated nuclear decay had presumably ceased only 4500 years ago. He therefore focused on Tertiary and Quaternary tuffs and volcanic glasses, as well as man-made and natural glasses of known historical age. This was because most geologists who are studying the rocks within the framework of a young earth and global catastrophic Flood would place the boundary between Flood and post-Flood rocks either at the beginning or near the end of the Tertiary. However, as in this present study of the Miocene Peach Springs Tuff, Bielecki found that the spontaneous fission track densities in the tuffs and natural glasses he studied from the Tertiary and Quaternary of western North America still indicated that millions of years of nuclear decay had occurred in them. He thus concluded that his attempt to distinguish between Flood and post-Flood rocks had failed.

If the Miocene Peach Springs Tuff, for example, were a post-Flood rock that should therefore only be thousands of years old, then in the zircons there should only be fission tracks representing just a few thousand years of nuclear decay. This is of course assuming accelerated nuclear decay was confined to the Flood event only. This present study has therefore cast no further light on this dilemma. However, it is unwarranted to conclude that, for example, the Miocene Peach Springs Tuff must therefore be a Flood rock, because *Bielecki* [1998] found that even Pleistocene natural glasses (contemporaneous with the post-Flood Ice Age) still contained an over-abundance of spontaneous fission tracks commensurate with their million year plus radioisotope age. Because there is much other geologic evidence that is relevant to placement of the Flood/post-Flood boundary with which this fission track evidence clearly appears to be in conflict, it can only be concluded that there is much more to learn yet with respect to fission tracks, nuclear decay, and radioisotopes in the rock strata through earth history. It may well be that at the end of the Flood there was a gradual deceleration of decay

rates that continued on well into the post-Flood period, rather than an abrupt termination of accelerated decay. Thus it is premature to use the fission tracks as a criterion for deciding where to put the Flood/post-Flood boundary in the geologic record.

11. Conclusions

The observed fission track densities measured in zircons from samples of Cambrian, Jurassic, and Miocene tuffs in the Grand Canyon-Colorado Plateau region were found to exactly equate to the quantities of nuclear decay measured by radioisotope age determinations of these same rocks. Though thermal annealing has occurred in some zircon grains in the two Cambrian tuffs from the western Grand Canyon, the U-Pb radioisotope system has also been thermally reset, the resulting reset ages in both instances coinciding with the onset of the Laramide uplift of the Colorado Plateau. The fact that the thermal annealing of the fission tracks and the thermal resetting of the U-Pb radioisotope system in those zircons are exactly parallel is confirmation that the radioisotope ratios are a product of radioactive decay in just the same way as the fission tracks are physical evidence of nuclear decay. Furthermore, because the resetting of the U-Pb radioisotope system in zircons will only occur at elevated temperatures, the fact that it has been reset in these zircons could therefore be due to them having been heated by accelerated nuclear decay.

There has clearly been thermal annealing of the fission tracks and thermal resetting of the U-Pb radioisotope system in the zircons from the Cambrian tuff units in the western Grand Canyon. However, there remains sufficient strong evidence to conclude that both the fission tracks and radioisotope ratios in the zircons in these tuff units record more than 500 million years worth (at today's rates) of nuclear and radioisotope decay during deposition of the Phanerozoic strata sequence in the Grand Canyon-Colorado Plateau region. Given the evidence in that strata sequence of catastrophic deposition and independent evidence that most of this strata sequence was deposited during the year-long global catastrophic Biblical Flood only 4500 years ago,

then 500 million or more years worth (at today's rates) of nuclear and radioisotope decay had to have occurred during the Flood year only 4500 or so years ago. Thus, this nuclear and radioisotope decay had to have occurred at accelerated rates, and the fission tracks in the zircons in the tuffs within that strata sequence are physical evidence of that accelerated nuclear decay.

12. Further Work

For completeness sake, it is recommended that further work be undertaken on the Cambrian Muav and Tapeats tuffs in the western Grand Canyon to further resolve the discrepancy between the zircon fission track dates obtained in this study and those obtained in the previously published study. There is a brief mention in *Elston* [1989] of other outcrops of the Muav tuff (in particular) in the western Grand Canyon and beyond in Nevada, so these should be located and sampled for zircon fission track dating, because of the possibility that those zircons may not all have had their fission tracks thermally annealed. Then second, zircon grains from the outcrops sampled in this study, as well as those from outcrops sampled in future work, should be submitted for SHRIMP (sensitive high resolution ion microprobe) U-Pb radioisotope analyses and age determinations. Given that the SHRIMP can obtain U-Pb radioisotope analyses of microscopic spots in the zircon grains, this is a far more effective way of controlling the results obtained, particularly if zircon grains have growth zones. Furthermore, many more zircon grains can be cost effectively analyzed using the SHRIMP, compared with the twelve grains analyzed by TIMS in this study, which was a statistically small sample set. As a side benefit to this further work, the extent of these tuff beds may thus be better delineated because they could represent a catastrophic event horizon of considerable areal extent.

The phenomenon of annealing is a separate process from radioisotope and nuclear decay that most likely is also time dependent. This could thus provide the basis for tests of the hypothesis that decay rates have changed in the past, or may help discriminate the limits of when decay

rates were different. For example, tests of annealing of minerals in contact metamorphic zones versus the host rock and intrusive body could be constructive lines of research that may identify annealing independent of internal heating due to accelerated decay.

Otherwise, there is a lot still to learn about the history of nuclear and radioisotope decay during accumulation of the geologic record. In particular, the dilemma of whether fission tracks do or do not help to define the Flood/post-Flood boundary in the geologic record needs further investigation and resolution. For example, did accelerated decay terminate abruptly at the end of the Flood, or did gradual deceleration extend well into the post-Flood period? It is suggested that further work might focus on an extensive literature search to compile all fission track dating results obtained right through the Phanerozoic strata record, particularly where such dating results are cross-linked with radioisotope age determinations. It may be that some pattern emerges that enables the history of nuclear decay recorded in the strata to be deciphered and the Flood/post-Flood boundary placement in the geologic record be resolved. Also, evidence may emerge consistent with variations in decay rates during historic events.

Acknowledgments

While they would not agree with all interpretations and conclusions, the following people need to be acknowledged for the tremendous help they gave during the course of this study—Dr. Paul Green of the Geotrack International laboratory, Melbourne, for his skills in zircon fission track dating and for his patience and helpfulness through many discussions; Dr. Charles Naeser of the U.S. Geological Survey, Reston, Virginia, for his helpfulness in rechecking his past work and for his suggestions; Dr. Sam Iyengar of the Technology of Materials laboratory, Wildomar, California, for his analytical work and advice; Dr. Dennis Eberl and Dr. Richard Pollastro of the U.S. Geological Survey in Boulder and Denver, Colorado, respectively for helpful advice; Professor Warren Huff of the Geology Department at the University of Cincinnati for the information he so willingly provided; and Dr. Yakov Kapusta, the geochronology

laboratory manager at Activation Laboratories, Ancaster, Ontario, for his helpful analytical work. The assistance given to me with fieldwork and sampling of the Morrison Formation tuffs and Peach Springs Tuff by William (Bill) Hoesch of the Geology Department at the Institute for Creation Research, and of the Muav and Tapeats tuffs in the western Grand Canyon by Tom Vail of Canyon Ministries, was greatly appreciated and is duly acknowledged. The advice and encouragement of the other members of the RATE group is also acknowledged. Finally, this study was only made possible by donations to the RATE project from many supporters, and they are thanked for those donations.

Appendix: Fission Tracks and Fission Track Dating

A1. Fission Track Formation

When charged particles travel through a solid medium, they leave a trail of damage resulting from the transfer of energy from the particles to the atoms of the medium. The spontaneous fission of ^{238}U releases about 200 MeV of energy, much of which is transferred to the two product nuclides as kinetic energy. They travel about 7 μm in opposite directions, leaving a single trail of damage through the medium which is about 15 μm long. Such fission fragment tracks were first observed by *Silk and Barnes* [1959] during examination of irradiated solids under very high magnification with an electron microscope.

Fleischer et al. [1964] discovered that fission tracks are only found in insulating materials. In what is known as the ion-explosion spike model of fission track formation, *Fleischer et al.* [1965a] proposed that the passage of the highly charged, massive fission fragments causes ionization of atoms by violently repelling electrons away from a cylindrical tube surrounding their path (Figure 24). The positively charged ions at the crystal lattice sites along this path then mutually repel each other so that they are forced into the surrounding lattice away from the path of the fission particle, creating a cylindrical zone of damaged, disordered structure. This, in turn, causes relaxation stress in the surrounding matrix, resulting in a 100 Å (10 nm)-wide zone of strain

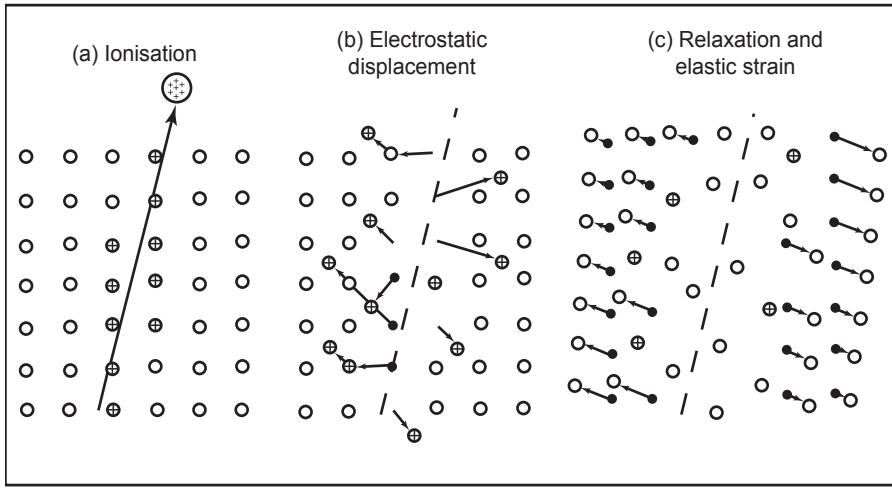

Figure 24. Schematic illustration of the process of formation of a fission track in a crystalline insulating solid (after *Fleischer et al.* [1975]).

which can actually be seen under an electron microscope. Conductors do not display fission tracks because the free movement of electrons in their lattice structures neutralizes the charged damage zones. However, if the solid in which the tracks form is an insulator at low temperatures, then the tracks may be preserved for times comparable to the claimed age of the universe.

The ability to generate fission tracks depends on the mass of the ionizing particle and the density of the material. In muscovite (white mica), the lowest mass particle which can generate tracks by irradiation is about 30 atomic mass units (amu). Fragments generated by fission of ^{238}U, with masses of about 90 and 135 amu respectively, are well above this threshold, so that they always generate tracks. On the other hand, α-particles, the major product of radioactive decay of ^{238}U, are so far below the critical mass that they cannot create tracks. Neither can they cause fission track erasure [*Fleischer et al*, 1965b].

Price and Walker [1962a] demonstrated that when irradiated materials were abraded to expose fission tracks at their surfaces, the damage zones could be preferentially dissolved by mineral acids, leading initially to very fine channels only 25 Å wide. However, these

could be enlarged by further chemical etching to yield wide pits which are observable under an optical microscope. *Price and Walker* [1962b] were the first to discover "fossil" fission tracks in minerals, generated by the spontaneous fission of the dispersed ^{238}U atoms in them. Indeed, they verified that fission tracks in natural minerals are due primarily to spontaneous fission of ^{238}U [*Price and Walker*, 1963] and proposed that the density of such fission tracks could be used as a dating tool for geological materials (such as micas) up to a billion years old in which they found track densities of up to 5×10^4 per cm^2. They found that induced fission of ^{238}U by natural thermal neutrons can be ignored, as can cosmic ray-induced fission of U and cosmic ray-induced spallation tracks. Consequently, *Fleischer et al.* [1965a] verified that the density of fission tracks in various geological materials and minerals could be used to obtain dates. They found that fission track dating of artificial and natural glasses and minerals produces results in agreement with those from radioisotope dating methods (Figure 25).

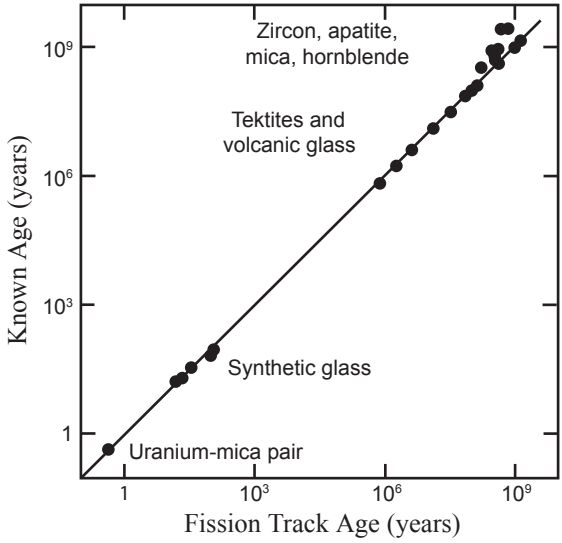

Figure 25. A comparison of specimen ages determined by fission track analysis with those from historical or other radiometric sources (after *Fleischer et al.* [1965a]).

A2. The Methodology of Fission Track Dating

The fission track method is now widely used for dating a wide variety of minerals, and therefore, the rocks containing them. It is regarded as being especially applicable to relatively young samples that have not been reheated since the time of their formation [*Fleischer and Price*, 1964b]. However, the method is also regarded as providing useful information about the thermal histories of older rocks, because the preservation of fission tracks is subject to annealing, with different minerals losing their tracks at different temperatures [*Fleischer et al*, 1969].

In order to date a mineral specimen by the fission track method, an interior surface is exposed by grinding and is then polished and etched with a suitable solvent under appropriate conditions [*Naeser*, 1967]. After etching the polished surface is examined with a petrographic microscope (magnification of 800 to 1800×) equipped with a flat-field eyepiece with a graticule to permit the counting of tracks in a known area. Fission tracks are readily distinguished by their characteristic tubular shape from other etched pits that result from imperfections or other causes. The track density due to spontaneous fission of ^{238}U is determined by counting a statistically significant number of tracks in a known area. Counting becomes difficult when the track density is less than 10 tracks per cm^2, but many minerals and glasses have much higher track densities so that from several hundred to several thousand tracks can be counted. The observed track density is related to the length of time during which tracks have accumulated and to the U concentration in the mineral or glass. *Fleischer and Price* [1964b] have estimated the dating range of fission track analyses with different types of minerals or glasses. Using the criterion that dates of reasonable precision can only be determined when the track density is at least 100 per cm^2, the lower end of the dating range can be estimated for the different minerals and glasses according to their U content (Figure 26) [*Wagner*, 1978].

The U concentration can be measured by a procedure that involves counting fission tracks produced by induced fission of ^{235}U due to irradiation of the sample with thermal neutrons in a nuclear reactor.

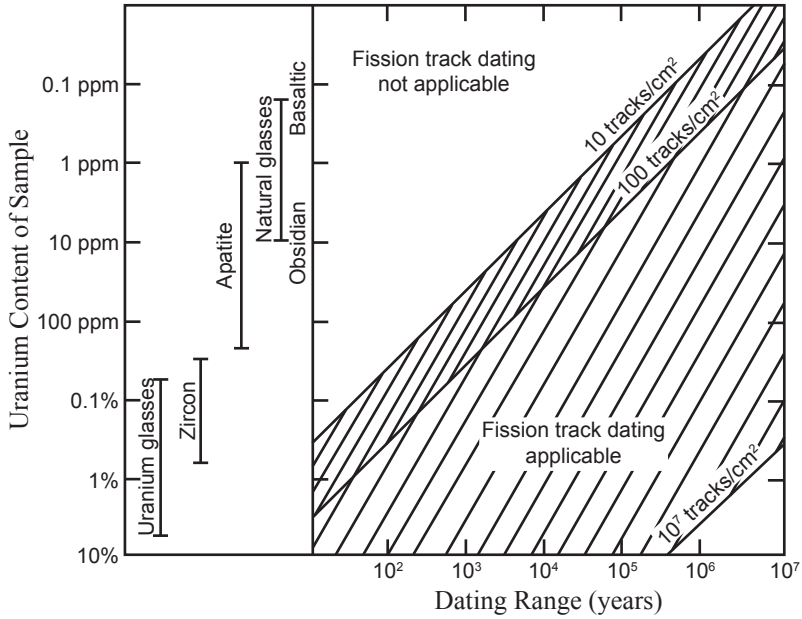

Figure 26. Diagram to show the dating range for fission track analysis of different kinds of geological material according to U content (after *Wagner* [1978]).

This can be accomplished in several ways described by *Gleadow* [1981] and *Hurford and Green* [1982]. The ideal is for the induced track count to be performed on the identical material to the spontaneous track count. Several different experimental methods are available which attempt to reach this ideal.

The method adopted by the earliest workers, such as *Price and Walker* [1963], was the population method, an expression coined by *Naeser* [1979]. This designation refers to the fact that the spontaneous and induced tracks are counted in different splits or sub-populations of the material being dated, which are nevertheless assumed to sample the same population. The success of the method depends on the material having a homogeneous distribution of U between the two splits. The method has proved particularly successful for dating glass and apatite, but unsuccessful for sphene and zircon, where U distribution is very

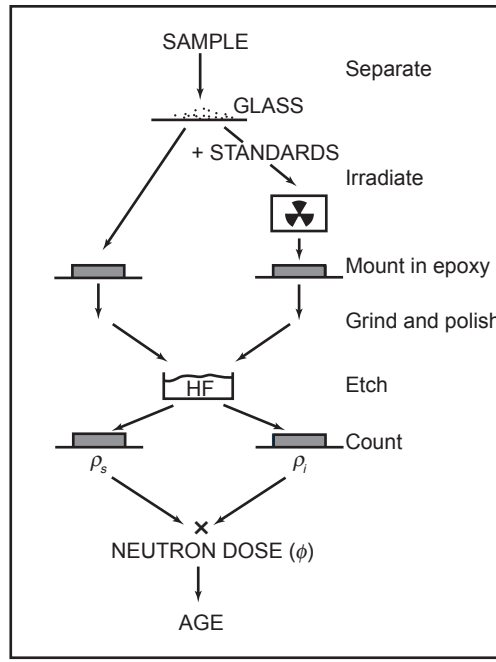

Figure 27. Schematic illustration of the population method of fission track analysis (after *Naeser and Naeser* [1984]).

variable both within and between grains. The sample is separated into two splits, one being irradiated with thermal neutrons along with the standard (flux monitor) (Figure 27). After irradiation of the induced track split, both splits are mounted in epoxy, ground, polished, and etched under identical conditions. This reveals an internal surface of the material and also removes any extraneous superficial tracks generated by U-bearing dust particles. Track densities are counted in both splits. The induced track density is calculated by subtracting the spontaneous track density (un-irradiated sample) from the total track density (irradiated sample). The population method can be statistically tested by counting track densities in numerous grains in each split.

An alternative procedure is after polishing, etching, and counting of the spontaneous tracks, they are destroyed by heating the specimen to cause annealing. The specimen in then exposed to thermal neutrons in

a nuclear reactor in order to produce new tracks by induced fission of ^{235}U. After the irradiation, a new surface is polished and etched, and the density of the induced tracks is determined. The U concentration of the sample is indicated by the observed density of the induced fission tracks, provided the effective thermal neutron flux and the duration of the irradiation are known. A variation of this method involves irradiating the sample after polishing, etching, and counting of the spontaneous tracks. However, the sample itself is then re-etched and re-counted to determine the induced track density by subtraction. Some disadvantages of this re-etching method are that the induced tracks are formed with only 50% efficiency due to the 2π geometry (Figure 28), and the spontaneous track pits may be unduly enlarged after the second etch so as to obscure some of the induced tracks.

The re-polishing method [*Naeser et al*., 1989b] is an improvement on the re-etching method. The sample is polished, etched, and counted for spontaneous track density. After irradiation it is re-polished to depths of at least 20 μm to reveal a new internal face with what is known as 4π track geometry yielding 100% efficiency (Figure 28). This new polished surface is then etched and counted to determine the induced track density by subtraction. This method has the advantage that both spontaneous and induced tracks are recorded under identical geometry, and spontaneous tracks are not over-enlarged by double etching. Also, surface contamination during irradiation is not a problem. The spontaneous and induced tracks are not generated by exactly the same sample material, but the two etched surfaces are so close together U inhomogeneity in the grain as a whole is unlikely to significantly bias the data. A disadvantage compared with the normal population method is that the two etching steps are performed separately, and may therefore vary slightly in efficiency.

The most popular method in use is the external detector method [*Fleischer et al*., 1965a] in which the U content of the material to be dated is determined by registration of the induced fission tracks in an external detector held against the same surface in which the spontaneous tracks are to be counted, rather than in the sample material itself. The sample is ground, polished, etched, and counted, after which a sheet

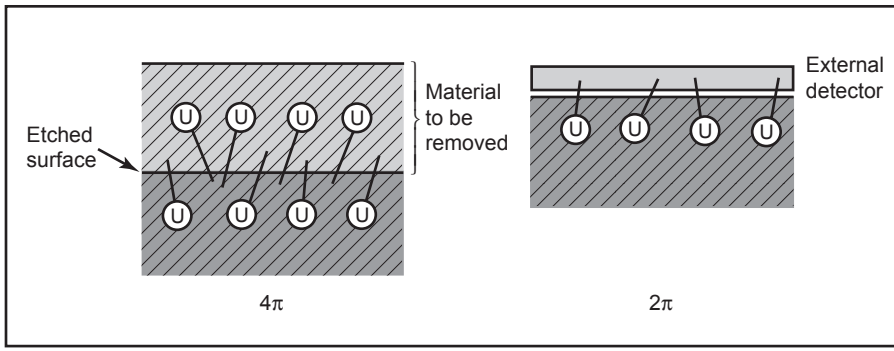

Figure 28. Schematic illustration of the difference between 4π (spherical) and 2π (hemi-spherical) geometry in track formation (after *Dickin* [1995]).

of detector material, often a sheet of low-U muscovite (white mica) or a plastic material like lexan, is placed in intimate contact with the etched surface. This must be done with absolute cleanliness to exclude U-bearing dust grains. After the neutron irradiation, the external detector is removed from the sample, etched, and the tracks caused by induced fission of ^{235}U in the specimen are counted (Figure 29). The advantage of this method is that both spontaneous and induced tracks are generated by the same sample material. It also eliminates problems caused by irregular distribution of U, and hence it is suited to the analysis of material with a very heterogeneous distribution of U, such as grains of zircon and sphene. On the other hand, the main disadvantage of this method is that the spontaneous and induced tracks are recorded under different spatial geometry conditions (see Figure 28 again). The spontaneous tracks are generated in the interior of the rock, and can therefore be formed by U atoms both above and below the polished and etched surface (spherical or 4π geometry). In contrast, the tracks induced in the external detector originate only from the U atoms in the surface of the analyzed material and are therefore generated with approximately one-half the frequency (hemi-spherical or 2π geometry). Therefore, a correction factor must be used to either reduce the observed density of spontaneous tracks by one-half, or increase the U concentration by a factor of 2. However, *Reimer et al.* [1970] question whether the efficiency of induced track formation is exactly 50%, or

whether small biases are introduced by the use of external detectors. Nevertheless, the use of external detectors was supported by *Gleadow and Lovering* [1977] and *Green and Durrani* [1978], and subsequent experiments showed that in most cases the ideal efficiency of 50% is achieved [*Hurford and Green*, 1982]. Thus external detectors are now widely used to measure the U concentrations of minerals dated by the fission track method.

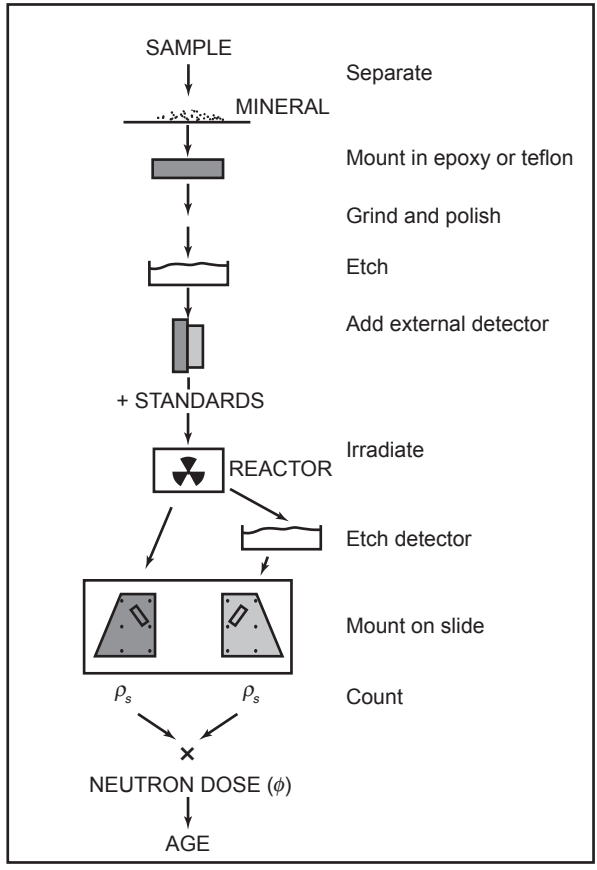

Figure 29. Schematic illustration of the external detector method of fission track analysis, as described by *Naeser* [1979]. In this version the counting of spontaneous tracks is performed after irradiation, unlike the sequence described in the text (after *Naeser and Naeser* [1984]).

The observed density of the fission tracks induced by the irradiation procedure is indicative of the U concentration of the specimen, provided the effective thermal neutron flux and the duration of the irradiation are known. The neutron "dose" (flux density × irradiation time) is determined by means of various flux monitors. One method is to include pieces of foil of Au, Cu, or Co of known weight with the mineral specimens being irradiated with thermal neutrons. After the irradiation, the induced γ-ray activity of these flux monitors can be used to determine the neutron dose, provided the neutron capture cross-section and the efficiency of the counting system are known. Alternately, one can irradiate glass of known U concentration (NBS series SRM 610 to 617 or Corning glasses U1 to U7 described by *Schreurs et al*. [1971]) and count the tracks resulting from induced fission of ^{235}U in an external detector. However, the relationship between the neutron dose and the resulting track density in U-bearing glass recorded in an external detector must be established by independent calibrations. *Hurford and Green* [1982] reported considerable scatter in that relationship over a six-year period and concluded that measurements of a neutron dose are very difficult and may be uncertain by up to ±10% of their absolute value.

The principle cause of systematic errors in fission track dates of natural samples is the fading of tracks due to annealing of the sample at elevated temperatures. For this reason, it is usually insisted that fission track dates of natural samples must be interpreted as "cooling ages" and do not necessarily coincide with the times at which the minerals crystallized in an igneous or metamorphic rock.

Another source of uncertainty inherent in fission track dating is the effectiveness of the etching process. The precise process of etching depends on the composition of the matrix and the nature, concentration, and temperature of the acid or alkali leaching solutions. This can give rise to a very large variation in the appearance of etched tracks in different materials and may thus affect the accuracy of track counting. These problems have been discussed by *Fleischer and Price* [1964a]. The three-dimensional profile or outline of an etched track depends on the rate of etching down the axis of the track (from its intersection with the surface), relative to the general rate of attack of the polished

surface. One problem in accurate track counting is to distinguish etched tracks from other features. Another source of uncertainty is caused by tracks which barely register in the etched surface. For example, tracks which are almost tangential to the surface may be completely erased by etching. Other tracks may not have intersected the original polished surface, but are exposed by the general attack of the surface during etching. These discrepancies will average out statistically if large numbers of tracks are counted with identical spatial geometry, but may cause large errors when spatial geometry varies. A more detailed discussion of track formation and track etching is given by *Fleischer et al*. [1975].

Other sources of error in fission track dating are statistical errors in counting tracks, and the possible uneven distribution of U in the specimen.

In conclusion, the prerequisite conditions for dating minerals by the fission track method are:-

- the concentration of U must be sufficient to produce a track density of >10 tracks per cm^2 in the time elapsed since cooling of the sample;
- the tracks must be stable at ordinary temperatures for time intervals comparable to the age being measured;
- the material must be sufficiently free of inclusions, defects, and lattice dislocations to permit identification and counting of etched fission tracks; and
- depending on the counting method used, the U distribution in the specimen must be uniform to permit the concentration of ^{238}U to be determined from the density of induced fission tracks in a different portion of the sample.

Because it is well known that chemical weathering adversely affects dates determined by radioisotope methods, *Gleadow and Lovering* [1974] made a study of the effect of weathering on the retention of fission tracks in apatite, sphene and zircon. They concluded that chemical weathering has no affect on fission track dates of sphene and zircon, but did result in a modest reduction of the date of apatite. The latter was attributed to the difficulty in identifying tracks in badly corroded crystals and to partial fading of tracks caused by the action of

groundwater. However, the apparent loss of tracks was partly offset by a lowering of the U concentration.

A3. Derivation of the Fission Track "Age" Equation

Several naturally occurring isotopes of high atomic number are known to decay by spontaneous fission and therefore produce fission tracks in minerals and glass. However, *Price and Walker* [1963] showed that in most cases such tracks are due primarily to spontaneous fission of ^{238}U. Track densities caused by spontaneous fission of ^{235}U and ^{232}Th are negligible. They also concluded that induced fission of ^{235}U due to absorption of natural thermal neutrons produced by spontaneous fission of ^{238}U is not important and can be ignored (because U concentrations in almost all rocks and minerals are too low for this process to occur), as can cosmic ray-induced fission of U and cosmic ray-induced spallation tracks. For these reasons, fission tracks in natural materials can be attributed to spontaneous fission of ^{238}U alone.

The decay constant for spontaneous fission of ^{238}U (λ_f) is approximately 7×10^{-17} yr^{-1}, which equates to a half-life ($t_{½}$) of 9.9×10^{15} yr [*Naeser et al*., 1989b]. There is some disagreement as to its exact value, but this uncertainty is not relevant to geological age determinations. Because the fission decay constant of ^{238}U is over a million times lower than the α-decay constant of ^{238}U, the decay of ^{238}U can be attributed entirely to α-emission, so its fission decay can be ignored in determining the isotope abundance of U through time.

Therefore, in a mineral grain containing ^{238}U atoms distributed evenly throughout its volume, the total number of decays of ^{238}U in a given volume of sample during time t is:

$$D = {}^{238}\mathrm{U}(e^{\lambda_\alpha t} - 1) \tag{8}$$

where D is the number of decay events per cm^3 of the sample, ^{238}U is the number of ^{238}U atoms per cm^3 of the sample at the present time, and λ_α is the decay constant of ^{238}U for α-emission, which is 1.55125×10^{-10} yr^{-1}.

The fraction of ^{238}U decays that are due to spontaneous fission and leave a track is thus:

$$F_s = \left(\frac{\lambda_t}{\lambda_a} \right)^{238} \mathrm{U}(e^{\lambda_\alpha t} - 1) \tag{9}$$

Only a certain fraction q of these tracks will cross the polished surface of the mineral grain and will be visible after etching to be counted. The area density of spontaneous fission tracks in that surface is therefore given by:

$$\rho_s = F_s q = \left(\frac{\lambda_f}{\lambda_\alpha} \right)^{238} \mathrm{U}\left(e^{\lambda_\alpha t} - 1\right) q \tag{10}$$

The number of fissions of ^{235}U induced by the thermal neutron irradiation per cm^3 of sample is:

$$F_i = {}^{235}\mathrm{U}\varphi\sigma \tag{11}$$

where ^{235}U is the number of ^{235}U atoms per cm^3 of sample at the present time, φ is the thermal neutron dose in units of neutrons per cm^2, and σ is the cross-section for induced fission of ^{235}U by thermal neutrons, which is equal to $580.2 \times 10^{-24} cm^2$.

The fraction of induced tracks that cross an interior surface and that will be counted after etching is also equal to q, provided the U atoms are evenly distributed throughout the volume of the specimen, and provided the etching is performed exactly as before. Thus the density of induced tracks is equal to:

$$\rho_i = F_i q = {}^{235}\mathrm{U}\varphi\sigma q \tag{12}$$

Combining equations (10) and (12) yields:

$$\frac{\rho_s}{\rho_i} = \left(\frac{\lambda_f}{\lambda_\alpha} \right) \left(\frac{e^{\lambda_\alpha \mathrm{t}} - 1}{\varphi\sigma \mathrm{I}} \right) \tag{13}$$

where I is the atomic ratio of $^{235}U/^{238}U$. Equation (13) can now be solved

for t and thus yield the "age" equation, first formulated by *Price and Walker* [1963]:

$$t = \frac{1}{\lambda_\alpha} \ln \left[1 + \left(\frac{\rho_s}{\rho_i} \right) \left(\frac{\lambda_\alpha}{\lambda_f} \right) \varphi \sigma \mathrm{I} \right] \tag{14}$$

It is important to equalize the densities of the spontaneous and induced tracks in order to reduce the error of measurement of ρ_s/ρ_i.

A4. The Zeta Calibration

Fission track dates determined by the methods outlined above are subject to systematic errors arising from the uncertainty of the decay constant for spontaneous fission of ^{238}U (λ_f) [*Bigazzi*, 1981], and from difficulties with measurements of the neutron dose (φ). Of course, it is possible to determine φ and σ directly by using flux monitors, such as iron wire or copper foil, but these types of flux monitors may not respond to reactor conditions in exactly the same way as geological materials. Therefore, an alternative procedure is to do a fission track analysis of a standard material with known U concentration. *Fleischer et al*. [1965a] used fragments of glass microscope slides to calibrate a reactor in this way, but this does not avoid the uncertainty of the ^{238}U fission decay constant. Furthermore, the problem is compounded by the fact that experimental determinations of λ_f by counting fission tracks in U-bearing glasses of known age of manufacture require knowledge of the neutron dose used to determine the U contents of the glasses. Therefore, any method used affects the value of λ_f that is obtained.

Thus, to eliminate both the flux term and the decay constant term, many workers started to use minerals dated by K-Ar as internal standards for the irradiation. *Fleischer and Hart* [1972] formalized this system into the "zeta calibration." Likewise, *Hurford and Green* [1982] proposed to calibrate the fission track method of dating against minerals of known age that had been dated by other radioisotope methods. Accordingly, the parameters in equation (13) whose magnitudes are in doubt are combined into one calibration factor termed "zeta" and symbolized by

ζ:

$$\zeta = \frac{\varphi \sigma \mathrm{I}}{\lambda_f} \tag{15}$$

The age equation for a sample of unknown age (t_{unk}) now becomes:

$$t_{unk} = \frac{1}{\lambda_\alpha} \ln \left[1 + \left(\frac{\rho_s}{\rho_i} \right)_{unk} \zeta \lambda_\alpha \right] \tag{16}$$

The value of ζ is determined by irradiating a mineral standard of known age (determined by radioisotope dating) with each batch of unknowns. Consequently, ζ is calculated from the measured ratio of the spontaneous and induced track densities of the standard. From equation (13):

$$\zeta = \frac{\left(e^{\lambda_\alpha t_{std}} - 1 \right)}{\lambda_\alpha (\rho_s / \rho_i)_{std}} \tag{17}$$

The value of ζ is then used to calculate dates for the unknown samples that were irradiated with the standard. The resulting fission track dates depend on the assumptions that:

- the age of the standard is known accurately;
- the fission track densities of the standard and unknowns were determined by the same procedure; and
- that the unknowns and the standard were irradiated together.

When the age of the standard is significantly less than the half-life of ^{238}U, equation (17) can be simplified by letting $e^{\lambda_\alpha t_{std}} - 1 = \lambda_\alpha t_{std}$. In this case:

$$\zeta = \frac{t_{std}}{(\rho_s / \rho_i)_{std}} \tag{18}$$

The fission track date of unknowns then becomes:

$$t_{unk} = \frac{1}{\lambda_\alpha} \ln \left[1 + \frac{(\rho_s / \rho_i)_{unk}}{(\rho_s / \rho_i)_{std}} \lambda_\alpha t_{std} \right] \tag{19}$$

The failure to resolve the fission decay constant problem can perhaps be attributed to the use of this calibration method, which transfers the uncertainty into the age determination of the geological reference material. Use of such material was recommended for all fission track

dating studies by a working group of the International Union of Geological Sciences (I.U.G.S.) Subcommission on Geochronology [*Hurford*, 1990]. Minerals to be used as calibration standards for fission track dating must have cooled rapidly and must yield concordant dates by different appropriate radioisotope methods. Moreover, they must be readily obtainable in pure form and adequate quantity. These criteria are best met by volcanic rocks that cooled rapidly and remained unaltered after crystallization. *Hurford and Green* [1983] selected zircons from three volcanic deposits and from kimberlite pipes in South Africa as standards, the most well-known of these being the zircon from the Fish Canyon Tuff in the San Juan Mountains of Colorado, U.S.A., described by *Naeser et al.* [1981] with an age of 27.9±0.7 Ma.

An alternative to the procedure outlined above is to use the standard minerals to calibrate U-bearing dosimeter glasses. The neutron dose (φ) is related to the density of induced fission tracks in the dosimeter glass (ρ_d) by the relationship:

$$\varphi = B\rho_d \tag{20}$$

where B is a calibration constant and ρ_d is measured by an external mica track-detector. Substituting equation (20) into equation (14) yields:

$$t_{unk} = \frac{1}{\lambda_\alpha} \ln\left[1 + \left(\frac{\rho_s}{\rho_i}\right)_{unk} \left(\frac{\lambda_\alpha}{\lambda_f}\right) B\rho_d \sigma \mathrm{I}\right] \tag{21}$$

Next, ζ is redefined as:

$$\zeta = \frac{B\sigma \mathrm{I}}{\lambda_f} \tag{22}$$

Thus, the "age" equation now becomes:

$$t_{unk} = \frac{1}{\lambda_\alpha} \ln\left[1 + \left(\frac{\rho_s}{\rho_i}\right)_{unk} \lambda_\alpha \rho_\alpha \zeta\right] \tag{23}$$

The new ζ is determined by irradiating dosimeter glasses with mineral standards of known age. After irradiation, the induced track density in

the dosimeter (ρ_d) and in the standard mineral (ρ_i) are determined by counting tracks in the external detectors used with both. The value of ζ for a given glass dosimeter is then calculated by means of equation (13), in which φ is replaced by $B\rho_d$ as per equation (20) to yield:

$$\left(\frac{\rho_s}{\rho_i}\right)_{std} = \left(\frac{\lambda_t}{\lambda_\alpha}\right)\frac{\left(e^{\lambda_\alpha t_{std}} - 1\right)}{B\rho_d \sigma \mathrm{I}} \tag{24}$$

Next, ζ as defined by equation (22) is inserted to yield:

$$\left(\frac{\rho_s}{\rho_i}\right)_{std} = \left(\frac{e^{\lambda_\alpha t_{std}} - 1}{\lambda_\alpha \zeta \rho_d}\right) \tag{25}$$

from which it follows that:

$$\zeta = \frac{\left(e^{\lambda_\alpha t_{std}} - 1\right)}{\lambda_\alpha \left(\rho_s / \rho_i\right)_{std} \rho_d} \tag{26}$$

Therefore, the modified ζ parameter for a glass dosimeter can be used to determine the age of an unknown mineral from equation (23), provided the dosimeter is irradiated with the unknown mineral and ρ_d is determined by counting the resultant tracks in an external detector. In essence, the ζ parameter enables the neutron dose to be determined directly from the density of induced tracks in the dosimeter glass. *Hurford and Green* [1983] determined values of ζ for three glass dosimeters which they irradiated numerous times with each of the zircon standards they had selected. Of course, equation (26) depends on the age of the standard (t_{std}) having been accurately determined by the radioisotope "dating" methods. However, because there is evidence that radioisotope decay was accelerated at some time or times in the past [*Humphreys et al*., 2003a, b, 2004; *Snelling et al*., 2003a; *Austin*, 2005; *Humphreys*, 2005; *Snelling*, 2005a, b], such past accelerated radioisotope decay would render the radioisotope "dating" of the standard suspect, which in turn makes the value of ζ suspect. Thus at best fission track dating, like radioisotope dating, would only yield relative "ages." Nevertheless, the quantity of fission tracks is physical evidence of how much nuclear decay has occurred in the past during accumulation of the geologic record.

A5. Annealing and the Closing Temperature

In most materials, fission tracks are stable for long periods of time at room temperature. However, at elevated temperatures the tracks fade as the damage done by the charged particles is healed. During this process the displaced ions within the damaged track lose their charge and return to their normal lattice positions, after which the track is no longer susceptible to preferential acid attack. The rate at which tracks fade (or are annealed) at a given temperature varies among different minerals and glasses. Consequently, two different minerals in the same rock that have been exposed to the same elevated temperature for the same length of time may have differing fission track dates. Such discordance of dates of cogenetic minerals may thus provide information about the temperature history of the rock.

In experiments on track annealing in mica, *Fleischer et al*. [1964] claimed that track annealing progressed by the accumulated "healing up" of short segments at random points along the length of tracks. However, subsequent work on other materials (for example, on glass by *Storzer and Wagner* [1969]) has shown that the healing process occurs principally at the ends of each track, causing irregular and progressive shortening. As the length of the tracks is diminished by healing they have a smaller probability of intersecting the free surface during the etching treatment. Hence, fewer tracks become etched and the apparent track density decreases. This correlation between track length and track density is termed the "random line segment model" [*Fleischer et al*., 1975].

Early studies showed that different materials have different degrees of resistance to fission track annealing [*Fleischer and Price*, 1964b]. In addition, however, a temperature-time relationship is found for the annealing process. The higher the temperature, the shorter the time required for complete annealing of tracks in any given material. To examine this behavior, *Fleischer and Price* [1964a] performed laboratory annealing experiments in which the reduction in track density in a chosen mineral was measured as a function of increasing temperature and duration of heating. It was found that annealing obeyed

a Boltzmann's law relationship:

$$t = Ae^{E/kT} \tag{27}$$

where t is the annealing time for a specific reduction in track density, A is a constant, E is the activation energy in units of kcal/mol or electron volts (eV), k is Boltzmann's constant, which equals 8.6171×10^{-5} eV/K, and T is the absolute temperature in K. Much work has subsequently been devoted to determining accurate Boltzmann relationship annealing curves for different minerals and materials, both by laboratory and apparently well-constrained geological studies.

By taking natural logarithms of both sides a linear equation is obtained:

$$\ln t = \ln A + \frac{E}{kT} \tag{28}$$

This is the equation of a straight line in co-ordinates of ln t and $1/T$ having a positive slope equal to E/k and an intercept on the y-axis equal to ln A. The linear relationship between ln t and $1/T$ permits the extrapolation of laboratory measurements obtained at elevated temperatures and short time periods to lower temperatures and the claimed geological time periods.

Detailed laboratory experiments were performed on apatite and sphene by *Naeser and Faul* [1969]. These showed that annealing is a progressive process, with different degrees of track annealing in these two minerals each defining their own Boltzmann's relationship lines when the experimental results were plotted on what is known as an Arrhenius diagram of time against reciprocal temperature (Figure 30). The fan of annealing lines in Figure 30 is evidence for the existence of a range of activation energies for track annealing within each mineral. This implies that as annealing progresses (as measured by the fraction of tracks lost) it also becomes progressively more difficult [*Storzer and Wagner*, 1969]. Hence, when comparing the annealing properties of different minerals it is necessary to compare equal fractions of track loss, such as 50%.

Thus the data of *Naeser and Faul* [1969], shown in Figure 30, indicate that the tracks in apatite and sphene, which are common accessories

in igneous and metamorphic rocks, fade at very different rates. This diagram can then be ostensibly used to predict track fading in these minerals in response to an increase in temperature for a given rate of heating. For a heating period of one million years, apatite would

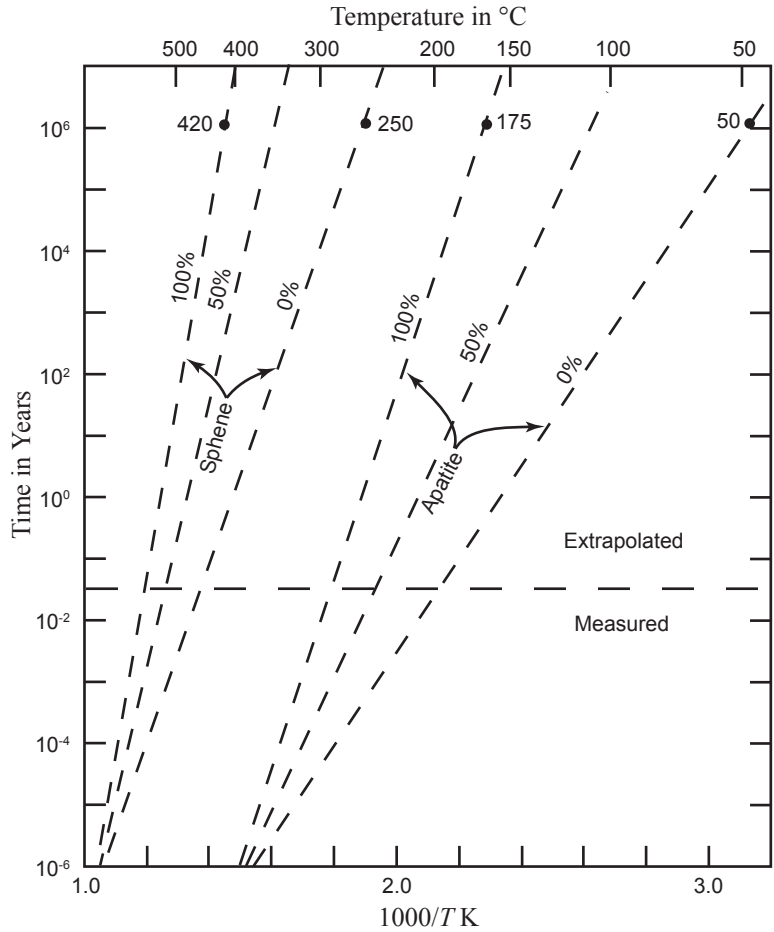

Figure 30. Fading of fission tracks in apatite and sphene (after *Naeser and Faul* [1969]). The lines marked 0% indicate temperatures and time periods at which no tracks are lost. The lines labeled 100% indicate conditions when all tracks are lost. The effective temperature recorded by the fission track age of a mineral is the value at which about 50% of the tracks are preserved. *T* is temperature in degrees Kelvin (K).

appear to begin losing tracks at about 50°C and would be completely annealed at about 175°C, while tracks in sphene would not fade unless the temperature is raised to 250°C and the mineral would be annealed completely only at 420°C. Therefore, fission track dates of apatite can be completely reset by episodic heating under conditions implied by its track-fading curve for 100% track loss. Under the same conditions, sphene loses no tracks at all, and its fission track date remains unaffected. Therefore, when fission track dates of these two minerals extracted from the same rock are concordant, the rock presumably cooled rapidly and was not reheated at a later time. On the other hand, when the dates are discordant, that is, the sphene date is greater than the apatite date, the rock presumably either cooled slowly or was reheated to a temperature at which track fading occurred in apatite but not in sphene.

Apatite is regarded as a particularly good indicator of the cooling history of a rock, because apparently it retains fission tracks only at temperatures that are significantly less than the so-called "blocking temperatures" for the Rb-Sr or K-Ar radioisotope geochronometers in coexisting micas. The exact temperature at which apatite retains all tracks (0% loss curve in Figure 30) depends on the cooling rate. When the rate of cooling is high, the cooling time is short, and complete track retention occurs at a higher temperature than when the cooling rate is slow. At any given cooling rate, track retention increases from 0 to 100% as the temperature drops so that the observed track density represents approximately the time elapsed since the temperature passed through the value at which 50% of the tracks are retained. Consequently, fission track dates can be interpreted as the time elapsed since they cooled through their 50% retention temperatures. This temperature is also known as the "closing temperature" by analogy with the "blocking temperature" defined with respect to retention of radiogenic ^{40}Ar and ^{87}Sr.

The closing temperatures of different minerals at different cooling rates are shown in Figure 31, based primarily on a review of the literature by *Sharma et al.* [1980]. The diagram demonstrates that minerals have widely differing closing temperatures and that these temperatures increase with faster cooling rates. The closing temperatures, at a cooling

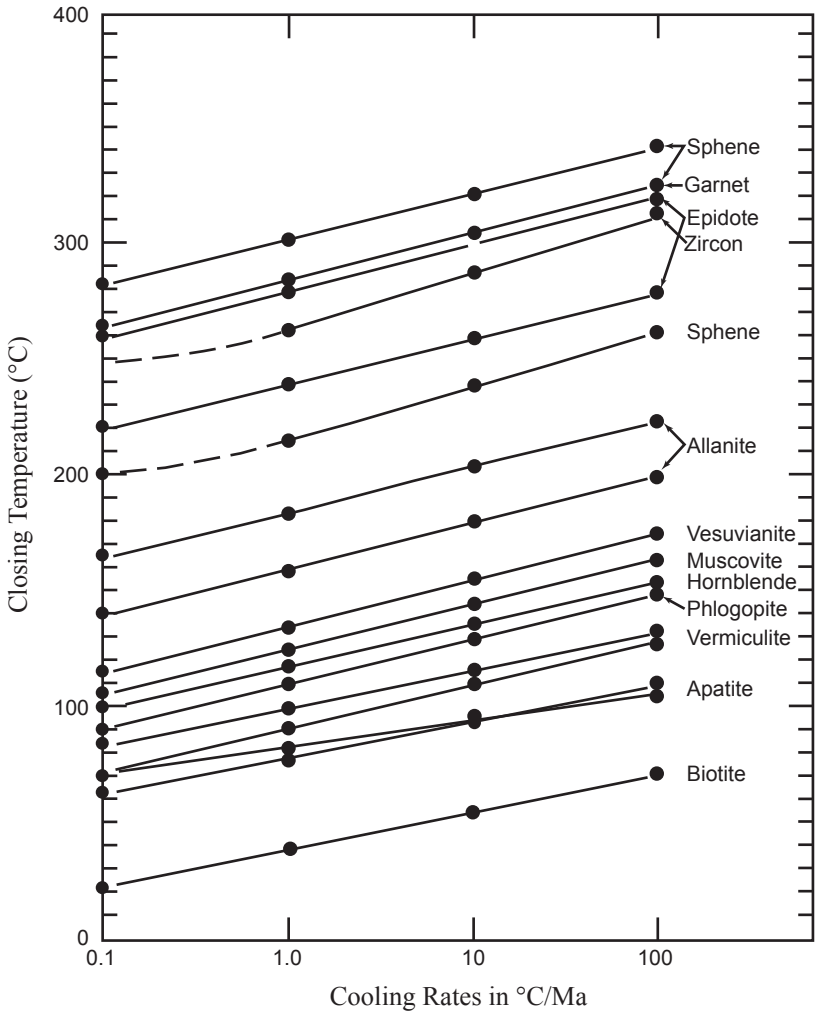

Figure 31. Closing temperatures for retention of fission tracks for minerals cooling at different rates. The closing temperature is defined as the temperature below which all fission tracks are retained in the mineral corresponding to the 50% track retention temperature. The closing temperature of chlorite is similar to that of apatite. (After *Haack* [1977]; *Sharma et al.* [1980]; *Bal et al.* [1983]; *Faure* [1986]; *Faure and Mensing* [2005].)

rate of 1°C/Ma, range from about 300°C for sphene to about 40°C for biotite. Therefore, the minerals of plutonic igneous or high-grade metamorphic rocks, that are claimed to have cooled slowly, potentially record a sequence of dates at which the temperature passed through their respective closing temperatures. Differences between fission track dates of two coexisting minerals, such as sphene and apatite, therefore would seem to indicate how long it took for the temperature to decrease from the closing temperature of sphene to that of apatite. For this reason, the fission track dates of different minerals and their closing temperatures have been used to reconstruct the apparent cooling histories of igneous and metamorphic rocks.

The closing temperatures of some minerals in Figure 31 are highly discrepant. For example, the closing temperature of sphene at a cooling rate of 1°C/Ma is 302°C according to *Nagpaul et al.* [1974], 284°C according to *Naeser and Dodge* [1969], and only 215°C according to *Bal et al.* [1983]. Similarly, discrepant closing temperatures have been reported for epidote, allanite, and vermiculite, according to the tabulation of *Sharma et al.* [1980]. These differences are caused primarily by the different etching conditions that were used to reveal the tracks during the annealing experiments from which the closing temperatures were determined. The different etchants used were not equally effective in retrieving fission tracks that had begun to fade as a result of annealing. Therefore, the experimentally determined closing temperatures depend on the etching solution used, its temperature, and the duration of the exposure. In addition, variations in the chemical compositions of the minerals being etched may affect their responses to a particular etchant. For these reasons, fission track dates of minerals should be determined by the same etching procedure as that used to determine their closing temperatures in order to avoid errors in cooling rates claimed to be derived from such data.

Fortunately, the differences in the closing temperatures of minerals do not depend on the cooling rates, as shown by the fact that the lines in Figure 31 are approximately parallel. After the presumed cooling rate has been determined as described above, the actual temperatures corresponding to the fission track dates of the minerals can apparently

be determined from the relationship between cooling rates and closing temperatures [*Haack*, 1977; *Faure*, 1986; *Faure and Mensing*, 2005].

Nevertheless, it has been found that the fading of fission tracks causes fission track dates of minerals and natural glasses to be lower than their geologic ages. In some cases, it is believed that the discrepancy can be reduced by employing longer etching times or by using etchants that are more effective in retrieving partially annealed tracks. To some extent, the effect of track fading is taken into consideration when fission track dates are interpreted as the time elapsed since the temperature dropped below the 50% track retention value. However, it needs to be noted that fission tracks are still sometimes used to determine the "ages" of rocks and minerals that may not be datable by other radioisotope methods. For this reason, several procedures have been developed to ostensibly correct fission track dates for the effects of track fading, such as "plateau dating" [*Storzer and Poupeau*, 1973; *Poupeau et al*., 1978, 1979; *Poupeau*, 1981; *Storzer and Wagner*, 1982].

References

Anderson, O.J., and S.G. Lucas, Synopsis of the Morrison Formation, in *Guidebook for the Geological Excursion of the Continental Jurassic Symposium*, edited by M. Morales, pp. 79–86, Museum of Northern Arizona, Flagstaff, 1996.

Austin, S.A. (editor), *Grand Canyon: Monument to Catastrophe*, Institute for Creation Research, Santee, California, 1994.

Austin, S.A., Do radioisotope clocks need repair? Testing the assumptions of isochron dating using K-Ar, Rb-Sr, Sm-Nd, and Pb-Pb isotopes, in *Radioisotopes and the Age of the Earth: Results of a Young-Earth Creationist Research Initiative*, edited by L. Vardiman, A.A. Snelling, and E.F. Chaffin, pp. 325–392, Institute for Creation Research, El Cajon, California, and Creation Research Society, Chino Valley, Arizona, 2005.

Austin, S.A., J.R. Baumgardner, D.R. Humphreys, A.A. Snelling, L. Vardiman, and K.P. Wise, Catastrophic plate tectonics: a global Flood model of earth history, in *Proceedings of the Third International Conference on Creationism*, edited by R.E. Walsh, pp. 609–621, Creation

Science Fellowship, Pittsburgh, Pennsylvania, 1994.

Baadsgaard, H., U-Th-Pb dates on zircons from the early Precambrian Amîtsoq Gneisses, Godthaab District, West Greenland, *Earth and Planetary Science Letters, 19*, 22–28, 1973.

Bal, K. D., N. Lal, and K. K. Nagpaul, Zircon and sphene as fission-track geochronometer and geothermometer: a reappraisal, *Contributions to Mineralogy and Petrology, 83*, 199–203, 1983.

Barrenechea, J. F., M. Rodas, and J. R. Mas, Clay mineral variations associated with diagenesis and low-grade metamorphism of early Cretaceous sediments in the Cameros Basin, Spain, *Clay Minerals, 30*, 119–133, 1995.

Baumgardner, J. R., ^{14}C evidence for a recent global Flood and a young earth, in *Radioisotopes and the Age of the Earth: Results of a Young-Earth Creationist Research Initiative*, edited by L. Vardiman, A. A. Snelling, and E. F. Chaffin, pp. 587–630, Institute for Creation Research, El Cajon, California, and Creation Research Society, Chino Valley, Arizona, 2005.

Baumgardner, J. R., A. A. Snelling, D. R. Humphreys, and S. A. Austin, Measurable ^{14}C in fossilized organic materials: confirming the young earth Creation-Flood model, in *Proceedings of the Fifth International Conference on Creationism*, edited by R. L. Ivey, Jr., pp. 127–142, Creation Science Fellowship, Pittsburgh, Pennsylvania, 2003a.

Baumgardner, J. R., A. A. Snelling, D. R. Humphreys, and S. A. Austin, The enigma of the ubiquity of ^{14}C in organic samples older than 100 ka, *EOS, Transactions of the American Geophysical Union, 84*(46), Fall Meeting Supplement, Abstract V32C-1045, 2003b.

Bielecki, J. W., *A Study in Spontaneous Fission Track Density in Resting Spring Range Obsidian (Miocene) near Shoshone, California*, Unpublished M. S. dissertation, Graduate School, Institute for Creation Research, Santee, California, 1994.

Bielecki, J. W., Search for accelerated nuclear decay with spontaneous fission of ^{238}U, in *Proceedings of the Fourth International Conference on Creationism*, edited by R. E. Walsh, pp. 79–88, Creation Science Fellowship, Pittsburgh, Pennsylvania, 1998.

Bigazzi, G., The problem of the decay constant λ_f of ^{238}U, *Nuclear Tracks, 5*, 35–44, 1981.

Bilbey, S. A., R. L. Kerns, Jr., and J. T. Bowman, Petrology of the Morrison

Formation, Dinosaur Quarry Quadrangle, Utah, *Utah Geological and Mineral Survey Special Studies 48*, 1974.

Billingsley, G.H., and D.P. Elston, Geologic log of the Colorado River from Lees Ferry to Temple Bar, Lake Mead, Arizona, in *Geology of Grand Canyon, Northern Arizona (with Colorado River Guides)*, edited by D.P. Elston, G.H. Billingsley, and R.A. Young, pp. 1–36, American Geophysical Union, Washington, DC, 1989.

Blenkinsop, T.G., Definition of low-grade metamorphic zones using illite crystallinity, *Journal of Metamorphic Geology, 6*, 623–636, 1988.

Brime, C., Metamorfismo de bajo grado: Diferencias en escala o diferencias en grado metamórfico?, *Trabajos de Geologia, 21*, 61–66, 1999.

Brime, C., J.A. Talent, and R. Mawson, Low-grade metamorphism in the Palaeozoic sequence of the Townsville hinterland, northeastern Australia, *Australian Journal of Earth Sciences, 50*, 751–767, 2003.

Bowring, S.A., I.S. Williams, and W. Compston, 3.96 Ga gneisses from the Slave Province, Northwest Territories, Canada, *Geology, 17*, 971–975, 1989.

Bucher, K., and M. Frey, *Petrogenesis of Metamorphic Rocks*, seventh edition, Springer-Verlag, Berlin, 2002.

Buesch, D.C., and G.A. Valentine, Peach Springs Tuff and volcanic stratigraphy of the southern Cerbat Mountains, Kingman, Arizona, in *Cenozoic Stratigraphy, Structure and Mineralization in the Mojave Desert, Guidebook and Volume, Field Trip Nos. 5 and 6*, compiled by P.E. Ehlig, pp. 7–14, 82nd Annual Meeting, Cordilleran Section, Geological Society of America, Los Angeles, California, 1986.

Chaffin, E.F., A young earth?—a survey of dating methods, *Creation Research Society Quarterly, 24*, 109–117, 1987.

Chaffin, E.F., Theoretical mechanisms of accelerated radioactive decay, in *Radioisotopes and the Age of the Earth: A Young-Earth Creationist Research Initiative*, edited by L. Vardiman, A.A. Snelling, and E.F. Chaffin, pp. 305–331, Institute for Creation Research, El Cajon, California, and Creation Research Society, St. Joseph, Missouri, 2000.

Chaffin, E.F., Accelerated decay: theoretical considerations, in *Radioisotopes and the Age of the Earth: Results of a Young-Earth Creationist Research Initiative*, edited by L. Vardiman, A.A. Snelling, and E.F. Chaffin,

pp. 525–585, Institute for Creation Research, El Cajon, California, and Creation Research Society, Chino Valley, Arizona, 2005.

Cherniak, D. J., and E. B. Watson, Pb diffusion in zircon, *Chemical Geology, 172*, 5–24, 2000.

Cherniak, D. J., and E. B. Watson, Diffusion in zircon, in *Zircon*, edited by J. M. Hanchar and P. W. O. Hoskin, pp. 113–143, Mineralogical Society of America, Washington, DC, Reviews in Mineralogy and Geochemistry, vol. 53, 2003.

Dickin, A. P., *Radiogenic Isotope Geology*, Cambridge University Press, New York, 1995.

Dumitru, T. A., I. R. Duddy, and P. F. Green, Mesozoic-Cenozoic burial, uplift, and erosion history of the west-central Colorado Plateau, *Geology, 22*(6), 499–502, 1994.

Elston, D. P., Correlations and facies changes in the Lower and Middle Cambrian Tonto Group, Grand Canyon, Arizona, in *Geology of Grand Canyon, Northern Arizona (with Colorado River Guides)*, edited by D. P. Elston, G. H. Billingsley, and R. A. Young, pp. 131–136, American Geophysical Union, Washington, DC, 1989.

Epstein, A. G., J. B. Epstein, and L. D. Harris, Conodont color alteration—an index to organic metamorphism, *U. S. Geological Survey, Professional Paper 995*, 1977.

Essene, E. J., and P. R. Peacor, Clay mineral thermometry—a critical perspective, *Clays and Clay Minerals, 43*(5), 540–553, 1995.

Faure, G., *Principles of Isotope Geology*, second edition, pp. 341–353, John Wiley & Sons, New York, 1986.

Faure, G., and T.S. Mensing, *Isotopes: Principles and Applications*, third edition, John Wiley & Sons, Hoboken, New Jersey, 2005.

Finch, R. J., and J. M. Hanchar, Structure and chemistry of zircon and zircon-group minerals, in *Zircon*, edited by J. M. Hanchar and P. W. O. Hoskin, pp. 1–25, Mineralogical Society of America, Washington, DC, Reviews in Mineralogy and Geochemistry, vol. 53, 2003.

Fleischer, R. L., and H. R. Hart, Fission track dating: techniques and problems, in *Calibration of Hominoid Evolution*, edited by W. Bishop, J. Miller, and S. Cole, pp. 135–170, Scottish Academic Press, 1972.

Fleischer, R. L., and P. B. Price, Glass dating by fission fragment tracks,

Journal of Geophysical Research, 69, 331–339, 1964a.

Fleischer, R. L., and P. B. Price, Techniques for geological dating of minerals by chemical etching of fission fragment tracks, *Geochimica et Cosmochimica Acta, 28*, 1705–1714, 1964b.

Fleischer, R. L., P. B. Price, E. M. Symes, and D. S. Miller, Fission track ages and track-annealing behavior of some micas, *Science, 143*, 349–351, 1964.

Fleischer, R. L., P. B. Price, and R. M. Walker, Tracks of charged particles in solids, *Science, 149*, 383–393, 1965a.

Fleischer, R. L., P. B. Price, and R. M. Walker, Effects of temperature, pressure, and ionization on the formation and stability of fission tracks in minerals and glasses, *Journal of Geophysical Research, 70*, 1497–1502, 1965b.

Fleischer, R. L., P. B. Price, and R. M. Walker, Nuclear tracks in solids, *Scientific American, 220*, 30–39, 1969.

Fleischer, R. L., P. B. Price, and R. M. Walker, *Nuclear Tracks in Solids: Principles and Applications*, University of California Press, Berkeley, 1975.

Frey, M., and H. J. Kisch, Scope of subject, in *Low Temperature Metamorphism*, edited by M. Frey, pp. 1–8, Blackie, Glasgow, 1987.

Frey, M., and D. Robinson (editors), *Low-Grade Metamorphism*, Blackwell Science, London, 1999.

Galbraith, R. F., On statistical models for fission track counts, *Mathematical Geology, 13*, 471–488, 1981.

Galbraith, R. F., On statistical estimation in fission track dating, *Mathematical Geology, 16*, 653–669, 1984.

Galbraith, R. F., Graphical display of estimates having differing standard errors, *Technometrics, 30*(3), 271–281, 1988.

Galbraith, R. F., Radial plot: graphical assessment of spread in ages, *Nuclear Tracks and Radiation Measurements, 17*(3), 207–214, 1990.

Galbraith, R. F., and P. F. Green, Estimating the component ages in a finite mixture, *Nuclear Tracks and Radiation Measurements, 17*(3), 197–206, 1990.

Gentry, R. V., T. K. Sworski, H. S. McKown, D. H. Smith, R. E. Eby, and W. H. Christie, Differential lead retention in zircons: implications for nuclear waste management, *Science, 216*, 296–298, 1982.

Glazner, A. F., J. E. Nielson, K. A. Howard, and D. M. Miller, Correlation

of the Peach Springs Tuff, a large-volume Miocene ignimbrite sheet in California and Arizona, *Geology, 14*(10), 840–843, 1986.

Gleadow, A. J. W., Fission-track dating: what are the real alternatives?, *Nuclear Tracks, 5*, 3–14, 1981.

Gleadow, A.J. W., and J. F. Lovering, The effect of weathering on fission track dating, *Earth and Planetary Science Letters, 22*, 163–168, 1974.

Gleadow, A. J. W., and J. F. Lovering, Geometry factor for external track detectors in fission-track dating, *Nuclear Tracks, 1*, 99–106, 1977.

Gleadow, A. J. W., I. R. Duddy, P. F. Green, and J. F. Lovering, Confined fission track lengths in apatite: a diagnostic tool for thermal history analysis, *Contributions to Mineralogy and Petrology, 94*, 405–415, 1986.

Gleadow, A. J. W., A. J. Hurford, and R. D. Quaife, Fission track dating of zircon: improved etching techniques, *Earth and Planetary Science Letters, 33*, 273–276, 1976.

Green, P. F., A new look at statistics in fission-track dating, *Nuclear Tracks, 5*(1/2), 77–86, 1981.

Green, P. F., Comparison of zeta calibration baselines for fission-track dating of apatite, zircon and sphene, *Chemical Geology, 58*, 1–22, 1985.

Green, P. F., The relationship between track shortening and fission track age reduction in apatite: combined influences of inherent instability, annealing and anisotropy, length bias, and system calibration, *Earth and Planetary Science Letters, 89*, 335–352, 1988.

Green, P. F., Fission track dating of zircon from a sample of tuff, *Geotrack Report #823*, unpublished, Geotrack International Pty Ltd, Melbourne, 2001.

Green, P. F., Fission track dating of zircon from five volcanic rock samples, *Geotrack Report #841*, unpublished, Geotrack International Pty Ltd, Melbourne, 2002.

Green, P. F., Fission track dating of zircon from six volcanic rock samples, *Geotrack Report #860*, unpublished, Geotrack International Pty Ltd, Melbourne, 2003.

Green, P. F., and S. A. Durrani, A quantitative assessment of geometry factors for use in fission-track studies, *Nuclear Track Detectors, 2*, 207–213, 1978.

Green, P. F., I. R. Duddy, G. M. Laslett, K. A. Hegarty, A. J. W. Gleadow, and J. F. Lovering, Thermal annealing of fission tracks in apatite. 4, Qualitative

modelling techniques and extension to geological timescales, *Chemical Geology, 79*, 155–182, 1989.

Gregory, H.E., The San Juan country: a geographic and geologic reconnaissance of southeastern Utah, *U.S. Geological Survey, Professional Paper 188*, 1938.

Gusa, S., Recognition of the Peach Springs Tuff, California and Arizona, using heavy mineral suites, *U.S. Geological Survey, Open-File Report 86-522*, 1986.

Gusa, S., J.E. Nielson, and K.A. Howard, Heavy-mineral suites confirm the wide extent of the Peach Springs Tuff in California and Arizona, U.S.A., *Journal of Volcanology and Geothermal Research, 33*, 343–347, 1987.

Haack, U., The closing temperature for fission track retention in minerals, *American Journal of Science, 277*, 459–464, 1977.

Harris, A.G., Conodont color alteration, an organo-mineral metamorphic index, and its application to Appalachian Basin geology, in *Aspects of Diagenesis*, edited by A. Scholle and P.R. Schluger, pp. 3–16, Society of Economic Paleontologists and Mineralogists, Special Publication 26, Tulsa, Oklahoma, 1979.

Harris, A.G., Color and alteration: an index to organic metamorphism in conodont elements, *Treatise on Invertebrate Paleontology, Part W, Miscellanea Supplement 2, Conodonta*, edited by R.A. Robison, pp. W56–W60, Geological Society of America, Boulder, Colorado, 1981.

Harrison, T.M., R.L. Armstrong, C.W. Naeser, and J.E. Harakal, Geochronology and thermal history of the Coast Plutonic Complex, near Prince Rupert, British Columbia, *Canadian Journal of Earth Sciences, 16*, 400–410, 1979.

Hildreth, W., and G. Mahood, Correlation of ash-flow tuffs, *Geological Society of America Bulletin, 96*, 968–974, 1985.

Hillier, S., J. Mátyás, A. Matter, and G. Vasseur, Illite/smectite diagenesis and its variable correlation with vitrinite reflectants in the Pannonian Basin, *Clays and Clay Minerals, 43*(2), 174–183, 1995.

Hoskin, P.O.W., and U. Schaltegger, The composition of zircon and igneous and metamorphic petrogenesis, in *Zircon*, edited by J.M. Hanchar and P.O.W. Hoskin, pp. 27–62, Mineralogical Society of America, Washington, DC, Reviews in Mineralogy and Geochemistry, vol. 53, 2003.

Hower, J., Shale diagenesis, in *Clays and the Resource Geologist*, edited by F. J. Longstaffe, pp. 60–80, Mineralogical Association of Canada, Short Course Handbook 7, 1981.

Huang, W.-L., J. M. Longo, and D. R. Pevear, An experimentally derived kinetic model for smectite-to-illite conversion and its use as a geothermometer, *Clays and Clay Minerals, 41*(2), 162–177, 1993.

Humphreys, D. R., Accelerated nuclear decay: a viable hypothesis?, in *Radioisotopes and the Age of the Earth: A Young-Earth Creationist Research Initiative*, edited by L. Vardiman, A. A. Snelling, and E. F. Chaffin, pp. 333–379, Institute for Creation Research, El Cajon, California, and Creation Research Society, St. Joseph, Missouri, 2000.

Humphreys, D. R., Young helium diffusion age of zircons supports accelerated nuclear decay, in *Radioisotopes and the Age of the Earth: Results of a Young-Earth Creationist Research Initiative*, edited by L. Vardiman, A. A. Snelling, and E. F. Chaffin, pp. 25–100, Institute for Creation Research, El Cajon, California, and Creation Research Society, Chino Valley, Arizona, 2005.

Humphreys, D. R., S. A. Austin, J. R. Baumgardner, and A. A. Snelling, Helium diffusion rates support accelerated nuclear decay, in *Proceedings of the Fifth International Conference on Creationism*, edited by R. L. Ivey, Jr., pp. 175–195, Creation Science Fellowship, Pittsburgh, Pennsylvania, 2003a.

Humphreys, D. R., S. A. Austin, J. R. Baumgardner, and A. A. Snelling, Recently measured helium diffusion rate for zircon suggests inconsistency with U-Pb age for Fenton Hill granodiorite, *EOS, Transactions of the American Geophysical Union, 84*(46), Fall Meeting Supplement, Abstract V32C-1047, 2003b.

Humphreys, D. R., S. A. Austin, J. R. Baumgardner, and A. A. Snelling, Helium diffusion age of 6000 years supports accelerated nuclear decay, *Creation Research Society Quarterly*, *41*, 1–16, 2004.

Hurford, A. J., On the closure temperature for fission tracks in zircon, *Nuclear Tracks, 10*, 415, 1985.

Hurford, A. J., Standardization of fission track calibration: recommendations by the Fission Track Working Group of the I.U.G.S. Subcommision on Geochronology, *Chemical Geology, 80*, 171–178, 1990.

Hurford, A. J., and P. F. Green, A user's guide to fission track dating calibration, *Earth and Planetary Science Letters, 59*, 343–354, 1982.

Hurford, A. J., and P. F. Green, The zeta age calibration of fission-track dating, *Chemical Geology (Isotope Geoscience), 1*, 285–317, 1983.

Ireland, T. R., and I. S. Williams, Considerations in zircon geochronology by SIMS, in *Zircon*, edited by J. M. Hanchar and P. O. W. Hoskin, pp. 215–241, Mineralogical Society of America, Washington, DC, Reviews in Mineralogy and Geochemistry, vol. 53, 2003.

Karlstrom, K. E., B. R. Ilg, M. L. Williams, D. P. Hawkins, S. A. Bowring, and S. J. Seaman, Paleoproterozoic rocks of the Granite Gorges, in *Grand Canyon Geology*, edited by S. S. Beus and M. Morales, second edition, pp. 9–38, Oxford University Press, New York, 2003.

Kisch, H. J., Mineralogy and petrology of burial diagenesis (burial metamorphism) and incipient metamorphism in clastic rocks, in *Diagenesis in Sediments and Sedimentary Rocks, 2*, edited by G. Larsen and G. Chilingar, pp. 289–493, Elsevier, Amsterdam, 1983.

Kisch, H. J., Correlation between indicators of very low-grade metamorphism, in *Low Temperature Metamorphism*, edited by M. Frey, pp. 227–304, Chapman and Hall, New York, 1987.

Kisch, H. J., Illite crystallinity: recommendations on sample preparation, x-ray diffraction settings, and interlaboratory samples, *Journal of Metamorphic Geology, 9*, 665–670, 1991.

Kowallis, B. J., and J. S. Heaton, Fission-track dating of bentonites and bentonitic mudstones from the Morrison Formation in central Utah, *Geology, 15*, 1135–1142, 1987.

Kowallis, B. J., E. H. Christiansen, and A. L. Deino, Age of the Brushy Basin Member of the Morrison Formation, Colorado Plateau, western USA, *Cretaceous Research, 12*, 483–493, 1991.

Kubler, B., Les argiles, indicateurs de métamorphisme, *Revue de L'Institut Française de Pétrole, 19*, 1093–1112, 1964.

Kubler, B., La cristallinité d'illite et les zones tout à fait supérieures du métamorphisme, in *Etages Tectoniques, Colloque de Neûchatel*, pp. 105–122, Institute de Géologie, Université de Neûchatel, Neûchatel, Switzerland, 1967.

Kubler, B., Evaluation quantitative de métamorphisme par la cristallinité

de l'illite, *Centre de Recherches de Pau Société Nationale de Pétroles d'Aquitaine Bulletin, 2*, 385–397, 1968.

Kubler, B., and D. Goy-Eggenberger, La cristallinité de l'illite revisitée, un bilan des connaissances acquises ces trente derniéres années, *Clay Minerals, 36*, 143–157, 2001.

Ludwig, K.R., *Isoplot/Ex (Version 2.49): The Geochronological Toolkit for Microsoft Excel*, University of California, Berkeley, Berkeley Geochronology Center, Special Publication No. 1a, 2001.

Magomedov, Sh. A., Migration of radiogenic products in zircon, *Geokhimiya, 2*, 263–267, 1970.

McKee, E.D., and C.E. Resser, *Cambrian History of the Grand Canyon Region*, Carnegie Institution of Washington Publication 563, Washington, DC, 1945.

Middleton, L.T., and D.K. Elliott, Tonto Group, in *Grand Canyon Geology*, edited by S.S. Beus and M. Morales, first edition, pp. 83–106, Oxford University Press, New York, and Museum of Northern Arizona Press, Flagstaff, Arizona, 1990.

Middleton, L.T., and D.K. Elliott, Tonto Group, in *Grand Canyon Geology*, edited by S.S. Beus and M. Morales, second edition, pp. 90–106, Oxford University Press, New York, 2003.

Naeser, C.W., The use of apatite and sphene for fission track age determinations, *Geological Society of America Bulletin, 78*, 1523–1526, 1967.

Naeser, C.W., Fission-track dating and geological annealing of fission tracks, in *Lectures in Isotope Geology*, edited by E. Jäger and J.C. Hunziker, pp. 154–169, Springer-Verlag, Berlin, 1979.

Naeser, C.W., The fading of fission tracks in the geologic environment: data from deep drill holes, *Nuclear Tracks, 5*, 248–250, 1981.

Naeser, C.W., and F.C.W. Dodge, Fission-track ages of accessory minerals from granitic rocks of the central Sierra Nevada Batholith, California, *Geological Society of America Bulletin, 80*, 2201–2212, 1969.

Naeser, C.W., and H. Faul, Fission track annealing in apatite and sphene, *Journal of Geophysical Research, 74*, 705–710, 1969.

Naeser, N.D., and C.W. Naeser, Fission-track dating, in *Quaternary Dating Methods*, edited by W.C. Mahaney, pp. 87–100, Developments in Palaeontology and Stratigraphy 7, Elsevier, Amsterdam, 1984.

Naeser, C. W., I. R. Duddy, D. P. Elston, T. A. Dumitru, and P. F. Green, Fission-track dating: ages for Cambrian strata and Laramide and post-Middle Eocene cooling events from the Grand Canyon, Arizona, in *Geology of Grand Canyon, Northern Arizona (with Colorado River Guides)*, edited by D. P. Elston, G. H. Billingsley, and R. A. Young, pp. 139–144, American Geophysical Union, Washington, DC, 1989a.

Naeser, N. D., C. W. Naeser, and P. H. McCulloh, The application of fission-track dating to the depositional and thermal history of rocks in sedimentary basins, in *Thermal History of Sedimentary Basins*, edited by N. D. Naeser and T. H. McCulloh, pp. 157–180, Springer-Verlag, Berlin, 1989b.

Naeser, C. W., R. A. Zimmermann, and G. T. Cebula, Fission-track dating of apatite and zircon: an interlaboratory comparison, *Nuclear Tracks, 5*, 65–72, 1981.

Nagpaul, K. K., P. K. Mehta, and M. L. Gupta, Correction of fission-track dates due to thermal annealing in apatite, biotite and sphene, *Pure and Applied Geophysics, 112*, 131–139, 1974.

Nielson, J. E., D. R. Lux, G. B. Dalrymple, and A. F. Glazner, Age of the Peach Springs Tuff, southeastern California and western Arizona, *Journal of Geophysical Research, 95*(B1), 571–580, 1990.

Nutman, A. P., V. C. Bennett, C. R. L. Friend, and V. R. McGregor, The early Archaean Itsaq Gneiss Complex of southern West Greenland: the importance of field observations in interpreting age and isotopic constraints for early terrestrial evolution, *Geochimica et Cosmochimica Acta, 64*, 3035–3060, 2000.

Parrish, R. R., and S. R. Noble, Zircon U-Th-Pb geochronology by isotope dilution-thermal ionization mass spectrometry (ID-TIMS), in *Zircon*, edited by J. M. Hanchar and P. O. W. Hoskin, pp. 183–213, Mineralogical Society of America, Washington, DC, Reviews in Mineralogy and Geochemistry, vol. 53, 2003.

Petersen, L. M., and M. M. Roylance, Stratigraphy and depositional environments of the upper Jurassic Morrison Formation near Capitol Reef National Park, Utah, *Brigham Young University Geology Studies, 29* (2), 1–12, 1982.

Peterson, F., and C. E. Turner-Peterson, The Morrison Formation of the Colorado Plateau: recent advances in sedimentology, stratigraphy and

paleotectonics, *Hunteria, 2* (1), 1–18, 1987.

Pollastro, R. M., Considerations and applications of the illite/smectite geothermometer in hydrocarbon-bearing rocks of Miocene to Mississippian age, *Clays and Clay Minerals, 41*(2), 119–133, 1993.

Poupeau, G., Precision, accuracy and meaning of fission-track ages, *Proceedings of the Indian Academy of Sciences, Earth and Planetary Science, 90*, 403–436, 1981.

Poupeau, G., J. Carpena, A. Chambaudiet, and Ph. Romary, Fission-track plateau-age dating, in *Solid State Nuclear Track Detectors*, edited by H. Francois, J. P. Massue, R. Schmitt, N. Kurtz, M. Monnin, and S. A. Durrani, pp. 965–971, Pergamon, Lyon, France, 1979.

Poupeau, G., Ph. Romary, and P. Toulhoat, On the fission-track plateau ages of minerals, *U.S. Geological Survey, Open File Report 78-701*, 339–340, 1978.

Price, P. B., and R. M. Walker, Chemical etching of charged particle tracks in solids, *Journal of Applied Physics, 33*, 3407, 1962a.

Price, P. B., and R. M. Walker, Observation of fossil particle tracks in natural micas, *Nature, 196*, 732, 1962b.

Price, P. B., and R. M. Walker, Fossil tracks of charged particles in mica and the age of minerals, *Journal of Geophysical Research, 68*, 4847–4862, 1963.

Pytte, A. M., and R. C. Reynolds, The thermal transformation of smectite to illite, in *Thermal History of Sedimentary Basins*, edited by N. D. Naeser and T. H. McCulloh, pp. 133–140, Springer-Verlag, Berlin, 1989.

Reimer, G. M., D. Storzer, and G. A. Wagner, Geometry factor in fission track counting, *Earth and Planetary Science Letters, 9*, 401–404, 1970.

Rejebian, V. A., A. G. Harris, and J. S. Huebner, Conodont color and textural alteration: an index to regional metamorphism, contact metamorphism and hydrothermal metamorphism, *Geological Society of America Bulletin, 99*, 471–479, 1987.

Renac, C., and A. Meunier, Reconstruction of palaeothermal conditions in the passive margin using illite-smectite mixed-layer series (BA1 scientific deep drill-hole, Ardeche, France), *Clay Minerals, 30*, 107–118, 1995.

Robinson, D., and R. J. Merriman, Low-temperature metamorphism: an overview, in *Low-Grade Metamorphism*, edited by M. Frey and D.

Robinson, pp. 1–9, Blackwell, Oxford, 1999.

Schreurs, J.W.H., A.M. Friedman, D.J. Rockop, M.W. Hair, and R.M. Walker, Calibrated U-Th glasses for neutron dosimetry and determination of uranium and thorium concentrations by the fission-track method, *Radiation Effects, 7*, 231–233, 1971.

Sharma, Y.P., N. Lal, K.D. Bal, R. Parshad, and K.K. Nagpaul, Closing temperatures of different fission-track clocks, *Contributions to Mineralogy and Petrology, 72*, 335–336, 1980.

Silk, E.C.H., and R.S. Barnes, Examination of fission fragment tracks with an electron microscope, *Philosophical Magazine, 4*, 970, 1959.

Smart, G., and T. Clayton, The progressive illitization of interstratified illite-smectite from Carboniferous sediments of northern England and its relationship to organic maturity indicators, *Clay Minerals, 30*, 455–466, 1985.

Smith, M.J., and P. Leigh-Jones, An automated microscope scanning stage for fission track dating, *Nuclear Tracks, 10*, 395–400, 1985.

Snelling, A.A., Geochemical processes in the mantle and crust, in *Radioisotopes and the Age of the Earth: A Young-Earth Creationist Research Initiative*, edited by L. Vardiman, A.A. Snelling, and E.F. Chaffin, pp. 123–304, Institute for Creation Research, El Cajon, California, and Creation Research Society, St. Joseph, Missouri, 2000a.

Snelling, A.A., Radiohalos, in *Radioisotopes and the Age of the Earth: A Young-Earth Creationist Research Initiative*, edited by L. Vardiman, A.A. Snelling, and E.F. Chaffin, pp. 381–468, Institute for Creation Research, El Cajon, California, and Creation Research Society, St. Joseph, Missouri, 2000b.

Snelling, A.A., Radiohalos in granites: evidence for accelerated nuclear decay, in *Radioisotopes and the Age of the Earth: Results of a Young-Earth Creationist Research Initiative*, edited by L. Vardiman, A.A. Snelling, and E.F. Chaffin, pp. 101–207, Institute for Creation Research, El Cajon, California, and Creation Research Society, Chino Valley, Arizona, 2005a.

Snelling, A.A., Isochron discordances and the role of inheritance and mixing of radioisotopes in the mantle and crust, in *Radioisotopes and the Age of the Earth: Results of a Young-Earth Creationist Research Initiative*, edited by L. Vardiman, A.A. Snelling, and E.F. Chaffin, pp. 393–518, Institute for

Creation Research, El Cajon, California, and Creation Research Society, Chino Valley, Arizona, 2005b.

Snelling, A. A., and M. H. Armitage, Radiohalos—a tale of three granitic plutons, in *Proceedings of the Fifth International Conference on Creationism*, edited by R. L. Ivey, Jr., pp. 243–267, Creation Science Fellowship, Pittsburgh, Pennsylvania, 2003.

Snelling, A. A., S. A. Austin, and W. A. Hoesch, Radioisotopes in the diabase sill (Upper Precambrian) at Bass Rapids, Grand Canyon, Arizona: an application and test of the isochron dating method, in *Proceedings of the Fifth International Conference on Creationism*, edited by R. L. Ivey, Jr., pp. 269–284, Creation Science Fellowship, Pittsburgh, Pennsylvania, 2003a.

Snelling, A. A., J. R. Baumgardner, and L. Vardiman, Abundant Po radiohalos in Phanerozoic granites and timescale implications for their formation, *EOS, Transactions of the American Geophysical Union, 84*(46), Fall Meeting Supplement, Abstract V32C-1046, 2003b.

Sparks, R. S. J., S. Self, and G. P. L. Walker, Products of ignimbrite eruptions, *Geology, 1*, 115–118, 1973.

Stacey, J. S., and J. D. Kramers, Approximation of terrestrial lead isotope evolution by a two-stage model, *Earth and Planetary Science Letters, 26*, 207–221, 1975.

Steiger, R. H., and B. Jäger, Subcommission on geochronology: convention on the use of the decay constants in geo- and cosmochronology, *Earth and Planetary Science Letters, 36*, 359–362, 1977.

Storzer, D., and G. Poupeau, Age-plateaux de verres et mineraux par la methode des traces de fission, *Comptes Rendu Academie Sciences Paris, 276D*, 137–139, 1973.

Storzer, D., and G. A. Wagner, Correction of thermally lowered fission track ages of tektites, *Earth and Planetary Science Letters, 5*, 463–468, 1969.

Storzer, D., and G. A. Wagner, The application of fission track dating in stratigraphy: a critical review, in *Numerical Dating in Stratigraphy*, edited by G. S. Oldin, pp. 199–221, John Wiley & Sons, New York, 1982.

Turner, C. E., and N. S. Fishman, Jurassic Late T'oo'dichi': a large alkaline, saline lake, Morrison Formation, eastern Colorado Plateau, *Geological Society of America Bulletin, 103*(4), 538–558, 1991.

Turner, C. E., and F. Peterson, Reconstruction of the Upper Jurassic Morrison Formation extinct ecosystem—a synthesis, *Sedimentary Geology, 167*, 309–355, 2004.

Velde, B., and J. Espitalié, Comparison of kerogen maturation and illite/smectite composition in diagenesis, *Journal of Petroleum Geology, 12*(1), 103–110, 1989.

Velde, B., and B. Lanson, Comparison of I/S transformation and maturity of organic matter at elevated temperatures, *Clays and Clay Minerals, 41*(2), 178–183, 1993.

Wagner, G. A., Archaeological applications of fission-track dating, *Nuclear Track Detectors, 2*, 51–63, 1978.

Wardlaw, B. R., and A. G. Harris, Conodont-based thermal maturation of Paleozoic rocks in Arizona, *American Association of Petroleum Geologists Bulletin, 68*(9), 1101–1106, 1984.

Warr, L. N., and A. H. N. Rice, Interlaboratory standardization and calibration of clay mineral crystallinity and crystallite size data, *Journal of Metamorphic Geology, 12*, 141–152, 1994.

Young, R. A., and W. J. Brennan, Peach Springs Tuff: its bearing on structural evolution of the Colorado Plateau and development of Cenozoic drainage in Mojave County, Arizona, *Geological Society of America Bulletin, 85*(1), 83–90, 1974.

Zeitler, P. K., Closure temperature implications of concordant $^{40}Ar/^{39}Ar$ potassium feldspar and zircon fission-track ages from high-grade terranes, *Nuclear Tracks, 10*, 441–442, 1985.